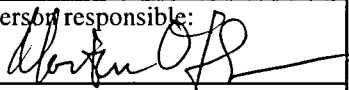


Report no.: 96.123		ISSN 0800-3416	Grading: Open
Title: The geology and ore deposits of the Pechenga Greenstone Belt. (Field trip guidebook).			
Authors: Melezhik, V.A. & Often, M.		Client: IGCP Project 336	
County: Murmansk region		Commune: Pechenga district	
Map-sheet name (M=1:200.000) Zapolyarny		Map-sheet no. (M=1:50.000) R-35-86-CD, R-35-87-AB, R-35-87-CD	
Deposit name and grid-reference: Pechenga Ore Field		Number of pages: 91	Price (NOK): 350.-
		Map enclosures: one	
Fieldwork carried out: 1990-1995	Date of report: 30.07.96	Project no.: 67.6421.02	Person responsible: 
<p>Summary:</p> <p>This field excursion guide, 'The geology and ore deposits of the Pechenga Greenstone Belt', prepared for the International Field Conference and Symposium 'Layered Mafic Complexes and Related ore Deposits of Northern Fennoscandia, Finland, Norway, Russia' in relation with the International Geological Correlation Program (IGCP) Project 336.</p> <p>A part from the excursion itinerary the guidebook contains description on: (1) 'General geology and evolutionary history of the Early Proterozoic Pechenga Greenstone Belt'; (2) 'Differentiated gabbro-wehrlite intrusions, 'ferropicritic' lava flows and associated sulphide Ni-Cu ores'; (3) 'Early Proterozoic layered mafic-ultramafic massif of Mt. General'skaya'.</p> <p>The geological map of the Pasvik-Pechenga Greenstone Belt 1: 200,000 is provided.</p>			
Keywords: Malmgeologi	Geologisk undersøkelse	Prekambrium	
Petsamo	Nikkel	Kobber	
Fagrapport			

**FIELD TRIP GUIDEBOOK**  
**THE GEOLOGY AND ORE DEPOSITS OF THE PECHENGA**  
**GREENSTONE BELT**

Geological Survey of Norway, Trondheim

Pechenga Exploration Expedition, Pechenga Nickel Combinat, Zapolyarny-  
Nickel

*Compiled by*  
Victor A. Melezhik

*Edited by*  
Victor A. Melezhik & Morten Often

Prepared for the  
International Geological Correlation Program (IGCP) Project 336  
Field Conference and Symposium

**Layered Mafic Complexes and Related ore Deposits of Northern Fennoscandia**  
**Finland, Norway, Russia**  
**Kemi, Penikat, Keivitsa, Seiland, General'skaya, Pechenga**  
August 18-30, 1996

**Part III: The Geology and Ore Deposits of the Pechenga Greenstone Belt**  
August 27-30, 1996

---

Trondheim, Norway

## **GUIDEBOOK CONTRIBUTORS**

**Andrey A. Bol'shakov**, Pechenga Exploration Expedition, Pechenga Nickel Combine, Bredov, 14, 184420 Nickel, Murmansk region, Russia.

**Vadim V. Distler**, Institute of Geology of Ore Deposits, the Russian Academy of Sciences, Staromonentny per. 35, 109017 Moscow.

**Victor A. Melezhik**, Geological Survey of Norway, Department of Mineral Resources, Post Box 3006 - Lade, 7002 Trondheim.

**Stanislav V. Sokolov**, Pechenga Nickel Combine, 184414 Zapolyarny, Murmansk region, Russia.

**Vladimir A. Tel'nov**, Pechenga Exploration Expedition, Pechenga Nickel Combine, Bredov, 14, 184420 Nickel, Murmansk region, Russia.

**Dmitry M. Turovzev**, Institute of Geology of Ore Deposits, the Russian Academy of Sciences, Staromonentny per. 35, 109017 Moscow.





# FIELD TRIP GUIDEBOOK

---

## THE GEOLOGY AND ORE DEPOSITS OF THE PECHENGA GREENSTONE BELT



Mining and Smelting  
Combine



Pechenga Nickel

PREPARED FOR  
THE 1996 IGCP PROJECT 336  
FIELD CONFERENCE AND  
SYMPOSIUM, FINLAND,  
N NORWAY AND NW RUSSIA

---



International Geological Correlation Program  
**Project 336**  
PETROLOGY AND METALLOGENY OF  
INTRAPLATE MAFIC AND ULTRAMAFIC MAGMATISM

1996 Field Conference and Symposium

**Layered Mafic Complexes and Related Ore Deposits of Northern  
Fennoscandia  
Finland, Norway, Russia  
Kemi, Penikat, Keivitsa, Seiland, General'skaya, Pechenga**  
August 18-31, 1996

**Part III: The Geology and Ore Deposits of the Pechenga Greenstone Belt**  
Pechenga, August 27-30, 1996

## **Organising Committee**

T. Alapieti, University of Oulu, Finland  
V. Melezhik, Geological Survey of Norway  
M. Often, Geological Survey of Norway  
H. Papunen, University of Turku, Finland (Chairman)  
B. Robins, University of Bergen, Norway  
A. Silvennoinen, Geological Survey of Finland  
S. Sokolov, Pechenga Nickel Combinate, Zapolyarny, Russia  
V. Tel'nov, Pechenga Exploration Expedition, Pechenga Nickel Combinate, Nickel, Russia

## **Sponsors**

IAGOD/CODMUR  
Geological Survey of Finland, Rovaniemi  
Geological Survey of Norway  
Pechenga Nickel  
University of Turku  
University of Bergen

## PREFACE

This guidebook has been prepared for the field conference on 'The Geology and Ore Deposits of the Pechenga Greenstone Belt' that will take place in Zapolyarny, Russia in August of 1996 as an essential component of field conference and symposium on 'Layered Mafic Complexes and Related ore Deposits of Northern Fennoscandia, Finland, Norway, Russia (Kemi, Penikat, Keivitsa, Seiland, General'skaya, Pechenga) that will be held in the framework of International Geological Correlation Program (IGCP) Project 336 ('Petrology and Metallogeny of Intraplate Mafic and Ultramafic Magmatism'). The five-year-long IGCP project was begun in 1992 to investigate the petrology and metallurgy of various intracontinental mafic igneous provinces with an overall goal of establishing geological criteria for targeting mineral deposits in such environments.

The principal goal of the 1996 meeting is to introduce to the international scientific and exploration communities the world-class ultramafic hosted sulphide Ni-Cu deposits and certain advances in our understanding of the structure, stratigraphy, magmatic history and ore-forming processes of the Early Proterozoic Pechenga Greenstone Belt. The four-day-long field trip (August 27-30) is designed to provide an overview of the general geology of the Pechenga Belt, where it is most exposed in the central Pechenga area; and it will focus on the two ultramafic hosted sulphide Ni-Cu deposits. The two active mines, the Severny underground mine and Pilgujärvi open pit mine, highlight the stratigraphic and tectonic location of those deposits which provide ca. 80% of current mining activities in the area.

This excursion guide starts with a brief description of the bedrock geology of the Pechenga Greenstone Belt in the county of Murmansk, north-west Russia. The development of geological research in this area and current understanding and interpretation of the geological history are presented. The main part of the guide consists of description of 18 excursion localities with emphasis placed on stratigraphy, geochemistry and aspects of sedimentology, volcanology and palaeotectonics as well as on structural position, isotope geochemistry and origin of ultramafic-hosted sulphide Ni-Cu ores. Some localities are situated along or close to roads while other are located far away from any roads and can be accessed only by hiking as far as 5 kilometres both ways. All localities have references to east and north co-ordinates of the 1:50,000 topographic maps produced by the Topography and Geodesy Agency of the former USSR. A simplified map of the bedrock geology is included in the guide.

Descriptions of the localities are organised according to a fixed standard. In addition to the references to topographic maps, each locality includes key words referring to lithostratigraphic units and other important geological information which may be examined at this particular locality. The locality numbers are also indicated on the stratigraphic table.

We thank Å.K. Rønningen and P. Ryghaug for digitising the geological map and the section of the Mt. General'skaya layered gabbro massif.

C. Kandolf reviewed the English of the manuscript.

Victor Melezhik & Morten Often  
June 30, 1996

## CONTENTS

GENERAL GEOLOGY AND EVOLUTIONARY HISTORY OF THE EARLY PROTEROZOIC PECHENGA GREENSTONE BELT, <b>V.A. Melezhik</b> .....	6
DIFFERENTIATED GABBRO-WEHRLITE INTRUSIONS, 'FERROPICRITIC' LAVA FLOWS AND ASSOCIATED SULPHIDE Ni-Cu ORES, <b>V.A. Melezhik &amp; St.V. Sokolov</b> .....	31
EARLY PROTEROZOIC LAYERED MAFIC-ULTRAMAFIC MASSIF OF MT. GENERALSKAYA, <b>V.A. Tel'nov, A.N. Bolshakov, V.V. Distler, D.M. Tourovstev &amp; V.A. Melezhik</b> .....	51
EXCURSION ITINERARY .....	70
PLATE 1. GEOLOGICAL MAP OF THE PASVIK-PECHENGA BELT, 1:200,000. <b>Melezhik, V. A., Sturt, B.A., Mokrousov, V.A., Ramsay, D.M., Nilsson, L.P. &amp; Balashov, Yu.A.</b> 1995: The Early Proterozoic Pasvik-Pechenga Greenstone Belt: 1:200,000 geological map, stratigraphic correlation and revision of stratigraphic nomenclature. In: Roberts, D. & Nordgulen, O. (eds), Geology of the eastern Finnmark-western Kola region. <i>Norges Geol.Unders. Special Publ.</i> , 7, 81- 91.	

## GENERAL GEOLOGY AND EVOLUTIONARY HISTORY OF THE EARLY PROTEROZOIC PECHENGA GREENSTONE BELT

V.A. Melezhik

### 1. Introduction

Early reconnaissance geological work on the Norwegian side of the Pasvik-Pechenga area was carried out by Tellef Dahl (1891). The Pechenga area has been the subject of research since early Russian geological/geographical expeditions visited the area in the 1910s. An extensive study of the area by Finnish geologists followed in 1921, and resulted in the discovery of economically interesting Ni-Cu sulphide ore. Väyrynen (1938) subsequently published the first document directly related to the geology of the Petsamo (Pechenga) area, focusing on the Ni-Cu ore and ultramafic intrusions and making only a limited description of the regional geology. Later geological work in the Pasvik area was carried out by Hausen (1926), Wegmann (1929).

After World War II, reconnaissance geological work was continued in Pasvik Bugge (1960) while the Pechenga area was intensively mapped and drilled, resulting in numerous Russian exploration and prospecting reports and scientific papers. Zagorodny et al. (1964) summarised the major regional geological features, providing a comprehensive stratigraphic subdivision outlining the cyclic development of the 'Pechenga Complex'.

The 1960s and 1970s saw intense prospecting and related scientific investigations resulting from the discovery of new Ni-Cu deposits in the Pilgüarvi differentiated ultramafic intrusion. Predovsky et al. (1974) described general and detailed features of the geochemical evolution of the volcanic and sedimentary rocks of the Pechenga Complex; much of the reported major and trace element data are still used as a basis for the geochemistry of the Petsamo Supergroup rocks. Siedlecka et al. (1985) described and correlated the Pechenga-Pasvik stratigraphy. Lieungh (1988) mapped the Pasvik area at 1:50 000 scale.

In 1987 the project entitled 'Deep Mapping of the Pechenga Zone' was initiated by the Central Kola Survey Expedition (Mitrofanov & Smolkin, 1995). Since 1990, the project has been conducted as a joint endeavour between the Geological Survey of Norway (NGU), Central Kola Survey Expedition

and the Russian Academy of Sciences to produce the 1:250 000 international map-sheet Kirkenes which includes entire Polmak-Opukasjarvi-Pasvik-Pechenga Greenstone Belt. This international cooperation resulted in the compilation of the Special Publication volume (Roberts & Nordgulen 1995) which contains a number of comprehensive papers on the stratigraphy and geochemistry as well as a preliminary version of 200,000 bedrock map and correlation table of the Pasvik-Pechenga Belt (Melezhik et al. 1995).

### 2. Geological setting

The early Proterozoic Pasvik-Pechenga Greenstone Belt is located in the north-western corner of the Kola Peninsula (Fig. 1). The PP Belt is a part of

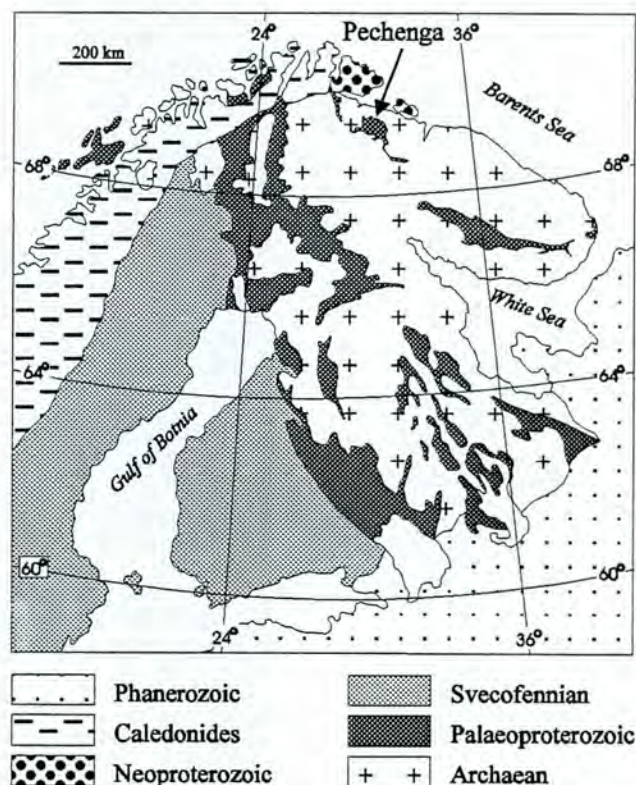


Fig. 1 Location of the Palaeoproterozoic Pechenga Greenstone Belt

the 1000 km long, discontinuously developed, early Proterozoic Polmak-Opukasjarvi-Pasvik-Pechenga-Imandra/Varzuga-Ust'Ponoy Greenstone Belt which traverses the north-eastern part of the Fennoscandian Shield (Fig. 1) and which formed initially in the easternmost part of the Kola Peninsula as the Imandra/Varzuga and Ust'Ponoy intracontinental rifts between two Archaean blocks, prior to the appearance of 2453±42 Ma-old layered



gabbro-norite intrusions (Melezhik & Sturt 1994). The rifts, and the sedimentary basins and zones of volcanic activity associated with them, subsequently migrated towards the north-west. The early stages of the Pasvik-Pechenga rift zone coincided with uplift and partial erosion of the layered gabbro-norite intrusions (Melezhik & Sturt 1994) including the gabbro-norite intrusion of the General'skaya Mountain (Bakushkin & Akhmedov 1975).

### 3. Structural build-up

Structurally, the Pasvik-Pechenga rift zone comprises the North and South Sub-Zones (Zagorodny et al. 1964) which later were renamed the North and South Zones (Melezhik et al. 1994a). The North and South Zones are separated by the major, longitudinal, probably at times synvolcanic, Poritash Fault Zone (Fig. 2, Zagorodny et al. 1964; Skuf' in 1995). The North

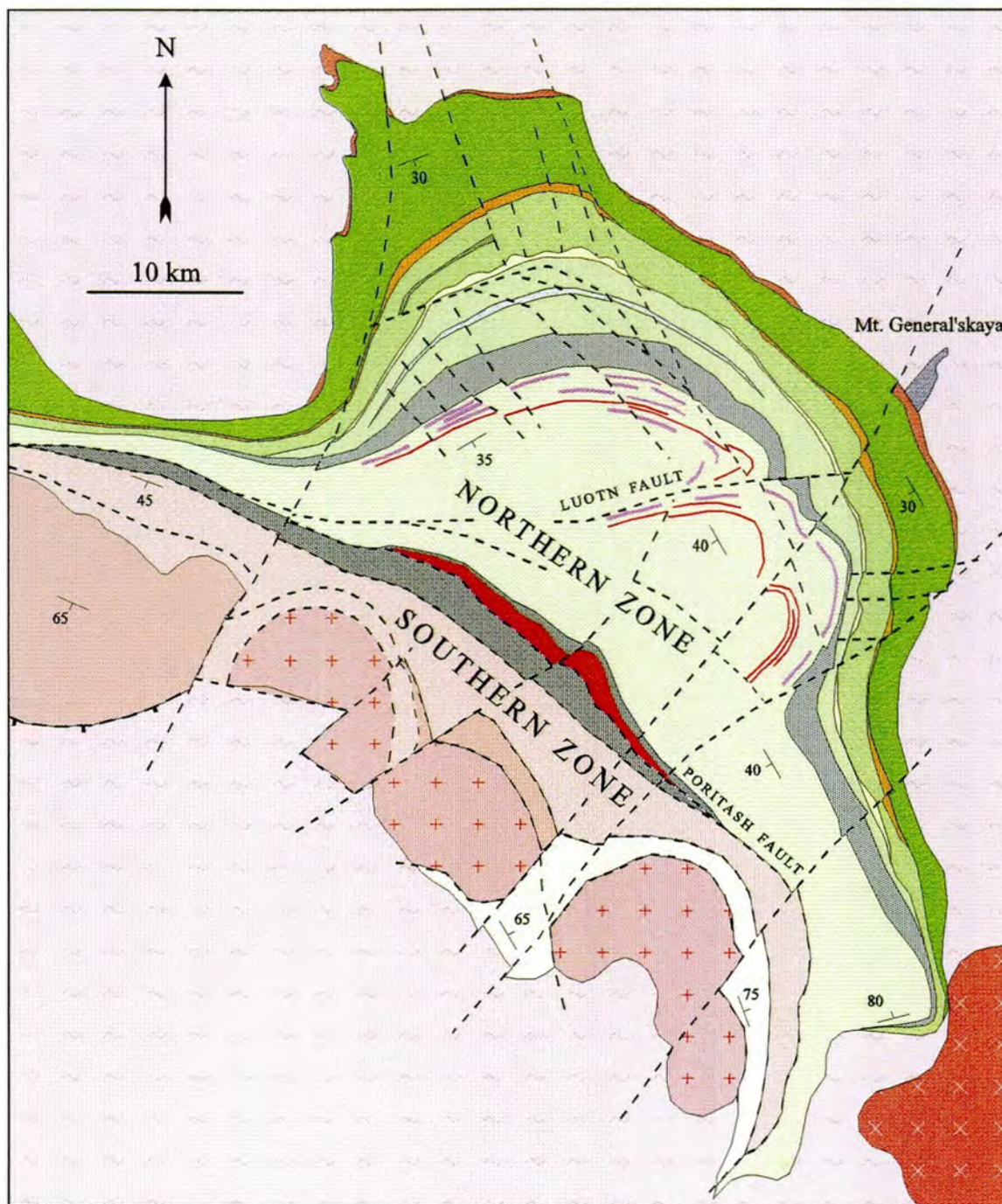


Fig. 2 General geology of the Pechenga Greenstone Belt (modified from Zagorodny et al. 1964 and Predovsky et al. 1974)



## Legend

### PLUTONIC ROCKS

#### LITZA-ARAGUBA COMPLEX



Porphyritic microcline granite

#### PORITASH COMPLEX



Andesite, dacite, rhyolite

#### KASKELJAVR COMPLEX



Granite, granodiorite, diorite, gabbro

#### MT. GENERAL'SKAYA MASSIF



Gabbro, gabbro-norite, norite

### METASUPRACRUSTAL AND INTRUSIVE ROCKS

### PETSAMO SUPERGROUP

#### SOUTH PECHENGA GROUP (MUTUAL AGE RELATIONS PARTLY UNCERTAIN)



LAKE PESTCHANOE FORMATION  
Tholeiitic pillowed and amygdaloidal basalt



TAL'YA FORMATION  
Andesitic volcanoclastic sandstone and siltstone



KASESJOKI, KAPLYA, MENNEL', BRAGINO FORMATIONS  
Rhythmic-bedded sandstone and siltstone, andesitic volcanoclastic polymict conglomerate, synorogenic andesitic lava, lava-breccia and tuff, synorogenic picritic pillowed and massive basalt, picritic lava, lava-breccia, tuff, volcanoclastic sediment, boninitic andesite, basalt



KOLLAJAVR FORMATION  
Black schist, cherty quartzite, amphibole-carbonate schist

#### NORTH PECHENGA GROUP

##### PILGUJÄRVI VOLCANIC FORMATION



*Suppavaara Member, Upper and Middle Basalt Members, Rhyolite Member, Basalt-Picrite Member*  
Tholeiitic massive and pillowed basalt with beds of basaltic volcanoclastic sediment and tuff; black shale; gabbro comagmatic with tholeiitic basalts



Ferropicritic massive, globular and pillowed lava



Rhyolitic, dacitic and andesitic lava and tuff

##### PILGUJÄRVI SEDIMENTARY FORMATION



*Lammas Member, Member B and Member A*  
Ferropicritic lava and tuff; highly carbonaceous and sulphidic sediment, subordinate polymict conglomerate; basalt and basaltic tuff, gabbro, pyroxenite peridotite and comagmatic ferropicritic volcanic rocks

##### KOLASJOKI VOLCANIC FORMATION



*Upper and Lower Basalt Members*  
Tholeiitic and pillowed basalt; lava-breccia, tuff



*Black Schist Member*  
Carbonaceous and sulphidic greywacke, chert, limestone; basaltic tuff and tuffite

##### KOLASJOKI SEDIMENTARY FORMATION



*Black Schist Member, Dolostone Member and Red Bed Member*  
Stromatolitic dolostone, red arkosic sandstone and polymict conglomerate

##### KUETSJÄRVI VOLCANIC FORMATION



*Orshoavi and Upper Basalt Member*  
Alkaline and subalkaline amygdaloidal basalt, ferropicrite, trachyandesite, dacite and rhyolite; lava-breccia; locally tuff



*Conglomerate Member*  
Volcanoclastic conglomerates, alkaline basalts with pillow structure and columnar joints

##### KUETSJÄRVI SEDIMENTARY FORMATION



*Quartzite Member, Dolostone Member*  
Dolostone, stromatolitic and oncolitic dolostone, dolostone breccia; arkosic and quartzitic sandstone



AHMALAHTI FORMATION  
Basalt and andesite; locally amygdaloidal structure; subordinate picritic tuff and basaltic graywacke



NEVERSKRUKK FORMATION  
Conglomerate with clasts of various gneisses, mafic volcanic rock and banded iron ore; arkose, basaltic tuff

### METAMORPHIC ROCKS; LATE ARCHAEOAN AGE



Tonalitic to granodioritic gneiss, amphibolite, banded iron ore

### GEOLOGICAL SYMBOLS



Lithological boundary



Fault



Thrust fault



Bedding, angle of dip indicated



Zone is an isometric, NW-SE-trending and SE-SW-dipping (20-60°) half-graben. A widespread, transversal fault system breaks the half-graben into several NW-SE and NE-SW-trending blocks, or smaller rift grabens, which controlled subsequent deposition (Melezhik et al. 1988). The three major tectonic blocks of the North Zone are the Western, Central and Eastern Rift Grabens (Fig. 3). The

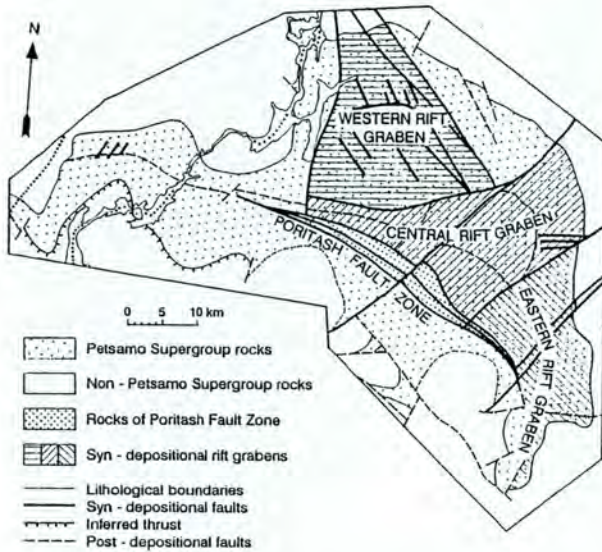


Fig. 3 Main syn-depositional blocks (grabens), and syn-depositional and post-depositional faults of the Pasvik-Pechenga Greenstone Belt (Melezhik et al. 1995).

South Zone (Plate 1) is represented by steeply-dipping (40-90°), strongly folded and probably tectonically imbricated rock assemblages. Two volcanic dome-like structures, made up of andesites, east of the Porojärvi, (Skuf' in et al. 1988), and picrites, south of the Bragino Lake, (Melezhik et al. 1988), are distinguished.

#### 4. Stratigraphic subdivision

The stratigraphic subdivision of the Pechenga Greenstone Belt has remained essentially unchanged since Zagorodny et al. (1964) published the first general description on the regional geology, tectonics and stratigraphy of what he called the Pechenga Series. Several attempts have been made to revise this stratigraphic subdivision (e.g. Kozlovsky, 1987; Smolkin et al., 1995). Strangely, neither of these cited accounts refer to the stratigraphy proposed by Zagorodny et al. (1964). One can consider that no viable case is made by either Kozlovsky (1987) or Smolkin et al. (1995) for revision of this stratigraphy according to the

International Stratigraphic Code (ISSC, 1976). 'New stratigraphic names' introduced by these authors are thus rejected and we will use Zagorodny's original stratigraphy as was done earlier (e.g. Hanski 1992; Hudson et al. 1992; Melezhik et al. 1994a, 1995). In the current lithostratigraphical subdivision, which has been used as a common legend for the forthcoming 1:250,000 international geological map-sheet for Kirkenes, only one exception was made. The exception is concerned with the basal formation which is more exposed and better specified in the northern Pasvik area. Because of this, we suggested the Norwegian name of the Neverskruck as a common name for the basal Formation of the Pechenga rocks (former Ahmalahti Sedimentary Formation) for the whole Pechenga-Pasvik Greenstone Belt (Table 1, Plate 1, Melezhik et al. 1995)

Lithologically, the Pasvik-Pechenga Belt is filled by the early Proterozoic Petsamo Supergroup (PSG, Melezhik & Sturt 1994), previously known as the Pechenga Series (Zagorodny et al. 1964). The Pechenga Series was originally subdivided into the North Pechenga and South Pechenga Sub-Series (Zagorodny et al. 1964), which were later renamed as the North Pechenga Group (NPG) and South Pechenga Group (SPG), respectively (Melezhik & Sturt 1994). The NPG is located mainly in the North (structural) Zone, and the SPG only within the South Zone. Although the NPG and SPG are presently separated in places by the Poritash Fault Zone, their primary contact relationship may have been more complex.

The nature of the basal contacts of the lowermost formations of the NPG in the Pechenga-Pasvik area has been a matter of dispute in the literature. The primary stratigraphic nature of the basal contacts (e.g. Zagorodny et al. 1964; Predovsky et al. 1974) has been called into question by one interpretation of the Superdeep Drillhole-cores (Kozlovsky 1987). The 'tectonic' nature of these contacts was emphasised and elevated to the status of the the Kola Collisional Suture between two major continental blocks (Marker 1985; Berheltensen & Marker 1986). Later the contacts were excavated, drilled and mapped on the scale of 1:5,000. As a result of this work the following conclusions were made (Sturt et al. 1994, 1995): (i) the development of the basal unit of the NPG was controlled by the existing topography, (ii) the basal contacts of the PSG is of a primary nature with well preserved palaeotopography, (iii) the Kola Collisional Suture as currently proposed along the northern margin of the Polmak-Pasvik-Pechenga Greenstone Belt does not exist



Table 1 Lithostratigraphic subdivision of the Pechenga-Pasvik Greenstone Belt (from Melezchik et al. 1995)

P E C H E N G A - P A S V I K B E L T					
ARCHAEAN					
E A R L Y P R O T E R O Z O I C T H R U S T					
P E T S A M O S U P E R - G R O U P	?	Tal'ya Fm.	Tholeiitic pillowed and amygdaloidal basalt (1000 m)		
		L. Pestchanov Fm.	Andesitic volcanoclastic siltstone, sandstone (1000 m)		
		Kasesjoki Fm.	Siltstone Mem.	Post-mid-Petsamo orogenic andesitic volcanoclastic siltstone (900 m)	
			Conglomerate Mem.	Post-mid-Petsamo orogenic andesitic volcanoclastic conglomerate, gritstone, sandstone with iron-banded quartzite pebbles (50 m)	
	M I D P E T S A M O O R O G E N I C U N C O N F O R M I T Y				
	South Pechenga Group	Kaplya Fm.	Synorogenic andesitic and dacitic lava and tuff, explosion breccia (cold and hot lahar) (1000 m)	1.85 Rb-Sr (1)	
		Mennel' Fm.	Synorogenic picritic basalt, picritic lava, lava-breccia, tuff, picritic volcanoclastic sandstone, gritstone, conglomerate (1200 m)	1.86 Rb-Sr (1)	
		Fagermo Fm.	Synorogenic picritic pillowed and massive lava, lava-breccia, tuff, picritic sediments (500 m)		
		Bragino Fm.	Synorogenic andesitic and dacitic lava, tuff and tuffite, andesitic volcanoclastic sediment, basalt, picrite, boninitic andesite (2300 m)	1.94 Rb-Sr (1)	
	T E C T O N I C C O N T A C T				
	Kallojavr Fm.	C- and S-rich sandstone, siltstone, mudstone with cherty quartzite and subordinate basalt and andesite (2000 m)			
P O R I T A S H F A U L T					
P E T S A M O S U P E R - G R O U P	Pilgüjärvi Volc. Fm.	Suppavara Mem.	Tholeiitic pillowed and massive basalt, C-rich siltstone (1000 m)	1.95 Rb-Sr (1)	
		Upper Basalt Mem.	Tholeiitic pillowed basalt, basaltic lava-breccia (800 m)		
		Middle Basalt Mem.	Tholeiitic pillowed basalt (500 m)	1.98 Rb-Sr (4)	
		Rhyolite Mem.	Rhyolitic lava, welded tuff, dacite, andesite, andesitic-dacitic explosion breccia (cold and hot lahar) (500 m)	1.97 U-Pb (3)	
		Lower Basalt Mem.	Massive tholeiitic basalt (600 m)		
		Basalt-Picrite Mem.	Massive tholeiitic basalt, tuff, massive and pillowed ferropicritic lava (750 m)	1.98 Sm-Nd (2) 1.99 Pb-Pb (2)	
	Pilgüjärvi Sed. Fm.	Lammas Mem.	Ferropicritic massive, amygdaloidal and pillowed lava, explosion breccia, tuff, C- and S-rich siltstone, subordinate basalt (500 m)		
		B Mem.	Finely laminated, sedimentary folded C- and S-rich sandstone to mudstone with abundant calcite and sulphide concretions (650 m)		
		A Mem.	C- and S-rich arkosic and greywacke sandstone with bodies of current-bedded and current-rippled greywacke gritstone, sandstone and conglomerate (alluvial fan), basalt (850 m)		
	W E A T H E R I N G C R U S T				
North Pechenga Group		Upper Basalt Mem.	Tholeiitic basalt with pillow and breccia structure (500 m)	2.11 Rb-Sr (1)	
	Kolasjoki Volc. Fm.	Black Shale Mem.	Tuffitic carbonaceous sulphide-bearing greywacke sandstone, siltstone with subordinate limestone, mafic tuff and tuffite (200 m)		
		Lower Basalt Mem.	Tholeiitic basalt with pillow and breccia structure (700 m)		
	Kolasjoki Sed. Fm.	Black Shale Mem.	Tuffitic carbonaceous sulphide-bearing siltstone (60 m)		
		Dolostone Mem.	Mn-rich dolostone, stromatolitic dolostone, dololite, subordinate limestone, jasper (50 m)		
		Red Bed Mem.	Red current-bedded polymict conglomerate, haematite-magnetite-rich gritstone, sandstone, muddy siltstone (150 m)		
	W E A T H E R I N G C R U S T				
		Basalt Mem.	Amygdaloidal sub-alkaline basalt, alkaline basalt, mugearite (500 m)		
	Kuetsjärvi Volc. Fm.	Trachyandesite Mem.	Amygdaloidal and columnar-jointed sub-alkaline basalt, alkaline basalt, basaltic andesite, andesite, mugearite (400 m)		
		Conglomerate Mem.	Red volcanoclastic conglomerate with volcanic bombs, volcanoclastic mudflow, siltstone with dolostone pebbles (80 m)		
Trachyandesite Mem.		Alkaline andesitic basalt, andesite, sub-alkaline andesitic dacite, mugearite and albitophyre with breccia structure (400 m)			
D I S C O N F O R M I T Y					
	Basalt Mem.	Amygdaloidal alkaline basalt, alkaline picrite (400 m)	2.21 Rb-Sr (1)		
Kuetsjärvi Sed. Fm.	Dolostone Mem.	Red and multicoloured dolostone, oncolithic dololite, ripple-marked dololite, dolomitic breccia and conglomerate (150 m)			
	Quartzite Mem.	Red and grey arkosic and quartzitic sandstone, ripple-marked siltstone, mudstone with ripple marks (100 m)			
W E A T H E R I N G C R U S T					
	Ahmalahki Volc. Fm.	Porphyritic and amygdaloidal sub-alkaline basalt, andesite, dacite, mafic and ultramafic tuff, greywacke sandstone (750 m)	2.32 Rb-Sr (1)		
	Neverskrukk Fm.	Basal polymict conglomerate, breccia, arkosic gritstone, sandstone (550 m)			
R E G O L I T H					
F I R S T - O R D E R U N C O N F O R M I T Y					
ARCHAEAN					

Age data are from: (1) Balashov et al. (1990); (2) Hanski (1992); (3) Hanski et al. (1990), (4) Mitrofanov et al. (1991). Radiometric ages are given in Ga.

and should be excluded from future geodynamic models.

The NPG, discordantly lying on Archaean basement, is composed of four major sedimentary-volcanic cycles (Zagorodny et al. 1964), each separated by a nondepositional unconformity generally marked by palaeoweathering (Melezhik & Sturt 1994), and each beginning with sedimentary rocks and ending with a thicker pile of mainly basaltic volcanic rocks. The cumulative stratigraphic thicknesses of the sedimentary and volcanic rocks are 1 000-1 600 m and 10 000-12 000 m, respectively. The NPG is divided into eight formations (previously known as 'subsuites', Zagorodny et al. 1964), which are, from oldest to youngest, the Neverskrukk (former Lower Ahmalahti Subsuites), Ahmalahti Volcanic, Kuetsjärvi, Kolasjoki and Pilgijärvi Sedimentary and Volcanic Formations (Table 1). The Pilgijärvi Sedimentary (other common name is the 'Productive' Formation, (e.g. Gorbunov 1968), hosts the Pechenga Ni-Cu deposits. The rocks have undergone zonal metamorphism from prehnite-pumpellyite to greenschist facies in the central part of the Pechenga and Pasvik portions of the belt to epidote-amphibolite facies towards the peripheral zones (Belyaev et al. 1977; Petrov & Voloshina 1995).

The lower age limit of the NPG is constrained by inclusions in the basal Neverskrukk conglomerates of pebbles (Bakushkin & Akhmedov 1975) of the  $2453 \pm 42$  Ma (Sm-Nd, Bakushkin et al. 1990) Mt. General'skaya layered gabbro-norite intrusion. The upper age limit of the NPG is younger than three ages obtained for rocks of the lower part of the Pilgijärvi Volcanic Formation:  $1990 \pm 66$  Ma old ferropicrites (Sm-Nd, Hanski et al. 1990);  $1970 \pm 5$  Ma old rhyolitic tuffs (U-Pb-zircon, Hanski et al. 1990); and  $1980 \pm 44$  Ma old tholeiitic basalts (Rb-Sr, Mitrofanov et al. 1991).

#### 4.1. North Pechenga Group

*The Neverskrukk Formation* is the basal formation of the NPG, lying unconformably on a sporadic Archaean regolith (Sturt et al. 1994) and comprising a base of immature closely packed, poorly sorted, framework-supported conglomerates which can be shown to have local sources. The boulder and pebble framework of the conglomerates generally is composed of Archaean plagioclase granites, plagioclase-microcline granites, gneisses and amphibolites. In the Mt. General'skaya area (Fig. 2) the formation also includes gabbro-norites derived

from the underlying layered intrusion (Bakushkin & Akhmedov 1975), and in Brattli it contains round to elliptical pebbles of Archaean iron formation (Siedlecka et al. 1985; Sturt et al. 1994).

The conglomerates become more matrix-supported in the upper part of the formation, giving way to grit- and sandstones. These are sub-aerial, cross-bedded to horizontally-bedded immature gritstones and sandstones, which are in turn overlain by tuffitic material and volcanic bombs.

The formation thickness ranges from 0 to 100 m, but is up to 250 m in palaeotectonic valleys (Predovsky et al. 1974) (Fig. 4). Alluvial channels and fans, in combination with shallow water ephemeral lakes are typical palaeoenvironments of the formation. At least two major NW-SE and NE-SW orientated rivers were active, recorded in thick fluvial deposits along two palaeovalleys (Melezhik 1992) (section 4 and 10, Fig. 4).

*The Ahmalahti Volcanic Formation* has a gradational contact with the underlying sedimentary formation and is composed of sub-aerially deposited amygdaloidal basalts, basaltic andesites and andesitic dacites (Predovsky et al. 1974). In eastern Pasvik, the lower part of the formation is locally represented by basalts and basaltic andesites with star-shaped glomerocrystic feldspar aggregates (Lieungh 1988). The upper part comprises mainly amygdaloidal sub-alkaline andesites with subordinate picritic lapilli tuff and thin lenses of volcanoclastic graywacke sandstones. The thickness of the formation is 50 to 1500 m (Fig. 4) and is controlled by transverse synvolcanic tectonic blocks, with the greatest thickness occurring in the north-west corner of the Western Rift Graben and in the Mt. General'skaya area within the Central Rift Graben (Fig. 3).

The formation consists of MgO-rich basalts and basaltic andesites (e.g. 51 wt% SiO<sub>2</sub>, 0.6 wt% TiO<sub>2</sub>, 10 wt% MgO), which were compared to komatiitic volcanics (Fedotov 1985). REE patterns of the volcanic rocks are characterized by weak enrichments in LREE (Fig. 5). Andesitic dacites located in the middle part of the formation have been dated at  $2330 \pm 38$  Ma (Rb-Sr, Balashov et al. 1991). An eruption centre exposed near Zapolyarny in the middle part of the formation contains numerous, partially melted and assimilated, basement-derived granite, granite-gneiss and



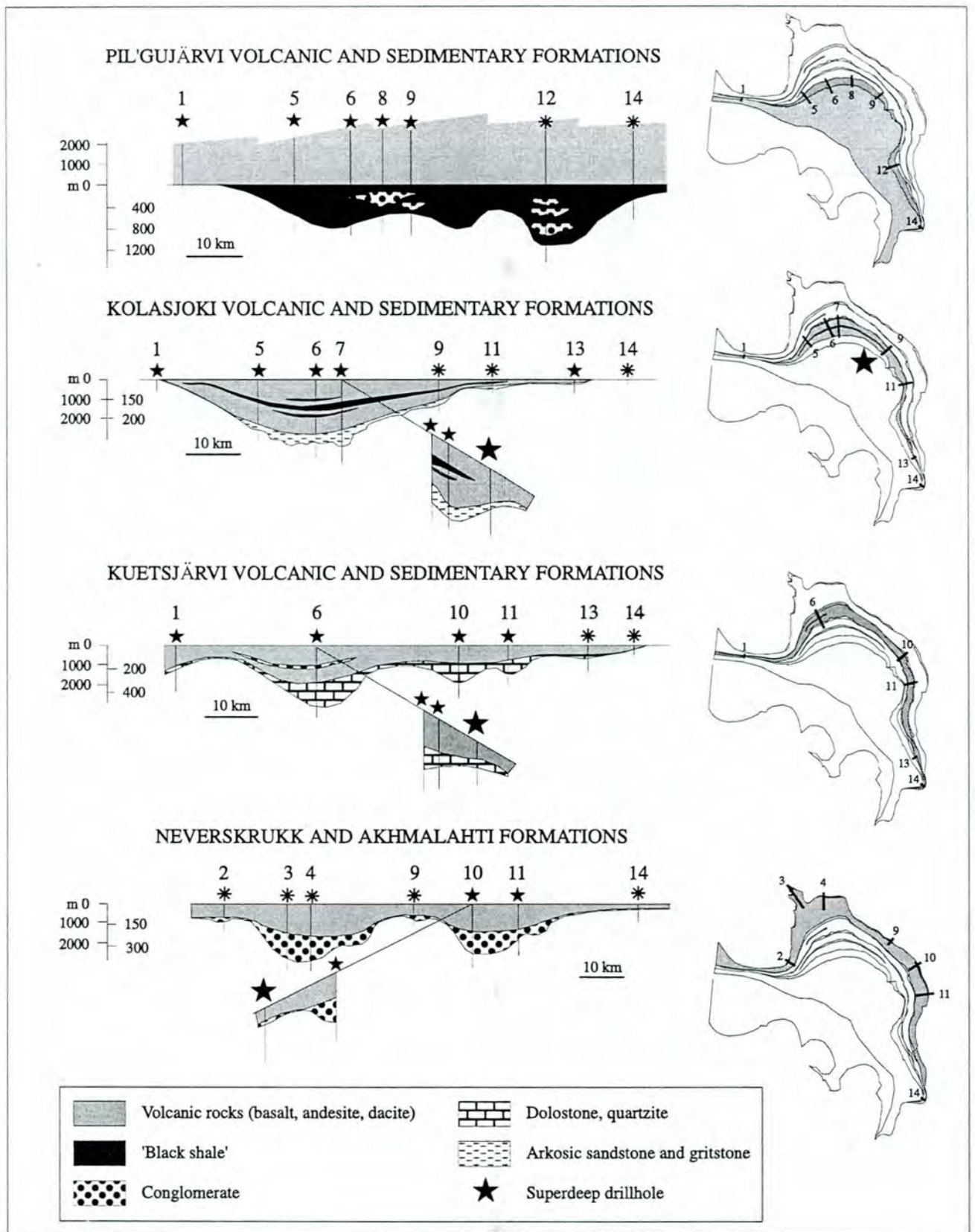


Fig. 4 Logitudinal sections illustrating thickness variations of sedimentary and volcanic formations of the Pechenga Belt.

Geographic location of sections: 1, Porojarvi; 2, Salmijarvi; 3, Bratli; 4, Piene Vohtastuni; 5, Nickel; 6, Kuvernerin-Luchlompolo-Souker; 7, 'Three Lakes'; 8, Kierdzhipori; 9, Zapolyarny; 10, Pechenga River; 11, Tul'javr; 12, Lammas; 13, Lake Gusinoe; 14, Kuchin. Note scale for volcanic rocks is on the left, for sedimentary rocks is on the right.



amphibolite fragments, suggesting the rift was underlain by continental crust at this time.

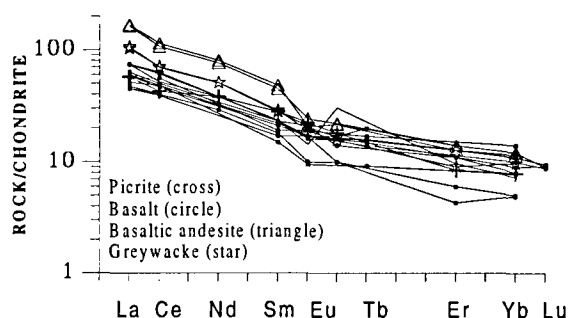


Fig. 5 Chondrite-normalized rare-earth element diagrams for Ahmalahti volcanites (Melezhik et al. 1994a).

The Akhmalahiti volcanic rocks do not show any features suggesting deposition in marine environments and are therefore considered to be a result of eruption and deposition in sub-aerial conditions (Predovsky et al. 1974), followed by local weathering, particularly in the Western and Central Rift Grabens.

**The Kuetsyarvi Sedimentary Formation** lies on weathered basalts of the Ahmalahti Volcanic Formation (Predovsky et al. 1974) and consists of basal current-bedded quartzitic gritstones to sandstones (*Quartzite Member*), overlain by red-coloured dolostones, dololutes, doloarenites, dolorudites, stromatolitic and oncolithic dolostones, and subordinate amounts of sedimentary dolomite breccia with tuff matrix (*Dolomite Member*). Ripple marks, mud cracks, syndepositional folds, sedimentary breccias, planar and small scale trough cross-bedding are typical features of these rocks. The formation thickness is 15 to 150 m (Fig. 4) and is strongly influenced by a number of transverse syndepositional faults (Melezhik 1992), with the greatest thicknesses observed in sections located within the Western and Central Rift Grabens (Fig. 3 and 4).

Kuetsjärvi terrigenous and carbonate sediments are enriched in LREE (Fig. 6), indicating a continental crustal source. The carbonate rocks

display unusually 'heavy' carbon isotopes, up to 10‰ (Karhu & Melezhik 1992; Melezhik & Fallick

1996). The palaeoenvironment of these deposits is interpreted to include either delta plains and lagoons (Predovsky et al. 1974) or delta plains and evaporitic, shallow water lakes resembling present-day East African Rift environments (Melezhik 1988).

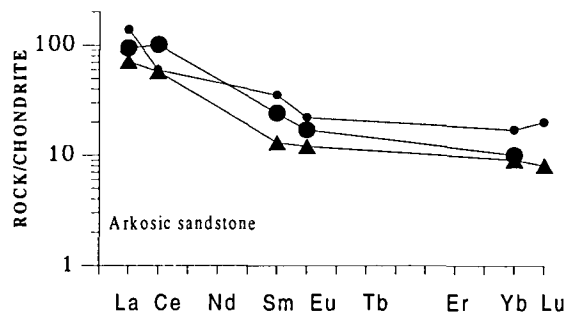


Fig. 6 Chondrite-normalized rare-earth element diagrams for Kuetsjärvi sandstones (Kozlovsky 1987).

**The Kuetsjärvi Volcanic Formation** has a gradational contact with underlying rocks. The lower part of the formation (*Orshoayvi Member*) comprises sub-aerial, amygdaloidal, magnetite- and haematite-bearing hawaiites trachybasalt, trachyandesite, mugearite and albitophyre with subordinate picrite (Predovsky et al. 1974): Acid volcanic rocks occur as thin flows, ignimbrites, flow-breccias and thinly-banded tuffs. Basic

volcanic rocks occur mainly as thin flows with occasional weathered flow-tops. Balashov et al. (1993) reported the Rb-Sr age for the Orshoayvi Member of  $2214 \pm 54$  Ma. The Orshoayvi Member is separated from the upper part of the formation by an irregular erosional surface and in the Western Rift Graben by a thin, volcanoclastic conglomerate-siltstone horizon capped with a 10 to 20 m thick either pillowed basalt flow or basalts with columnar joints (*Conglomerate Member*). The upper part (*Upper Basalt Member*) is represented mainly by sub-alkaline basalts with subordinate alkaline basalts and mugearites. Upper Member basalts are ubiquitously amygdaloidal and in places columnar, with palaeoweathering occurring on the surfaces of several flows, suggesting breaks in

deposition and emergence. The formation thickness varies from 50 m in Pasvik, to 2 000 m in the Western Rift Graben (Fig. 3 and 4). Variations in the thickness, facies and lithology of the volcanic rocks are controlled by syndepositional transversal faults. The Kuetsjärvi volcanic rock REE patterns are similar to those of the Ahmalahti volcanic rocks, but some alkaline rocks are slightly enriched in HREE (Fig. 7). The Kuetsyarvi volcanic rocks have high TiO<sub>2</sub> (1.4-3.0 wt%), Fe<sub>2</sub>O<sub>3</sub> (12.3-18.1 wt%), Na<sub>2</sub>O (3.0-5.4 wt%) and P<sub>2</sub>O<sub>5</sub> (0.2-0.4 wt%) contents compared to the Ahmalahti volcanic rocks (0.7-1.0 wt% TiO<sub>2</sub>, 9.3-13.0 wt% Fe<sub>2</sub>O<sub>3</sub>, 2.9-3.8 wt% Na<sub>2</sub>O, and 0.1-0.3 wt% P<sub>2</sub>O<sub>5</sub>) (Predovsky et al. 1974, 1987).

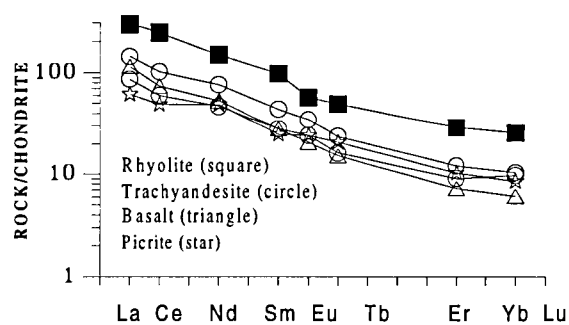


Fig. 7 Chondrite-normalized rare-earth element diagrams for Kuetsjärvi volcanites (Melezhik et al. 1994a).

Predovsky et al. (1987) described the Kuetsjärvi Volcanic Formation as a volcanic rock assemblage typical of intracontinental rift environments. The volcanic rocks were formed as a result of two stages of sub-aerial eruption and deposition, separated by a non-depositional break and by deposition of conglomerates and siltstones of the Conglomerate Member in ephemeral shallow water rift lakes.

**The Kolasjoki Sedimentary Formation** overlies an irregular palaeosurface which is cut by a number of palaeovalleys. At several localities near Luchlompolo the Kuetsjärvi volcanites immediately adjacent to the Kolasjoki show signs of subaerial weathering (Predovsky et al. 1974).

The weathered rocks, represented by altered 'patchy', black-and pink basalts, were only preserved in the palaeotopographic heights and were entirely removed by pre-Kolasjoki erosion in the palaeovalleys. The lower part of the formation comprises numerous current-bedded sand channels and red arkosic gritstones. The middle part is represented by coarse-grained, red, hematite-rich, arkosic gritstones and sandstones, and by sand- and gritstones with frameworks of quartz amygdules. The lower and middle parts are collectively named

the *Red Bed Member*. The upper part (*Dolomite Member*) consists mainly of red-coloured, Ba- and Mn-enriched (both up to 2 wt%) dolomites intercalated with and in the eastern Pechenga, dominated by, jasper. The uppermost part of the formation (*Black Shale Member*) is represented by organic carbon (C<sub>org</sub>)- and sulphur (S)-bearing siltstones and basaltic and picritic tuffs. The contact between the Dolomite and Black Shale Members is usually tectonic. The total formation thickness varies from 0 to 150 m in the Western Rift Graben (Fig. 3 and 4) and is controlled by palaeotopography and numerous transversal, syndepositional, regional- to small-scale faults (Melezhik 1992).

The Kolasjoki sediments contain clastic material derived exclusively from the underlying Kuetsyarvi volcanic rocks. In places the Red Bed Member contains 5 to 10 m thick sandstone to gritstone layers, composed of 80 to 90 % well-rounded quartz grains resembling quartz amygdules, implying deep erosion down to the amygdaloidal Ahmalahti volcanic rocks. Many of the Red Bed Member sediments were deposited within a number of narrow alluvial palaeovalleys (Predovsky et al. 1974) whose walls extended up to 50-100 m (Melezhik 1992).

The palaeoenvironment has been interpreted both as alluvial channels and fan delta deposits combined with other lagoon deposits palaeovalleys (Predovsky et al. 1974), and as a number of isolated, highly saline, shallow water evaporitic lakes within an intracontinental rift valleys (Melezhik 1987, 1992).

**The Kolasjoki Volcanic Formation** locally has a tectonised contact with the underlying sediments. The rocks are mainly tholeiitic basalts with subordinate Fe<sub>2</sub>O<sub>3</sub><sub>tot</sub>- and TiO<sub>2</sub>-enriched picrites (15.2 and 1.5 wt%, respectively), occurring as pillowed and massive basalt flows, flow breccias and hyaloclastites (Predovsky et al. 1974, 1987). A Rb-Sr age determination on tholeiites yielded 2114±52 Ma (Balashov et al. 1991). The volcanic succession is intruded by numerous gabbro sills which expose either massive or columnar appearance. REE patterns are flat but slightly LREE-enriched (Fig. 8). On the basis of bulk composition and the dominance of pillow basalt, the Kolasjoki tholeiites are considered to be intercontinental rift, submarine volcanic deposits (Predovsky et al. 1987).

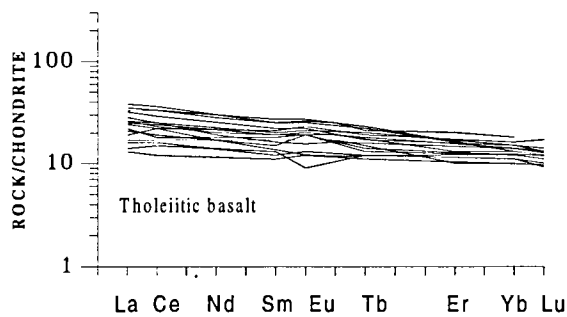


Fig. 8 Chondrite-normalized rare-earth element diagrams for Kolasjoki volcanites (Kremenetsky & Ovchinnikov 1986; Melezhik et al. 1994a).

A 50 to 150 m thick black shale horizon (*Black Shale Member*), thickest in the Western Rift Graben, divides the Kolasjoki volcanic pile into the *Lower* and *Upper Basalt Members*. This horizon is composed of S- and C<sub>org</sub>-bearing, thinly laminated, fine-grained graywacke sandstones and siltstones interbedded with basaltic tuffs, limestones and microfossil-bearing cherts. REE patterns for siltstones of the Black Shale Member (Fig. 9) are the same as those of the Kuetsyarvi sediments and thus reflect a similar type of continental crustal source.

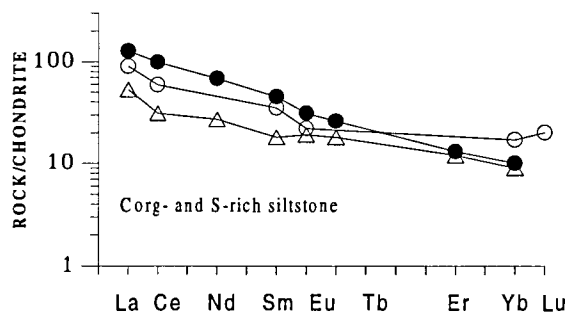


Fig. 9 Chondrite-normalized rare-earth element diagrams for Kolasjoki 'black shales' (Melezhik et al. 1994a).

Interpretations of the depositional environment of the black shales range from an oceanic, deep water trench (Negruzta 1984) or a lagoon (Predovsky et al. 1987) to a moderately deep water lake within an intercontinental rift (Melezhik 1992).

The Kolasjoki Volcanic Formation is absent in the eastern part of the Pechenga Zone, but attains a thickness of 2 000 m in the Western Rift Graben (Fig. 3 and 4). This implies that the two faults bounding the Western Rift Graben remained active during Kolasjoki deposition, causing the graben to deepen significantly. If a deep water trench (Negruzta 1984) existed at this time, it likely occurred within the Western Rift Graben. However,

the presence of photosynthesizing blue-green algae within the Black Shale Member (Melezhik et al. 1992), reflected by the microfossil-bearing cherts, precludes such a deep water environment (unless Proterozoic deep-water cyanobacteria have not yet been recognised).

*The Pilgujärvi Sedimentary Formation*, also known as the '*Productive Formation*', is the thickest sedimentary unit of the Pechenga Group. The total thickness generally is 600 to 800 m, but decreases to zero near the Russian-Norwegian and Norwegian-Finnish borders and rises to 1 000 m in the Western and Eastern Rift Grabens (Melezhik et al. 1988, Fig. 3 and 4). The sedimentary and sedimentary-volcanic rocks of the 'Productive' Formation are the host rocks for all the ultramafic intrusions and flows with economically interesting sulphide Ni-Cu deposits. This gives the 'Productive' Formation rocks a key position for the understanding of the ore-forming processes. The sedimentary succession is intruded by numerous gabbro sills.

The formation consists of three members: A, B and the 'Upper' or Lammas Members. *Member A* consists of C<sub>org</sub>- and S-bearing, horizontally laminated, arkosic and graywacke sandstones and siltstones with subordinate polymictic conglomerate lenses. *Member B* is dominated by black, highly carbonaceous and sulphidic graywacke and Bouma cycle rhythmites (Akhmedov & Krupenik 1990) interbedded with basaltic tuffs. Typical features of *Member B* are finely laminated rhythmites with pyritic layers and concretions, current-bedded sediments and symsedimentary folded and eroded layers. Also characteristic are sedimentary breccias and dikes, and abundant diagenetic carbonate layers and lenses (Melezhik & Abzalov 1989). These lithologies have been interpreted in many ways: a shallow water marine environment (Predovsky et al. 1974); a moderately deep- and fresh-water lake environment within a seismically active intercontinental rift system (Melezhik 1987; Melezhik et al. 1988) with short-lived embryonic 'black smokers' (Melezhik 1992); an oceanic, deep-water (3 000 to 5 000 m) trench (Negruzta 1984); and a deep-water oceanic continental slope environment (Akhmedov & Krupenik 1990). REE patterns for *Member B* of the Productive Formation (Fig. 10) are similar to those of the Kuetsjärvi and Kolasjoki sediments (Fig. 6, 9), suggesting that sediment was still continentally derived during the deposition of the Productive Formation.

The Lammas Member is represented by ferropicritic tuffs and tuffites with pyrite and



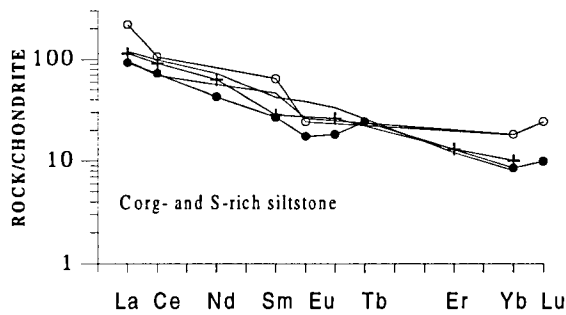


Fig. 10 Chondrite-normalized rare-earth element diagrams for Pilgularvi 'black shales' (Melezhik et al. 1994a).

carbonate nodules. The thickest section occurs in the Eastern Rift Graben, where it consists of mainly ferropicritic tuffites and occupies about 75 percent of the thickness of the Productive Formation (Predovsky et al. 1974). Two alluvial fan systems are developed near Kierdzhipori in the Western Rift Graben (Fig. 4, section 8) and Lammas in the Eastern Rift Graben (Fig. 4, section 12). The Kierdzhipori system comprises phosphorous-bearing (up to 5 wt%  $P_2O_5$ ), polymictic, current-bedded, fine-grained arkosic conglomerates, gritstones and sandstones. The Lammas fan is dominated by matrix-supported conglomerates. Pebbles and some large (up to 2 m) granite boulders of probable Archaean provenance lie in the graywacke and Productive Formation ferropicritic tuffitic matrix. Both fan systems are interpreted either as long-lived palaeoalluvial fans (Melezhik et al. 1988) or submarine slope slides (Akhmedov & Krupenik 1990).

**The Pilgularvi Volcanic Formation** has a gradational contact with the Productive Formation. The volcanic formation is dominated by tholeiitic basalts occurring as pillowed and massive flows, flow breccias and tuffs, with subordinate amounts of ferropicritic and acidic volcanic rocks (Zagorodny et al. 1964; Predovsky et al. 1974). The formation can be informally divided into six members (Melezhik et al. 1995). The succession starts with the *Basalt-Pycrite Member*, a 750 m thick unit of massive tholeiitic basalts interbedded with a number of ferropicritic flows. The *Lower Basalt Member* is a 600 m thick pile of tholeiitic basalts both massive and pillowed. It is overlain by the *Rhyolite Member* which is ca. 500 m thick horizon of rhyolite, dacite and andesite tuffs and flows alternating with tholeiitic lavas. This rock assemblage is developed in the Western and Central Rift Grabens (Fig. 3). The *Middle Basalt Member* is 500 m thick and is dominated by massive and pillowed tholeiitic basalts with a subordinate amount of basic tuffs. The *Upper Basalt Member*, also 800 m thick,

consists of massive and pillowed tholeiitic basalts intercalated with basaltic tuff and volcanoclastic sediments. The formation ends with the *Suppavaara Member* consists of predominantly tholeiitic pillowed lavas. The proportions of different volcanic rocks in each member are indicated in Table 2. The total formation thickness exceeds 3 000 m in the Western Rift Block, decreasing to 1 000 m to the east and west (Fig. 4).

Table 2. Volume percentages of various volcanic rocks in different members of the Pilgularvi Volcanic Formation (Rusanov 1981).

Member*	1	2	3	4	5	6
Massive and layered ferropicritic lavas	7	-	2	-	3	-
Ferropicritic pillow lavas	3	-	1	-	2	-
Ferropicritic tuffs	1	-	1	-	1	-
Massive tholeiitic lavas	60	47	50	57	45	28
Tholeiitic pillow lavas	5	50	30	40	40	70
Fine-grained basic tuffs	20	3	3	3	2	2
Medium- to coarse-grained basic and andesite tuffs	5	-	5	-	8	-
Dacite and dacite-liparite porphyrites	-	-	5	-	-	-
Felsic tuffs	-	-	3	-	-	-

The members are named according to Melezhik et al. (1995): 1-Basalt-Pycrite Member, 2-Lower Basalt Member, 3-Rhyolite Member, 4-Middle Basalt Member, 5-Upper Basalt Member, 5-Suppavaara Member.

Gabbro and gabbro-dolerite sills are most voluminous within the Pilgularvi Volcanic Formations. Major volume of gabbro and gabbro-dolerite sills are observed within both the Western Rift Block and Central Rift Block.

All mafic volcanic rocks of the Pilgularvi Volcanic Formation are enriched in  $TiO_2$  (1.8-2.2 wt%) and  $Fe_2O_3$  (14.1-18.7 wt%) and are classified as intercontinental rift volcanic rocks (Predovsky et al. 1987). REE patterns of the Basalt-Picrite Member are close to NMORB ( $La/Yb$ )<sub>N</sub>=1.0, Fig. 11a. The Lower Member basalts are characterized by a weak enrichment in LREE ( $La/Yb$ )<sub>N</sub>=1.2, Fig. 11b, while those of the Suppavaara Member are enriched in LREE ( $La/Yb$ )<sub>N</sub>=1.8, Fig. 11c. These data suggest that the Pilgularvi volcanic magma source was continually evolving, culminating in the production

of Upper Basalts with distinct continental characteristics.

REE patterns of the ferropicrites (Fig. 12a, b, c), gabbro-wehrlite bodies (Fig. 12b) and acidic volcanic rocks (Fig. 12d) are similar to each other, but are significantly different from those of the tholeiites (Fig. 11a, b, c).

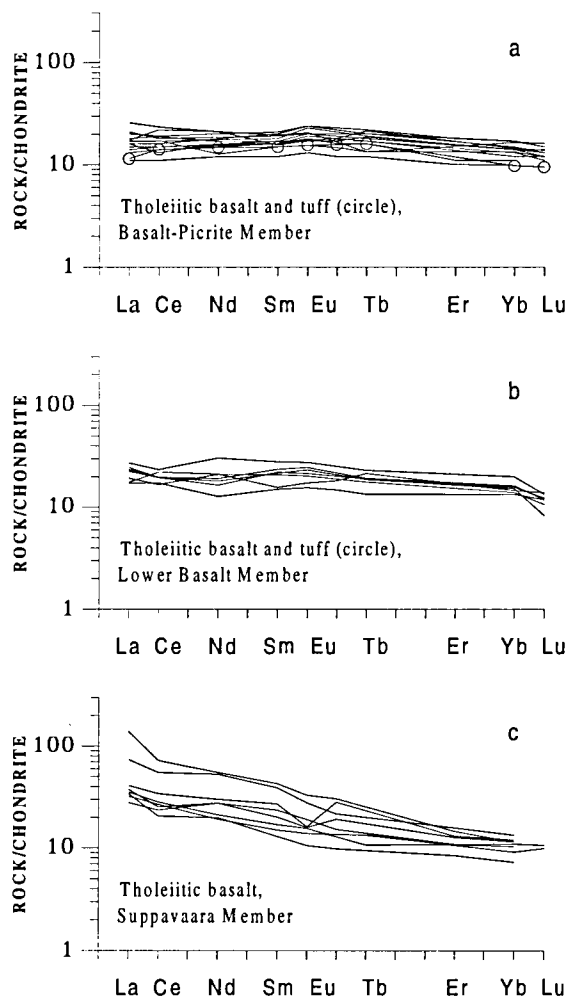


Fig. 11 Chondrite-normalized rare-earth element diagrams for Pilgūjärvi basalts (a-Kremenetsky & Ovchinnikov 1986; b, c-Melezhik et al. 1994a).

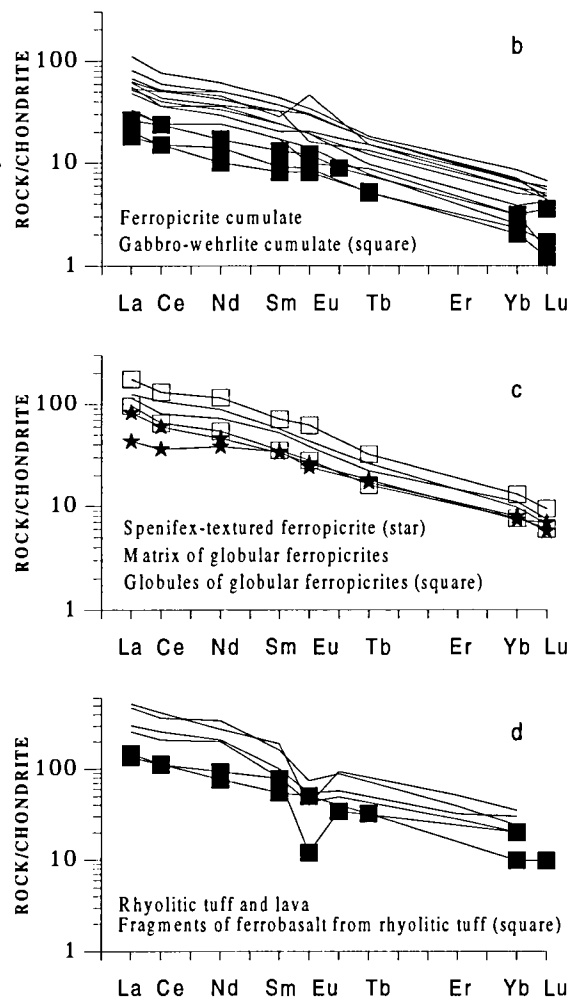
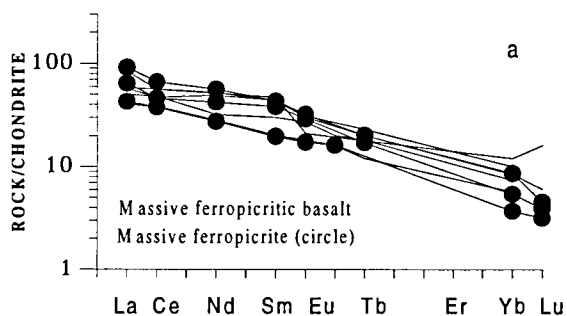


Fig. 12 Chondrite-normalized rare-earth element diagrams for Pilgūjärvi ferropicrites and gabbro-wehrlites (a, b-Hanski & Smol'kin 1989; Melezhik et al. 1994a; c-Hanski & Smol'kin 1989; d-Melezhik et al. 1994a).

#### 4.2. South Pechenga Group

The South Pechenga Group (SPG) has an approximate tectonostratigraphic thickness of 6000 m (Predovsky et al. 1974) and occurs entirely within the Southern (structural) Zone of the Pechenga-Pasvik Belt. The SPG generally is in fault contact with the NPG in the north, and is overthrust by an Archaean complex containing a number of the early Proterozoic granodiorite intrusions (Plate 1). According to the geotectonic model presented in Melezhik & Sturt (1994), the succession of the SPG is tectonostratigraphy rather than stratigraphy. From north to south, the SPG is composed of the following major formations or lithological units: the Kallojavr, Bragino, Mennel', Kaplya, Kasesjoki, Tal'ya and Lake Pestchanoe Formations (Ansemjoki tholeiitic basalts). Contact relationships between the formations are not well understood. The rocks are generally

metamorphosed under greenschist facies conditions, with the degree of metamorphism reaching amphibolite facies along the southern thrust contact and in the eastern flank of the Southern Zone (Belyaev et al. 1977; Petrov & Voloshina 1995). The five SPG formations, which we adapted from the previous study (Zagorodny et al. 1964; Predovsky et al. 1974) are as follows: the Kallajavr, Bragino, Mennel', Kaplya and Kasesjoki formations. We added three extra formations to the SPG for the same reasons as in Melezhik et al. (1994a). These are the Fagermo, Tal'ya and the Lake Pestchanoe formations (Ansemjoki basalts).

Apart from the dubious stratigraphy of the SPG, the relationship between the latter and NPG is not fully resolved (Zagorodny et al. 1964). Predovsky et al. (1974) considered the SPG to be younger than the NPG, although the SPG 'black shales' (Kallajavr Formation) (Plate 1) and the Productive Formation 'black shales' were thought to have formed synchronously though in different tectonic environments and from essentially different sources (Golubev et al. 1984; Melezhik et al. 1988). In other words, it was considered that the 'black shales' of the SPG are the stratigraphic equivalent of the rocks of the Productive Formation. Galdobina & Melezhik (1986), however, considered that the Ansemjoki tholeiitic basalts (Lake Pestchanoe Formation) (Plate 1) could be the stratigraphic equivalents of the Pilgujärvi tholeiites. The latter interpretation implies tectonic imbrication of the SPG (Melezhik & Sturt 1994).

The stratigraphic equivalent of the SPG of the Pechenga Belt at Pasvik is the Langvannet Group. This group is poorly exposed and little studied. Although all the lithology of the South Pechenga Group from the Pechenga Belt has been identified among the rocks of the Langvannet Group, their geological boundaries can not be yet drawn on the map. Therefore, all the lithologies are included in the undivided Langevannet Group. At this stage only the Fagermo Formation of the Langevannet Group can be separately shown on the map as its content and boundaries are well studied.

The radiometric age of the SPG has not been fully constrained. Balashov et al. (1991) obtained a Rb-Sr isochron age of  $1855 \pm 54$  Ma (Rb-Sr) on andesites of the Kaplya Formation and  $1865 \pm 58$  Ma (Rb-Sr) on picrites of the Bragino Formation. The youngest, but probably not reliable, reported SPG age is  $1729 \pm 35$  Ma (Rb-Sr, Balashov et al. 1991) for subvolcanic bodies of andesitic composition which are intruded along the Poritash Fault (Fig. 1, Plate. 1). The Litza-Araguba granites, considered to represent the latest magmatic event associated with

the Pechenga-Pasvik Belt, have been dated at  $1810 \pm 50$  Ma (U-Pb-zircon, Pushkarev et al 1978).

For the full lithological and geochemical description of all seven formations of SPG we refer to Predovsky et al. (1974), Melezhik et al. (1994a) and Mitrofanov & Smol'kin et al. (1995)

The seven SPG formations are described below, from oldest to youngest.

**The Kollajavr Formation** is generally separated from the Pilgujärvi Volcanic Formation by the Poritash Fault (Fig. 2) but the contact has not been fully investigated. The Formation comprises quartz-sericite-plagioclase siltstone and carbonate rhythmites, collectively named 'black shales', which are often highly enriched in S and  $C_{org}$  (up to 15 wt%). These rocks carry abundant, thin lenses of  $C_{org}$ - and S-rich chert. The Kollayavr black shales are entirely different from those of the NPG Productive Formation in that they are derived from andesites (Melezhik et al. 1988). The formational thickness is ca. 400-1,200 m (Predovsky et al. 1974).

**The Bragino Formation**, up to 2,300 m thick, consists of tuffs and lava flows of andesites, high-Mg andesites, basalts, microbasalts and picrites. The formation is poorly defined and apparently represents the rocks of different formations which are arranged as a number of small-scale plates overthrusting one above other.

**The Mennel' Formations**, up to 1,300 m thick, consists of picritic pillowed flows, flow-breccias and lapilli tuffs with subordinate picritic volcanoclastic rocks. Near Lake Bragino, the eastern flank of the South Zone, the picrites form a palaeovolcano where they occur as a complex assemblage of pillowed and massive picritic flows and flow-breccias with interbedded picritic conglomerates and gritstones. This palaeovolcano was probably coeval with the Porojarvi andesites, producing laterally interfingering andesitic and picritic volcanites (Melezhik et al. 1994a).

The high Ti contents (average 1.5 wt%) of the picrites (Predovsky et al. 1974, 1987) have been attributed to magmatism in an extensional environment (Predovsky et al. 1974, 1987; Hanski & Smol'kin 1989) such as a continental rift system, craton or collisional zone, but not an oceanic or plate margin setting (Condie 1989). REE patterns in the Mennel' Formation (Fig. 13a and 13b) are both flatter and less LREE-enriched than those of the Bragino andesites, suggesting that the coeval andesites and picrites have significantly different

sources. One explanation could be that the two rock types were tectonically emplaced, suggesting the overlap of an intercontinental rift with an arc system.

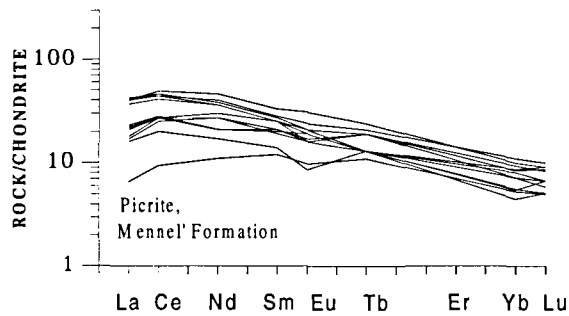


Fig. 13 Chondrite-normalized rare-earth element diagrams for Mennel' picrites (Melezhik et al. 1994a).

**The Fagermo Formation** consists of a complex assemblage of pillowed and massive picritic flows and flow-breccias with interbedded picritic conglomerate, graded,  $C_{org}$ -bearing sandstones, siltstones and mudstones and minor basaltic flows with a total thickness of 500 m. The picritic lavas are represented by Ti-rich ultramafic rocks consisting of serpentine, talc, tremolite and clinopyroxene. This picritic rock assemblage alternates and interfingers with andesitic volcanoclastic sediments and subordinate basalts. The Fagermo Formation is a stratigraphic equivalent of the Mennel' Formation of the Pechenga Belt. The reason that they are named differently is that both represent a local development and are separated by a 20 km gap (Plate 1).

**The Kaplya Formation** forms a volcanic pile with a thickness ranging from ca. 300 to 2 300 m. The formation is characterised by massive andesitic flows and banded tuffs with subordinate amounts of andesitic volcanoclastic sediments (Predovsky et al. 1974) and porphyritic syenites (Melezhik et al. 1994a). Near Lake Poroyarvi, the andesites form a palaeovolcano where they occur as andesitic flow breccias, volcanic agglomerates and tuffs, and rock assemblages that are typical of hot and cold lahars.

The rocks range in composition from Mg-rich andesites (53.1 wt%  $SiO_2$ , 8.5 wt% MgO) to Mg-rich basaltic andesites (50.0 wt%  $SiO_2$ , 12.4 wt% MgO, Skuf'in et al. 1988), reminiscent of the modern boninitic volcanic series (Hickey & Frey 1982). However, some of the andesites are Al-rich (up to 17.3 wt%  $Al_2O_3$ ) and their REE patterns are significantly different from those of real boninites (Fig. 14a, b, c and d). Boninites usually have a 'dish'-shaped (upward concave) chondrite-

normalised REE pattern with overall REE abundances around 2 to 10 times those of average chondrite (Hickey & Frey 1982). In this case, this characteristic pattern is not present.

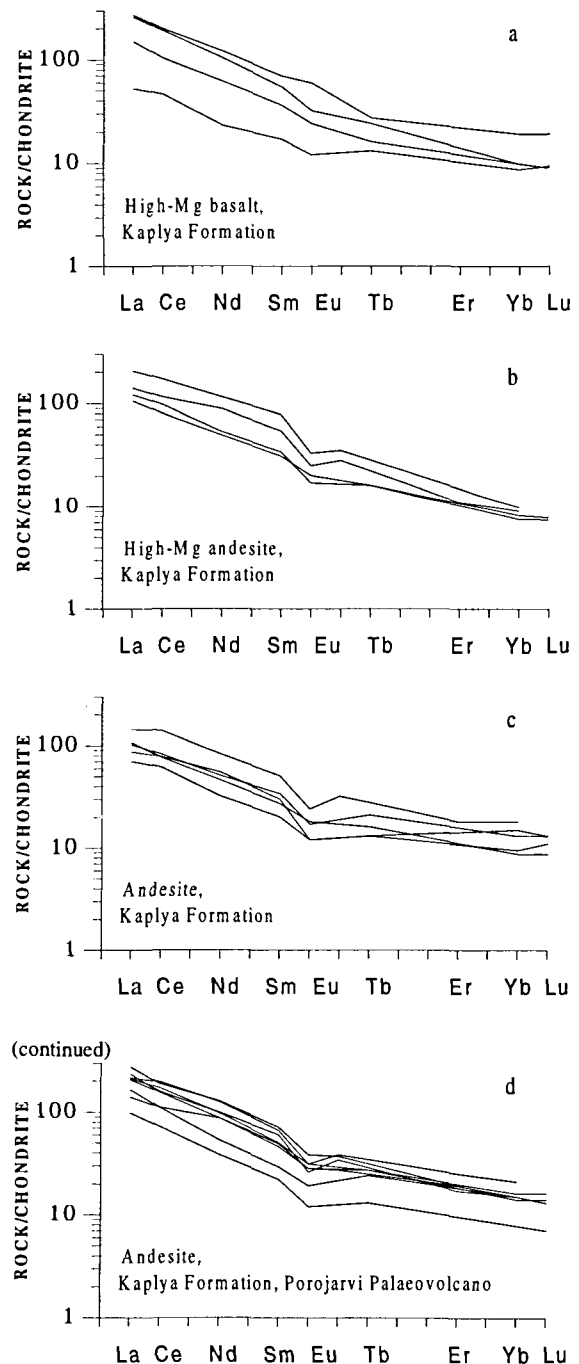


Fig. 14 Chondrite-normalized rare-earth element diagrams for high-Mg basalts (a), high-Mg andesites (b) and andesites (c) of the Kaplya Formation; and for andesites of the Poroyarvi Palaeovolcano (d) (Melezhik et al. 1994a).

Porphyritic syenites, with distinctly different REE patterns (Fig. 15) from those of the andesites (Fig. 14d), also are sporadically developed.



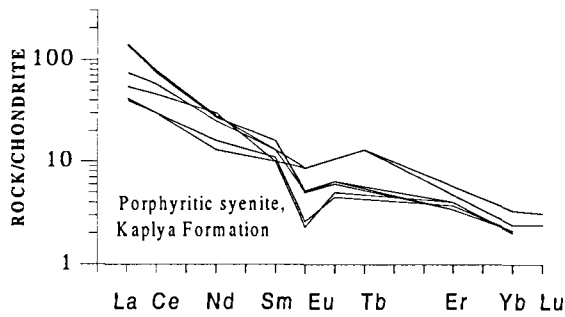


Fig. 15 Chondrite-normalized rare-earth element diagrams for porphyritic andesites of the Kaplya (Melezhik et al. 1994a).

The Kaplya andesites are described as typical orogenic association rocks (Predovsky et al. 1974, 1987; Skuf'in et al. 1988).

**The Kasesjoki Formation** is 1 000 to 3 000 m thick and is represented by andesitic volcanoclastic sediments with sporadic, 10 to 50 m thick conglomerate layers at the base and rhythmic-bedded sandstones and siltstones with subordinate basalts in the middle and upper parts. The conglomerates contain iron-quartzite pebbles and numerous andesite pebbles which bear pre-pebble tectono-metamorphic fabrics, implying that the Kaplya andesites were subjected to deformation and metamorphism probably related to a compressional orogenic event (Melezhik et al. 1991) prior to uplift and erosion.

**The Tal'ya Formation** is probably the youngest formation of the SPG. In the north, the formation has a normal stratigraphic contact with the Kasesyoki Formation. In the south, the formation is overthrust by an Archaean granite-gneiss complex that is penetrated by a number of granite, granodiorite and diorite intrusions, including the  $1810 \pm 50$  Ma (Pushkarev et al. 1978) Litza-Araguba granites (Plate 1). The 100 to 1 000-1 500 m thick Tal'ya Formation is represented mainly by highly metamorphosed, horizontally bedded, andesitic volcanoclastic sandstones. REE patterns (Fig. 16) are similar to those of the Kaplya andesites (Fig. 14b, c and d).

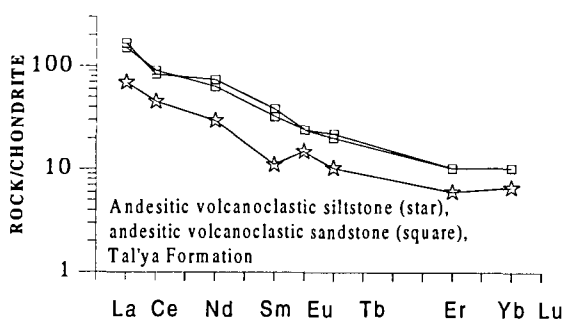


Fig. 16 Chondrite-normalized rare-earth element diagrams for andesitic volcanoclastic sediments of the Tal'ya Formation (Melezhik et al. 1994a)

**The Lake Pestchanoe (Ansemjoki) Formation**, mapped as pillow basalts of the South Pechenga Group (Plate 1), comprises pillow and amygdaloidal tholeiitic basalts and has a problematic stratigraphic position. The formation comprises an 800 m pile of pillow basalts occurring in the eastern flank of the South Zone at Lake Pestchanoe. On the basis of similar bulk compositions and REE patterns (Fig. 17), the Lake Pestchanoe Formation basalts can probably be correlated with the Pilgijärvi Volcanic Formation tholeiites (Fig. 11a, b, c).

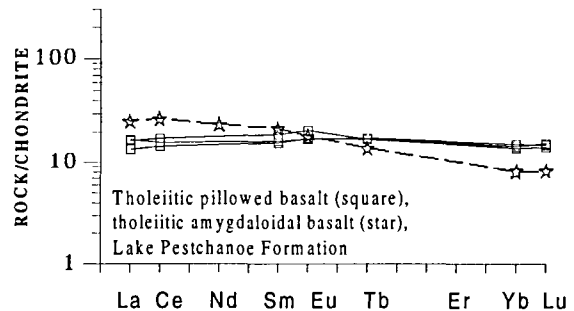


Fig. 17 Chondrite-normalized rare-earth element diagrams for basalts of the Lake Pestchanoe Formation (Melezhik et al. 1994a).

### 3. Position of intrusive rocks in the stratigraphic subdivisions of the Petsamo Supergroup

In the last few decades a substantial amount of different intrusive rocks types were recognised and mapped in the Pechenga-Pasvik Greenstone Belt. Although numerous sills and intrusions are shown on the map (Plate 1), only gabbro-wehrlite intrusions and ferropicritic sills were studied in detail (e.g. Predovsky et al. 1971; Zak et al. 1982; Hanski 1992; Smol'kin 1992). Table 3 intends to systematise all early Proterozoic intrusive rocks in a time scale showing the stratigraphic subdivisions of the Petsamo Supergroup. Positions of the gabbro-wehrlite intrusions and the Poritash sub-volcanic bodies as well as the undivided gabbro sills coeval with the Ahmalahti, Kuetsjärvi, Kolasjoki and Pilgijärvi formations, are indicated on the attached geological map (Plate 1). The Shuonijavr and Kaskeljavr granodiorites can be also seen on the map as the large sub-circular bodies south of the Pechenga Greenstone Belt. The western intrusion is called Shuonijavr, and the eastern one is Kaskeljavr. A considerable outcropping of the Litza-Araguba granites commences ca. 6 km east of the south-eastern flank of the Pechenga Greenstone Belt. It is represented by a small spot in the southeastern corner of the map. The main

development is further to the east, off the map, as the largest Early Proterozoic granite intrusions in the Kola region. The gabbro and gabbro-pyroxenites, sub-volcanic porphyritic picrites and andesitic dacites are not shown on the map as they developed as a number of very small bodies within the South Pechenga Group. The sub-volcanic porphyritic picrites intrude the Mennel' Formation, whilst sub-volcanic andesitic dacites were placed among the rocks of the Bragino Formation. The gabbro and gabbro-pyroxenites are less well developed and can be found within different formations of the South Pechenga Group. The Nyasyukka gabbro-pyroxenites developed as a dyke swarm ca. 8-10 km northeast of the northeast flank of the Pechenga Greenstone Belt. The largest dyke from this swarm is approximately 28 km long and 200 m wide. The Nyasyukka dykes are considered coeval at 2.00 Ga and comagmatic with the gabbro-wehrlites and ferropicrites of the Pechenga Greenstone Belt. Gabbro and gabbro-dolerite sills are most voluminous within the WRG when they occur in the Kolasjoki Volcanic and Pilgijärvi Sedimentary Formations. The Pilgijärvi Volcanic Formations contain major volume of gabbro and gabbro-dolerite sills within both the WRG and CRG.

Thus, the Early Proterozoic magmatic activity resulted in a series of intrusions which were placed within the Pasvik-Pechenga Belt. Their relationship with lithostratigraphical subdivision of the Petsamo Supergroup is shown in Table 3.

#### 4. Palaeoenvironment and history of development

The palaeotectonic evolution of the Pechenga-Pasvik Rift Zone has been the subject of many scientific discussions. Many authors (Barbey et al. 1984; Hanski & Smol'kin 1989; Melezhik 1988; Negrutza 1984; Predovsky et al. 1987; Sharkov 1984) favour an intercontinental rift model. Berthelsen and Marker (1986) have suggested a model involving continental rifting, subsequent ocean-floor subduction and arc-continent collision. Pharaoh et al. (1987) have proposed that the Pechenga-Pasvik Zone was developed in a mature continental volcanic arc. Smol'kin et al. (1995) has developed a model involving a complex cycle of evolution: arc formation-rifting-orogeny.

Based on the reviewed literature and the results of the international research in the Pechenga area (eg. Marker 1985; Hanski 1992; Melezhik et al. 1994a, 1994b; Sturt et al. 1994; Brewer & Daly 1994) we propose below a five-stage rift model for the

Pasvik-Pechenga Belt as based on Melezhik et al. (1994a) and Melezhik & Sturt (1994). The five stages of development are (Table 4): (i) an intracontinental rift stage (2450-2330 Ma), comparable with the present-day Afar Triangle and East African rifts; (ii) a rift inversion and a transitional stage from an intracontinental to an intercontinental rift environments (2330-2000 Ma); (iii) an intercontinental rift-aborted oceanic rift stage (2000-1970 Ma), comparable with the present-day Red Sea Rift System; (iv) a subduction related rift stage (ca. 1970-1870 Ma); (v) a collision related rift (1870 -1800? Ma).

#### **Intracontinental Rift Stage (2450-2330 Ma).**

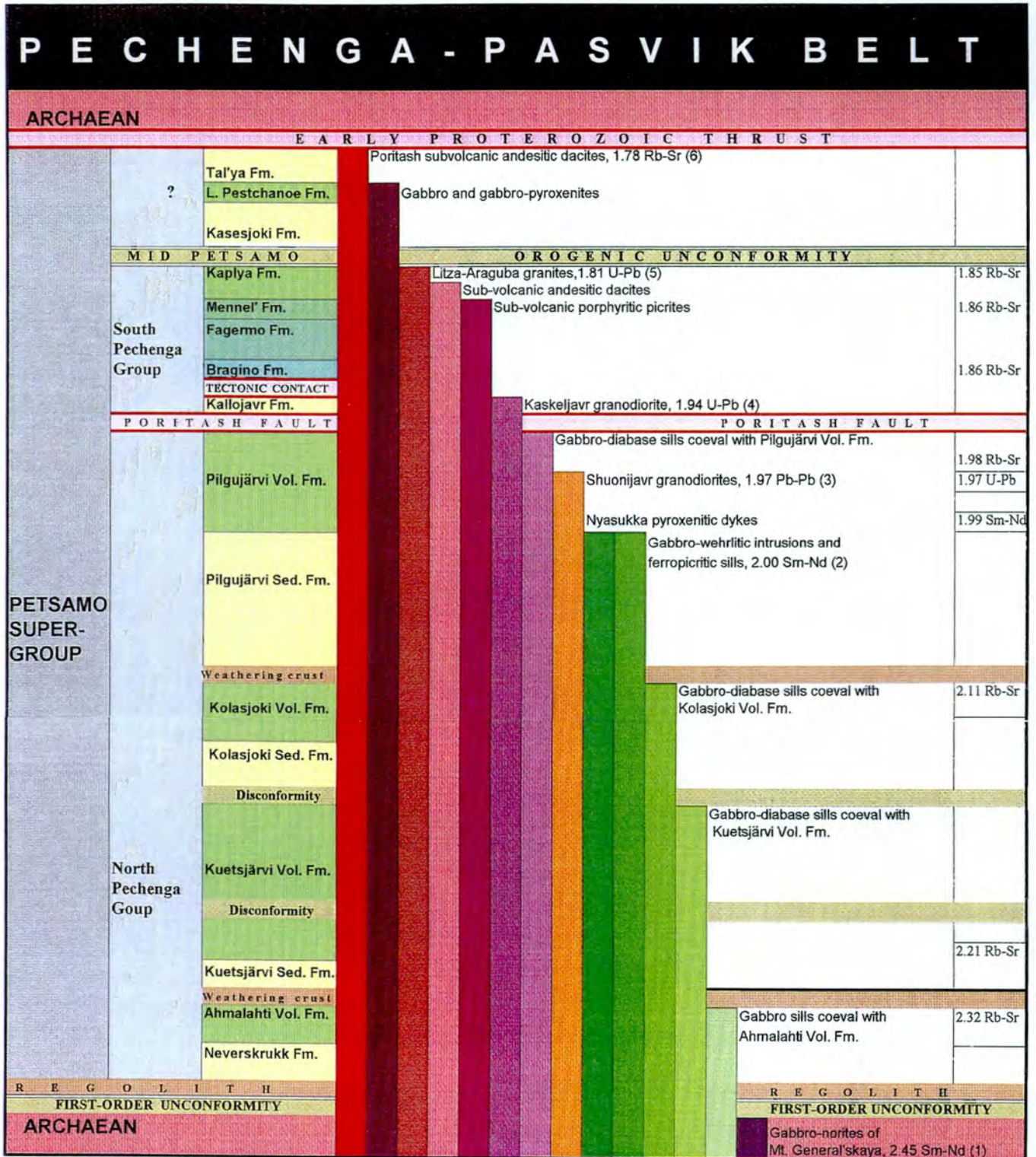
The main evidence of the initial stages of Early Proterozoic rifting on the Kola Peninsula is the chain of 2450 Ma-old layered gabbro-norite intrusions developed along the northern margin of the eastern part of the Polmak-Opukasjarvi-Pasvik-Pechenga-Imandra/Varzuga-Ust'Ponoy Greenstone Belt (Melezhik & Sturt 1994). After 2450 Ma, the Pechenga-Pasvik area was affected by continuous uplift, recorded by inclusions of Mt. General'skaya gabbro-norite pebbles in the basal North Pechenga Group Neverskrukk conglomerates (Fig. 18).

A combination of longitudinal and transverse fault systems controlled the development of the Pechenga-Pasvik rift and produced a half-graben configuration. The main Pechenga half-graben was separated by a number of long-lived, transverse, syndepositional faults into three main sub-grabens: the Western, Central and Eastern Rift Grabens. These grabens controlled the lithology, facies and thicknesses of sedimentary and volcanic rocks deposited within their respective basins.

The first rift sediments (Neverskrukk) were fluvial conglomerates and lacustrine grit- to sandstones in the Western and Central Graben. The first volcanic processes occurred earlier than 2330 Ma ago, and eventually produced Ahmalahti sub-aerial basaltic to dacitic volcanic rocks with crustal signatures. This sedimentary-volcanic cycle was subjected to surface weathering prior to the next phase of deposition.

The sedimentary-volcanic cyclic nature of deposition became an essential feature of the evolving Pechenga-Pasvik rift. Each cycle records a temporal change from alluvial through shallow to relatively deep water lacustrine conditions, interrupted by violent volcanism which caused cessation of sedimentation, except when surface weathering and erosion continued. The cyclic

Table 3 Stratigraphic subdivision of the Petsamo Supergroup and intrusive activity (from Melezhik et al. 1995)



Age data are from: (1) Bakushkin et al. (1990), (2) Hanski et al. (1990), (3) Central Kola Prospecting Expedition (unpublished data), (4) Vetrin et al. (1986); (5) Pushkarev et al. (1978), (6) Balashov et al. (1991). Radiometric ages are given in Ga.

repetition may have been caused by a correlation between high rates of crustal extension and graben

Table 4. Evolutionary scheme of Pechenga-Pasvik Greenstone Belt - continental rift model (modified from Melezhik et al. 1994a).

**Intracontinental Rift Stage (2450-2330 Ma), East African Type**

*Rifting, 2450-2100 Ma*

Layered gabbro emplacement.

Sub-aerial immature basal polymict conglomerate;  
Sub-aerial basaltic andesites with komatiitic affinities.

**Transitional Intra- and Intercontinental Rift Stage and Rift Inversion (2330-2000 Ma), Afar Triangle Type**

*Rifting, 2100-2000 Ma*

'Red beds', lacustrine evaporitic series 1;  
Sub-aerial alkaline volcanic association.

'Red beds', lacustrine evaporitic series 2;  
Submarine tholeiitic basalts, transitional to NMORB;  
Deep-water lake 'black shales' 1;  
Submarine tholeiitic basalts, transitional to NMORB.

**Intercontinental Rift-Aborted Oceanic Rift Stage (2000-1970 Ma), Red Sea Type**

*Rifting and short term spreading, 2000-1970 Ma*

Moderately deep-water lake 'black shales' 2;  
Moderately deep-water lake fossil 'black smokers';  
Submarine tholeiitic basalts, approximately NMORB;  
Ferropicritic lavas and co-magmatic shallow-seated differentiated ultramafic intrusions (Ni-type);  
Sub-aerial or shallow-water rhyolitic and dacitic tuffs and lavas;  
Submarine tholeiitic basalts.

**Subduction-Related Rift Stage (1970-1870 Ma)**

Andesites, boninites, high-Ti picrites.

**Collision-Related Rift Stage (1870-1800? Ma)**

Postorogenic andesitic conglomerates;  
Postorogenic shallow- to deep-water andesitic volcanoclastic rhyolites;  
Postorogenic granites.

Orogeny ———

Rift inversion - - - - -

Non-depositional break ·····

collapse related to low continental crust thickness (Melezhik 1988).

The second sedimentary-volcanic (Kuetsjärvi) cycle, comprised of lacustrine evaporites and alkaline volcanic rocks, represents the climax of sub-aerial continental volcanism and sedimentation within the Pechenga-Pasvik rift (Fig. c).

**Rift Inversion and Transitional Intra- and Intercontinental Rift Stage (2330-2000 Ma).**

Prior to the deposition of Kolasjoki sediments, the previously formed volcanic-sedimentary successions were uplifted and eroded to depths of more than 100 m by well-developed internal rift river systems, implying that surface uplift on the order of several hundreds of metres occurred (Fig. 19a). The rift appears to have been initiated as an intracontinental rift structure (2450-2100 Ma) that went through a stage of inversion prior to renewed rifting and deposition of huge volumes of NMORB-affinity tholeiites with minor black shales of the Kolasjoki Volcanic Formation (Fig.19b).

**Intercontinental Rift - Aborted Oceanic Rift Stage (2000-1970 Ma).**

The Pechenga sequence that was formed at the earlier stages, between 2450 and 1990 Ma, may be interpreted as the product of Palaeoproterozoic rifting with a progressive reduction of crustal influence over time (Brewer & Daly 1994). The Pechenga-Pasvik Rift Zone is thought to have been constantly floored by continental crust since its early development (Hanski 1992; Melezhik et al. 1994b), apart from a short period (Melezhik et al. 1994a) between the Pilgijärvi Lower Basalt Member formation (1990±66 Ma) and the occurrence of felsic tuffs and flows (1970±5 Ma). Oceanic conditions may have dominated during this short interval, as evidenced by NMORB basalts and mantle-like δ<sup>34</sup>S signatures of sulphides from the Pilgijärvi Formation (Fig. 20, Melezhik et al. 1994b). It is possible that this rift stage was caused by a rising mantle plume, like those described by Campbell and Griffiths (1990) and Davies and Richard (1992). This proposal has been also discussed in Melezhik et al. (1994b).

This stage resulted in the eruption of extensive volume of NMORB-like tholeiites and a subordinate volume of 'ferropicritic' magma with crustal geochemical signatures. Abundant shallow-seated, differentiated, sulphide Ni-Cu-bearing mafic-ultramafic (gabbro-wehrlite), comagmatic with 'ferropicrites' intrusions were placed synchronously with tholeiites and 'ferropicrites'



# EAST AFRICAN TYPE

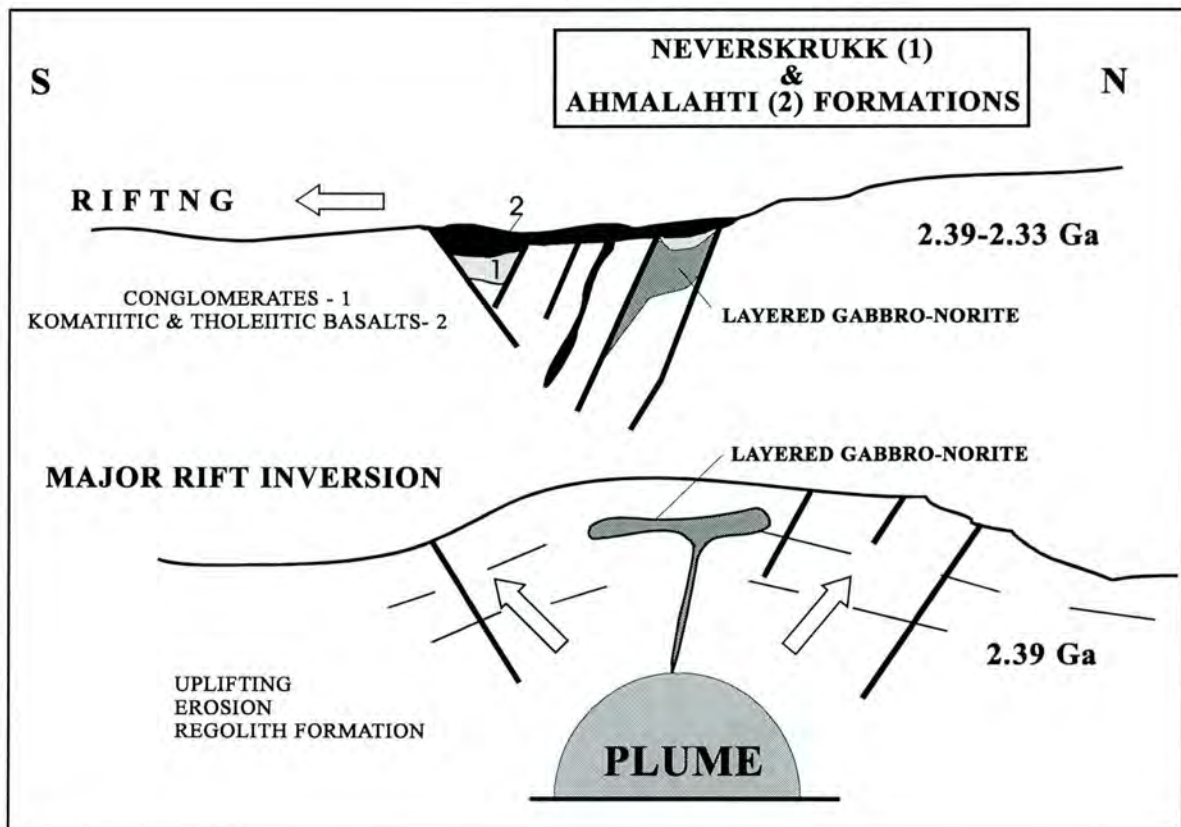
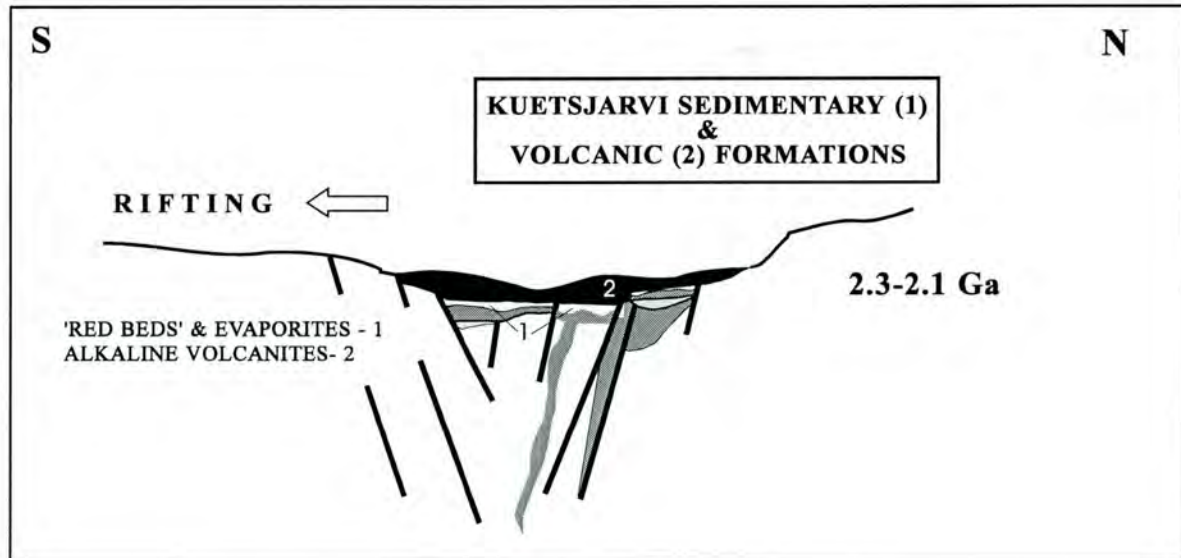


Fig. 18 Early stage of the Pechenga-Pasvik Belt development; an intracontinental rift (modified from Melezhik & Sturt 1994).

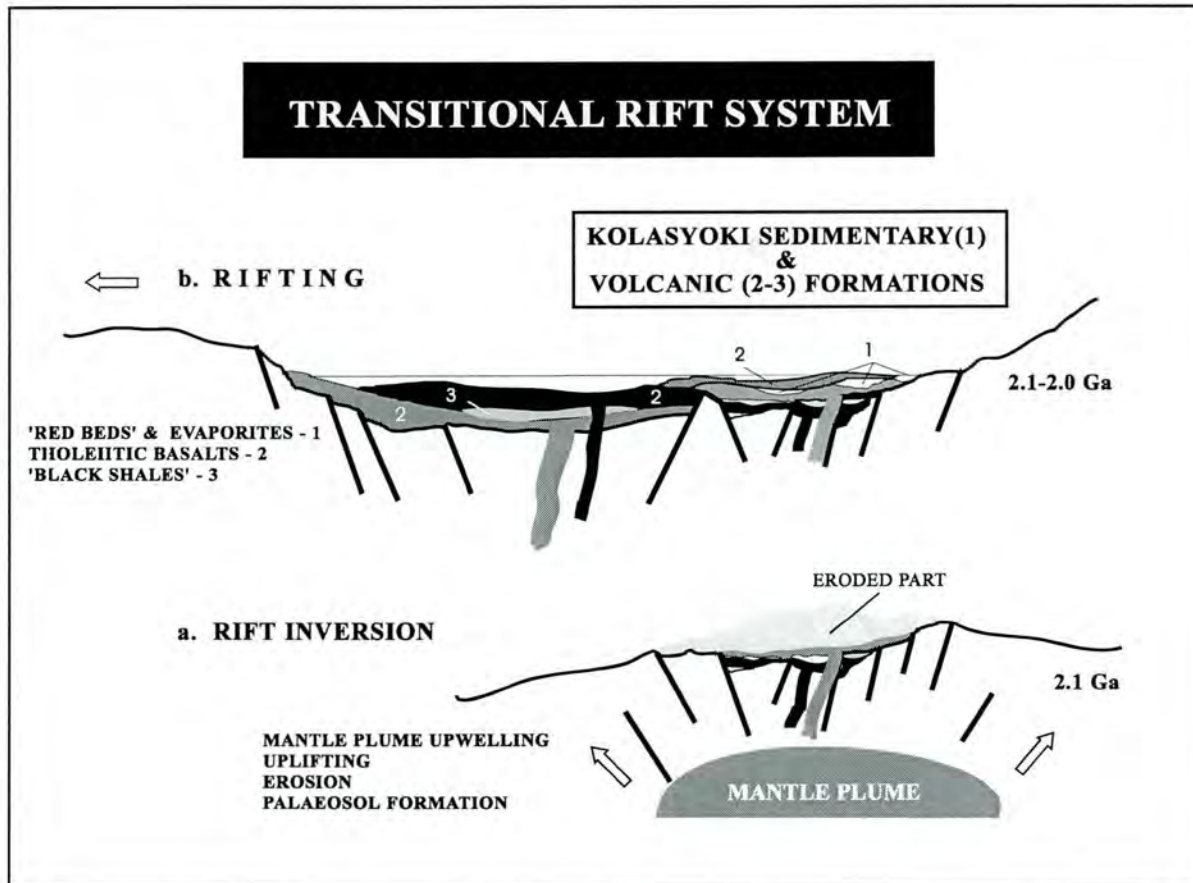


Fig. 19 Mid stage of the Pechenga-Pasvik Belt development. Rift inversion and stage transitional to an intercontinental rift (modified from Melezhik & Sturt 1994).

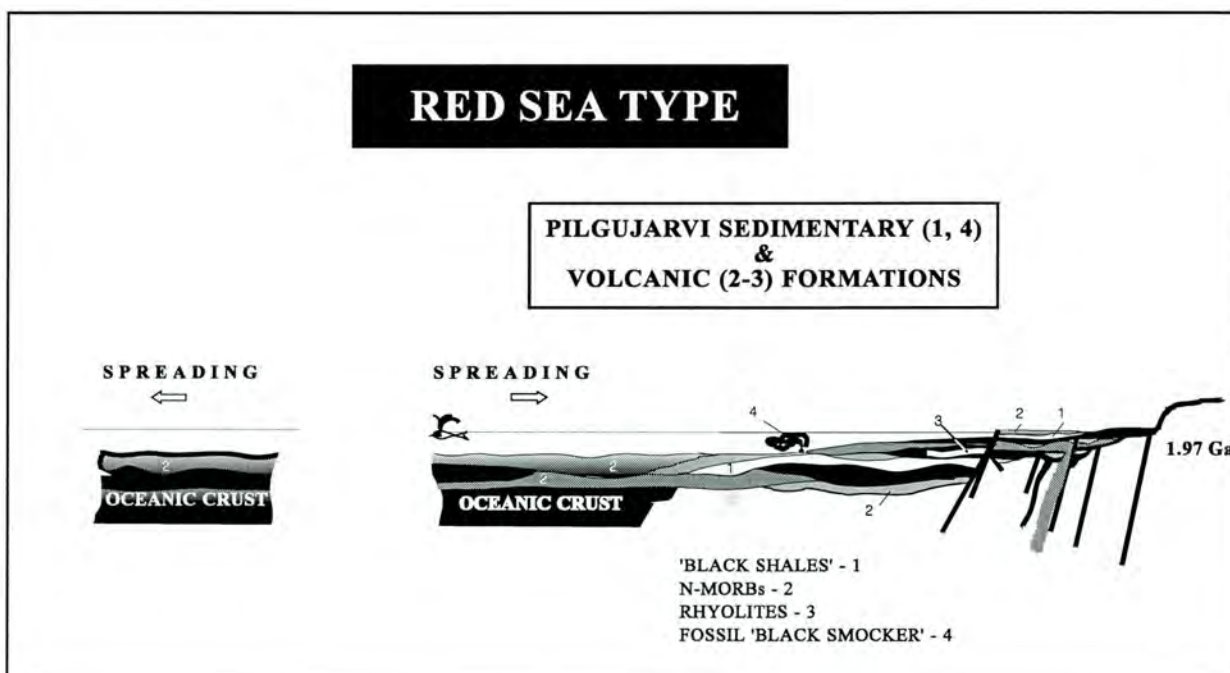


Fig. 20 The mid stage of the Pechenga-Pasvik Belt development. An intercontinental rift followed by aborted oceanic rift (modified from Melezhik & Sturt 1994).

(Predovsky et al. 1971; Hanski & Smol'kin 1989; Hanski et al. 1990; Hanski 1992)

Al<sub>2</sub>O<sub>3</sub> andesites of the Kaplya Formation (1970-1870 Ma) which bear the geochemical signature of calc-alkaline island-arc volcanics (Skufin et al. 1988).

**Subduction-Related Rift Stage (1970-1870 Ma).**

The first possible indications of subduction in the system (Fig. 21) are recorded by the high-MgO boninite-like andesites and basalts and by the high-

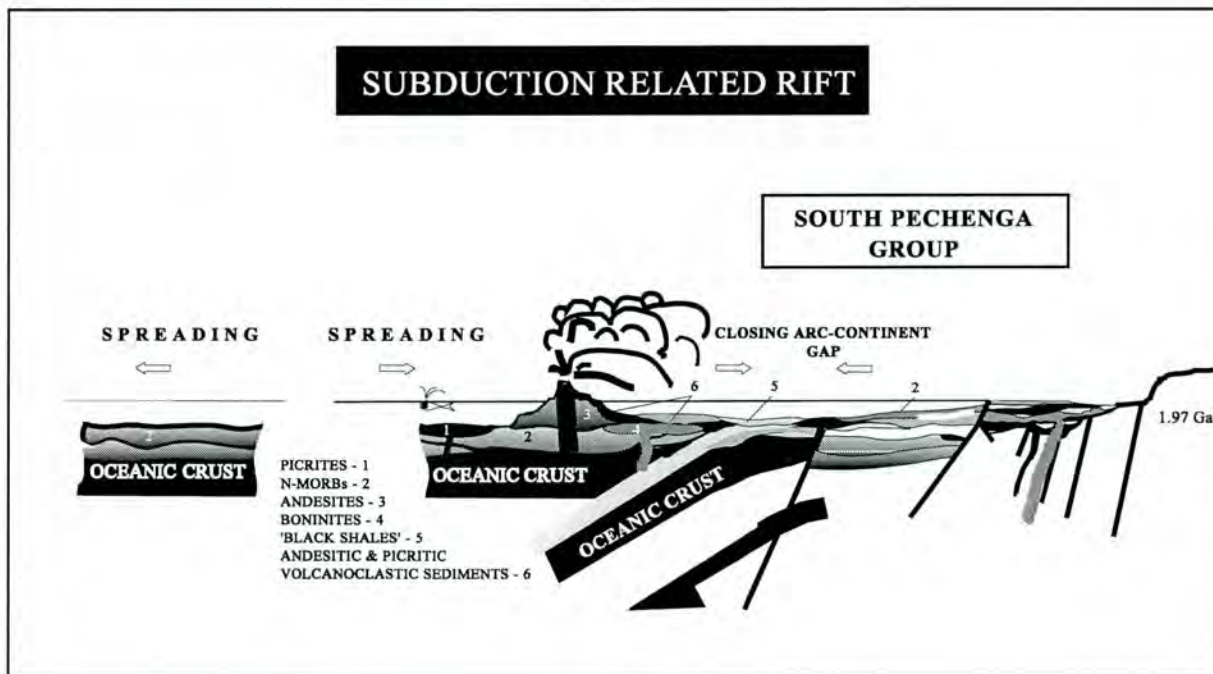


Fig. 21 The late stage of the Pechenga-Pasvik Belt development; a subduction-related rift (modified from Melezhik & Sturt 1994).

**Collision-Related Rift Stage (1870-1800? Ma)**

The rocks of the Kaplya Formation were deformed and metamorphosed prior to uplift, erosion and deposition of polymict conglomerates of the Kasesjoki Formation (Melezhik et al., 1991). This deformation and metamorphism may be related to a collision between the arc and the northern continent (Fig. 22). The polymict conglomerates are followed by a considerable thickness of high Al<sub>2</sub>O<sub>3</sub> andesites/volcanoclastic sediments which again bear the geochemical signature of calc-alkaline island arc volcanics. These rocks have been deformed and metamorphosed, probably in relation to the overriding southerly derived thrust plate of Archaean gneisses (Fig. 22). This stage may relate to a

continent-continent collision which brought the evolution of the Belt to an end in a Svecofenian orogeny at ca. 1800 Ma.

15-20 m per Ma (Melezhik 1992). This implies a number of extensive non-depositional breaks in the Belt history (Table 2). At least two factors played an important role in the Pechenga-Pasvik history: (1) the 2100 Ma-old non-depositional break separating the two major stages of rift zone development, which may have been caused by mantle plume-related up-lift, and (2) the non-depositional break and probable orogenic event recorded by the SPG andesitic volcanoclastic conglomerates which occurred sometime between 1970 and 1800 Ma ago.



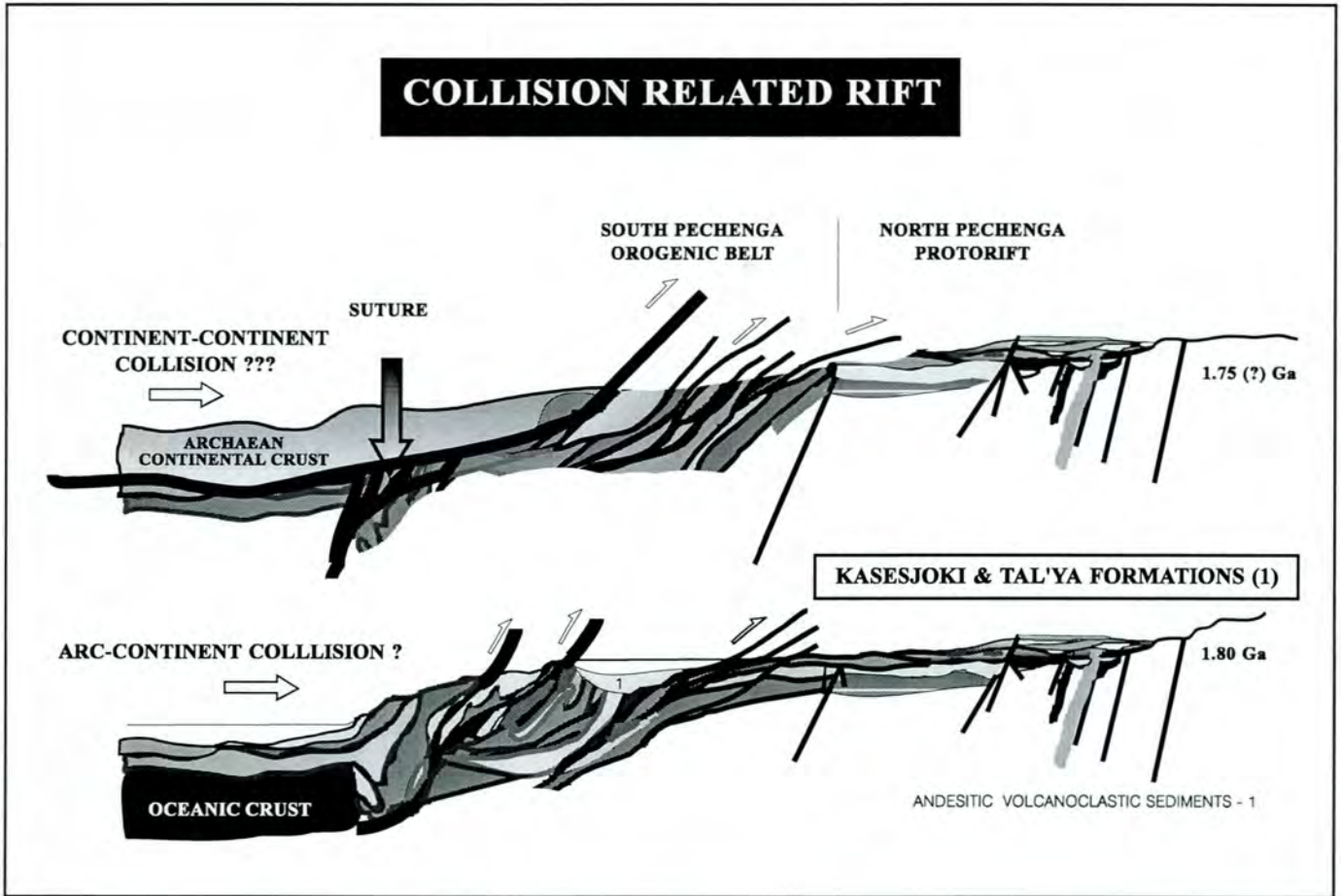


Fig. 22 The latest stage of the Pechenga-Pasvik Belt development; a collision-related rift (modified from Melezhik & Sturt 1994).

## References

- Akhmedov A. M. & Krupenik V. A. 1990: Turbidity regimes of the sedimentation and pyrite-forming processes in the Early Proterozoic Pechenga Basin. *Soviet Geol.*, 11, 51-60 (in Russian).
- Bakushkin Ye. M. & Akhmedov A. M. 1975: Basal conglomerate of the Pechenga Complex near the Mt. General'skaya. In: *Geology and Geochemistry of the Metamorphic Complexes of the Kola Peninsula*, Apatity, 70-77 (in Russian).
- Bakushkin Ye. M. *et al.* 1990: Mountain General'skaya. In: Mitrofanov. F. P. and Balashov Yu. A. (eds), *Geochronology and Genesis of the Layered Basic Intrusions, Volcanites and Granite-Gneisses of the Kola Peninsula*, Apatity, 14-15 (in Russian).
- Balashov Yu. A. *et al.* 1991: Rb-Sr age of volcanic and metamorphic processes in the Pechenga structure. In: *Methods of Isotopic Geology*, Institute of Precambrian Geology, St. Petersburg, 19-20 (in Russian).
- Balashov, Yu.A., *et al.* 1993: New data on geochronology of the Pechenga structure and its framing. In: *The Svecofennian Domain. Geological, Geophysical Aspects of the Continental Crust. Annual Meeting of IGCP-275*, Turku, August 23-25, 1993. Abstracts, pp. 7-8.
- Barbey P. *et al.* 1984: Petrogenesis and evolution of an Early Proterozoic collisional orogenic belt; the granulite belt of Lapland and the Belomorian (Fennoscandia). *Bull. Geol. Soc. Finland*, 56, 161-168.
- Belyaev, O. A. *et al.* 1977: *Regional Metamorphic Facies of the Kola Peninsula*, Leningrad, Nauka. (in Russian).
- Berthelsen A. & Marker M. 1986: Tectonics of the Kola collision suture and adjacent Archaean and Early Proterozoic terrains in the north-eastern region of the Baltic Shield. *Tectonophysics*, 126, 31-35.
- Bugge J. A. W. 1960: Precambrian of eastern Finnmark. In: Høltedahl O. (ed), *Geology of Norway, Norges Geol. Unders. Bull.*, 208, 78-92.
- Campbell I. H. & Griffiths R. W. 1990: Implications of mantle plume structures for the evolution of flood basalts. *Earth Planet. Sci. Lett.*, 99, 79-93.
- Condeci K. C. 1989: *Plate Tectonics and Crustal Evolution*. 3rd ed., Pergamon Press, 211 pp.
- Davies G. E. & Richards M. A. 1992: Mantle convection. *J. Geol.*, 100, 151-206.
- Fedotov Zh. A. 1985: *Evolution of Proterozoic Volcanism of the Pechenga-Varzuga Belt (Petrogeochemical Aspects)*, Kola Science Centre, Apatity. (in Russian).
- Galdobina L. P. & Melezhik V. A. 1986: Stratigraphy of the Ludicovian in the eastern part of the Baltic Shield. In: Sokolov V. A. and Heiskanen K. I. (eds), *Early Proterozoic of the Baltic Shield* (Proceedings of the Finnish-Soviet Symposium held in Petrozavodsk 19th-27th August, 1985), Petrozavodsk, 226-235.
- Golubev A. I. Akhmedov A. M. & Galdobina L. P. 1984: *Geochemistry of Black Shale Complexes of the Karelia-Kola Region*. Nauka, Leningrad, 193 pp. (in Russian).
- Gorbunov, G.I. 1968: *Geology and origin of the copper-nickel sulphide ore deposits of Pechenga (Petsamo)*. Moscow, Nedra, 352 pp (in Russian).
- Hanski E. J. 1992: Petrology of the Pechenga ferropicrites and cogenetic, Ni-bearing gabbro-wehrlite intrusions, Kola Peninsula, Russia. *Geol. Surv. Finland Bull.*, 367, 1-192.
- Hanski E. J. & Smolkin V. F. 1989: Pechenga ferropicrites and other Early Proterozoic picrites in the eastern part of the Baltic Shield. *Precambrian Res.*, 45, 63-82.
- Hanski E. *et al.* 1990: The age of the ferropicritic volcanics and comagmatic Ni-bearing intrusions at Pechenga, Kola Peninsula, USSR. *Bull. Geol. Soc. Finland*, 62, 123-133.
- Hausen H. 1926: Über die Praquartäre Geologie des Petsamo-Gebietes. *Bull. Comm. Geol. Finlande*, 76. (in German).
- Hickey R. L. & Frey F. A. 1982: Geochemical characteristics of boninite series volcanics: implications for their source. *Geochim. Cosmochim. Acta*, 46, 2099-2115.
- Hudson K. A. Melezhik V. A. & Green A. H. 1992: Potential for Pechenga-type Ni-Cu deposits in Pasvik, northern Norway. Abstract *Geology in Europe and Beyond*, Instn Min. Metall., April 22-23, 1992.
- ISSC (International Subcommission on Stratigraphic Classification of IUGS Commission on Stratigraphy), 1976: *International Stratigraphic Guide: A Guide to Stratigraphic Classification, Terminology and Procedure* (ed. Hedberg, H. D.), John Wiley & Sons, New York, , 200 p.
- Karhu, J.A. & Melezhik, V.A. 1992: Carbon isotope systematics of early Proterozoic sedimentary carbonates in the Kola Peninsula, Russia. In: *Balagansky, V.V. &*

- Mitrifanov, F.P., (eds) 'Correlations of Precambrian formations of the Kola-Karelian region and Finland'. Apatity, Kola Sci. Centre, 48-53.
- Kozlovsky Ye. A. (Ed). 1987: *The Superdeep Well of the Kola Peninsula*, Springer-Verlag, 558 pp.
- Kremenetsky A. A. & Ovshinnikov L. N. 1986: *Geochemistry of Deep Rocks*, Moscow, Nauka, 262 pp. (in Russian).
- Lieungh B. A. 1988: Geological description of the map sheets: Svanvik 2433I, Skogfoss 2433IV, Vaggatem 2333I & Krokfjellet 2333II. Norwegian Geological Survey, unpublished report. (in Norwegian)
- Marker, M. 1985: Early Proterozoic (c. 2000-1900 Ma) crustal structure on the northeastern Baltic Shield: tectonic division and tectogenesis. *Norges Geol.Unders. Bull.*, 403, 55-74.
- Melezhik V. A. 1987: Composition of waters of Precambrian basins as indicated by geochemical data. *Int. Geol. Rev.*, 29, 1188-1199.
- Melezhik V. A. 1988: Early Proterozoic Sedimentary Basins of the Baltic Shield. Ph.D. Thesis, USSR Academy of Sciences, Moscow, 446 pp. (in Russian).
- Melezhik V. A. 1992: *Early Proterozoic Sedimentary and Sedimentary Rock-Forming Basins of the Baltic Shield (Problems of the Reconstructions of Postsedimentary Processes)*, St. Petersburg, Nauka, 256 pp. (in Russian).
- Melezhik V. A. & Abzalov M. Z. 1989: Geochemistry of diagenetic concretions in the Early Proterozoic clastic rocks of the Kola Peninsula. *Int. Geol. Rev.*, 31, 506-517.
- Melezhik, V.A. & Fallick, A.E. 1996: A widespread positive  $\delta^{13}\text{C}_{\text{carb}}$  anomaly at around 2.33-2.06 Ga on the Fennoscandian Shield: a paradox. *TERRA Nova*,
- Melezhik V. A. Ivanova L. V. & Chapina O. S. 1992: The 2.1 billion year-old coccooid microfossils from non-stromatolitic cherts interbedded with pillow lavas (Pechenga, Baltic Shield). Is this evidence of deep-water life in the Precambrian? In *Abstract Volume, 2, 29th International Geological Congress*, Kyoto, Japan, 24 August-3 September, 1992.
- Melezhik V. A. & Sturt B. A. 1994: General geology and evolutionary history of the Early Proterozoic Polmak-Pasvik-Pechenga-Imandra/Varzuga-Ust'Ponoy Greenstone Belt in the northeastern Baltic Shield. *Earth-Sci. Rev.*, 205-241.
- Melezhik V. A. et al. 1988: *Carbonaceous Deposits of Early Stages of the Earth's Evolution (Geochemistry and Conditions of Accumulation on the Baltic Shield)*. Leningrad, Nauka, 200 pp. (in Russian).
- Melezhik V. A. et al. 1991: Development of the Early Proterozoic Pasvik-Pechenga-Imandra/Varzuga-Ust'Ponoy Greenstone Belt. Sixth Meeting of the European Union of Geosciences, Strasbourg, 24-28 March 1991. *Terra Abstr.*, 3, 194.
- Melezhik, V.A., Hudson-Edwards, K.A., Green, A.H. & Grinenko, L.I. 1994b: The Pechenga area, Russia. Part 2: nickel-copper deposits and related rocks. *Inst. Mining. Metall., Section B, Applied Earth Science* 103, 146-161.
- Melezhik, V. A., Hudson-Edwards, K. A., Skuf'in, P. K. & Nilsson, L.-P. 1994: The Pechenga area, Russia. Part 1: geological setting and comparison with Pasvik, Norway. *Inst. Mining. Metall., Section B, Applied Earth Science* 103, 129-145.
- Melezhik V. A. et al. 1995: The Early Proterozoic Pasvik-Pechenga Greenstone Belt: 1:200,000 geological map, stratigraphic correlation and revision of stratigraphic nomenclature. In: Roberts, D. & Nordgulen, O. (eds), *Geology of the eastern Finnmark-western Kola region. Norges Geol.Unders. Special Publ.*, 7, 81-91.
- Mitrofanov F. P. Balashov Yu. A. & Balagansky V. V. 1991: New geochronological data on lower Precambrian complexes of the Kola Peninsula. In: Mitrofanov F. P. and Balagansky V. V. (eds), *Correlation of Lower Precambrian Formations of the Karelia-Kola Region, USSR, and Finland*, Apatity, 12-16.
- Mitrofanov, F.P & Smol'kin V.F. (eds), *Magmatism, Sedimentogenesis and Geodynamics of the Pechenga Paleorift*. Apatity, 256 pp. (in Russian).
- Negrutza V. S. 1984: *Early Proterozoic Stages of Evolution in the Eastern Part of the Baltic Shield*. Leningrad, Nedra, 270 pp. (in Russian).
- Petrov, V.P & Voloshina, S.M. 1995: In: Mitrofanov, F.P & Smol'kin V.F. (eds), *Magmatism, Sedimentogenesis and Geodynamics of the Pechenga Paleorift*. Apatity, 164-182 pp. (in Russian).
- Pharaoh T. C. Warren A. & Walsh N. J. 1987: Early Proterozoic metavolcanic suites of the northernmost part of the Baltic Shield. In: Pharaoh T. C. Beckinsale R. D. and Rickard D. (eds). *Geochemistry and Mineralisation of Proterozoic Volcanic suites*, Geol. Soc. Spec. Publ., 33, 41-58.
- Predovsky A. A. Fedotov Zh. A. & Akhmedov A. M. 1974: *Geochemistry of the Pechenga Complex*. Leningrad, Nauka, 139 pp. (in Russian).



- Predovsky A. A. *et al.* 1987: *Volcanism and Sedimentology of the Precambrian in the North-Eastern Part of the Baltic Shield*. Leningrad Nauka, 185 pp. (in Russian).
- Predovsky, A. A., Zhangurov, A. A. & Fedotov, Zh. A., 1971. Evolution of the composition of mafic-ultramafic rocks and its relation to associated Ni-Cu ores in Pechenga. In: *Problems of Magmatism of the Baltic Shield*, Leningrad, Nauka, pp. 166-176. (in Russian).
- Pushkarev Yu. D. Kravchenko E. V. & Shestackov G. I. 1978: *The Precambrian Geochronological Markers of the Kola Peninsula*. Leningrad, Nauka, 136 pp. (in Russian)
- Roberts, D. & Nordgulen, O. (eds). 1995 Geology of the eastern Finnmark-western Kola region. *Norges Geol.Unders. Special Publ.*, 7, 378 pp.
- Rusanov, M.S. 1981: The tholeiit-komatiite formation of the Pechenga Complex. *Soviet Geology*, 2, 98-112 (in Russian).
- Sharkov Y. V. 1984: Lower Proterozoic continental rift volcanism in the Karelia-Kola region. *Geotectonics*, 18, 123-132.
- Siedlecka A. *et al.* 1985: Lithostratigraphy and correlation of the Archean and Early Proterozoic rocks of Finnmarksvidda and the Sørvaranger district. *Norges Geologiske Undersøkelse Bulletin*, 403, 7-36.
- Skufin P. K. 1995: Geology of the Poritash volcanic centre: new results. In: Roberts, D. & Nordgulen, O. (eds), Geology of the eastern Finnmark-western Kola region *Norges Geol.Unders. Special Publ.*, 7, 111-116.
- Skufin P. K. Gavrilenko B. V. & Fedotov Zh. A. 1988: Porayarvi volcanic dome structure in the South Pechenga Zone. *Bulletin of Moscow Soc. Investigators Nature*, 63, 98-107. (in Russian).
- Skufin P. K. Pushkarev Yu. D. & Kravchenko M. P. 1986: Volcanics of the mugearite-trachytic formation in the Pechenga palaeodepression. *News USSR Acad. Sci.*, 1, 18-29. (in Russian).
- Smol'kin, V.F. 1992: *Early Precambrian Picritic and Komatiitic Magmatism of the Baltic Shield*. St.-Petersbourg, Nauka, 272 pp. (in Russian).
- Smolkin V.F., Skufin, P.K. & Mokrousov, V.A. 1995: Stratigraphic position, geochemistry and genesis of volcanic associations of the Early Proterozoic area. In: Roberts, D. & Nordgulen, O. (eds), Geology of the eastern Finnmark-western Kola region *Norges Geol.Unders. Special Publ.*, 7, 93-110.
- Sturt, B.A, Melezhik, V.A & Ramsay, D.M. 1994: Early Proterozoic regolith at Pasvik, NE Norway: palaeoenvironmental implications for the Baltic Shield. *TERRA Nova*, 6, 618-633
- Sturt, B.A, Melezhik, V.A & Ramsay, D.M. 1995: The significance of the contact relationship of the lower formations of the Petsamo Supergroup. In: Roberts, D. & Nordgulen, O. (eds), Geology of the eastern Finnmark-western Kola region *Norges Geol.Unders. Special Publ.*, 7, 119-120.
- Tellef Dahl. 1891: Om fieldbygningen i Finnmarken og guldets forekomst sammesteds. *Norges Geologiske Undersøkelse*, 4, 1-21. (in Norwegian).
- Väyryanen H. 1938: Petrologie des Nickelerzfeldes Kaulatunturi-Kammikivitunguri in Petsamo. *Bull. Comm. Geol. Finlande*, 116, 1-198 (in German).
- Wegmann C. E. 1929: Zur Kenntnis der tectonischen Beziehungen meatlogenisher Provinzen in der nördlichsten Fennoscandia. *Zeitschr. für prakt. Geologie*, 37, 193-208. (in German).
- Zagorodny V. G. Mirskaya D. D. & Suslova S. N. 1964: *Geology of the Pechenga Sedimentary-Volcanogenic Series*. Leningrad, 218 pp. (in Russian).
- Zak S. I. *et al.* 1982: *Geology, Magmatism and Ore Formation in the Pechenga Ore Field*. Leningrad, Nedra, 112 pp. (in Russian).

# DIFFERENTIATED GABBRO-WEHRLITE INTRUSIONS, FERROPICRITIC LAVA FLOWS AND ASSOCIATED SULPHIDE Ni-Cu ORES

V.A. Melezhik and St.V. Sokolov

## 1. Introduction

The Ni-Cu deposits of the Pechenga ore field (Fig. 1) have been prolific producers since mining began in the early 1940s. Annual production is about 30-35 000 t nickel (Strishkov, 1989). Reserves of the Tsentralny, Zapadny and Severny deposits in the Pilgújärvi intrusion alone should enable mining operations to continue for another 40 to 50 years (Chadwick 1992).

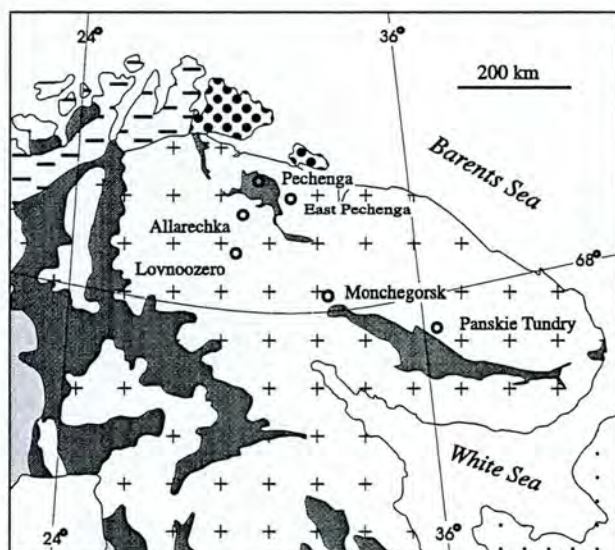


Fig. 1 Nickel deposit areas of Kola Peninsula, Russia.

Väyrynen (1938) described the Ni-Cu ores and was the first to suggest a magmatic-immiscible sulphide melt model for their formation. Eliseev et al. (1961) and Gorbunov (1968) made modifications to this model with respect to timing, depth of formation and precipitation of the sulphides, and Gorbunov (1968) proposed a compressional, ore-related tectonic regime and considered that the Luotna Fault (Fig. 2,

Melezhik 1996, this volume) was a major feeder channel for the ore-bearing magma.

Predovsky et al. (1971, 1974) were the first to describe the geochemical similarity between the Ni-Cu ore-bearing gabbro-wehrlite intrusions and associated picritic volcanic rocks. Their work has been developed by Hanski (Hanski & Smol'kin 1989; Hanski et al. 1990), who recently published a comprehensive petrogeochemical and petrological summary of the picrites and gabbro-wehrlites (1992), and suggested a model for their origin involving either a lithospheric or mantle plume.

Although the mode of formation of the Ni-Cu ores in the gabbro-wehrlite intrusions has been ascribed to a magmatic immiscibility, the mechanism of emplacement of the ultramafic rocks and the source of sulphur for the ores and ultramafics remains enigmatic. Mapping in Pasvik, Norway by A/S Sydvaranger in 1957 and subsequent exploration carried out sporadically in the area resulted in the discovery of ultramafic rocks similar to the ore hosts at Pechenga (Boyd & Nixon 1985). A new phase of investigation of the Pasvik ultramafic rocks was initiated in 1990 by A/S Sulfidmalm, in collaboration with the Geological Survey of Norway. One important result of this cooperative work was the recognition of two modes of sulphide Ni-Cu ore developments, namely one associated with differentiated mafic-ultramafic intrusions, and another related to weakly differentiated ultramafic flows (Melezhik et al. 1994a).

## 2. Geological Setting

Three of the six main nickel deposit areas in the Kola Peninsula, namely, Fedorovo-Panskie Tundry, Monchegorsk and Pechenga, are associated with the Pasvik-Pechenga-Imandra/Varzuga Belt (Gorbunov et al. 1985). The other three occur within the Archaean granulites (Lovnoozero) and gneisses (Allarechka, East Pechenga/Karikjavr) (Fig. 1).

The Ni-Cu sulphide ores of the Pechenga Greenstone Belt are hosted by differentiated mafic-ultramafic (gabbro-wehrlite) bodies which are located within a 600-1000 m-thick 'black shale' formation named the Pilgújärvi Sedimentary or 'Productive' Formation. All of the commercial Pechenga Ni-Cu deposits lie within the Western Rift Graben of the Northern Zone. This graben is bounded by two long-lived, syndepositional faults, and contains the thickest accumulations of each of the North Pechenga Group sedimentary and volcanic formations (Fig. 2).

### 3. Rocks Related to the Ore-Forming Processes

The economically viable Ni-Cu deposits are hosted by gabbro-wehrlite bodies and by 'ferropicrite' ultramafic flows lying within the Pilgijärvi Sedimentary, or 'Productive' Formation. These host rocks are genetically and spatially related to other volcanic rocks including 'ferropicrite' tuffs, and acidic tuffs and lesser flows, described below.

#### 3.1. Gabbro-Wehrlites

Two different sets of gabbro-wehrlite intrusions can presently be distinguished in the Pechenga Belt. The first set of intrusions is weakly differentiated gabbro-wehrlite bodies, which occur subconcordantly in the Kolasjoki Volcanic Formation along the NW-SE trending Kolasyoki Fault (Fig. 2). The second set is weakly differentiated ultramafic flows and well differentiated gabbro-wehrlite bodies. The latter occur both discordantly and subconcordantly in the Productive Formation. The ultramafic flows are observed both in the Pilgijärvi Sedimentary and Volcanic formations. More than 226 differentiated ultramafic-mafic bodies lie within the Productive Formation. Twenty-five of these contain Ni-Cu deposits of economic interest, 68 are classified as 'Ni-Cu-bearing', and the remaining 113 are described as 'barren' (Zak 1982), though several are host to Ni-Cu ores (Fig. 3). Thicknesses of the bodies generally range from 5 to 250 m, except for the 466 m thick Pilgijärvi intrusion, and strike lengths range from 100 m to 6.5 km (Zak 1982).

The ultramafic rocks have been partially metamorphosed under prehnite-pumpellyite to greenschist facies conditions, resulting in the formation of serpentinites and dolomite-magnesite-serpentinite-talc rocks where original textures and some primary minerals are preserved. Textural features reflecting rapid cooling in the upper part of ultramafic bodies (Eliseev et al. 1961; Hanski & Smol'kin 1990) and the widespread occurrence of devitrified glass (Akhmedov & Krupenik 1990) indicates that the bodies were placed at very shallow depths as both sills and flows. The presence of two different developments of ultramafic bodies is particularly evident in the western group of intrusions near Kaula (see below). A comprehensive description of ultramafic rocks in English is available in Hanski (1992), who gave the description for two extreme examples, namely for the voluminous Pilgijärvi intrusions and thin Kamikivi sill.

Gabbro-wehrlites show differentiation from peridotite through pyroxenite to gabbro, with most ultramafic cumulates not exceeding 39 wt% MgO, and the maximum gabbro SiO<sub>2</sub> content reaching 54 wt% (Table 1). REE patterns generally are straight,

negatively sloped and LREE-enriched (Fig. 12b, Melezhik 1996, this volume). Average sulphur concentrations for barren and ore-bearing bodies have been reported both as 0.2-0.4 wt% (Grinenko & Smol'kin 1991) and 0.31-0.37 wt% (Papushis 1952; Predovsky et al. 1974).

#### 3.2. Ferropicritic Volcanism

Ultramafic volcanic rocks at Pechenga with skeletal pyroxene structures were described by Zagorodny et al. (1964), and were subsequently named spinifex komatiites by Suslova (1979) and Rusanov (1981). Predovsky et al. (1971) showed, on the basis of bulk composition, that these ultramafic volcanic rocks had a different source from that of spatially associated tholeiites of the Pilgijärvi Volcanic Formation, and that the ultramafic volcanic rocks were co-magmatic with the Ni-Cu-bearing, differentiated gabbro-wehrlites. This was later supported by other analyses of bulk composition (Table 1, as well as data cited in Hanski & Smol'kin 1989, and Hanski 1992) and by REE patterns (Fig. 11, 12, Melezhik 1996, this volume). The ultramafic volcanic rocks and gabbro-wehrlites were also shown to be coeval (2001±77 Ma, Sm-Nd, Pb-Pb) within radiometric analytical error (Hanski et al. 1990).

Hanski and Smol'kin (1989) and Hanski (1992) classified the ultramafic volcanic rocks chemically as 'ferropicrites', as they are characterised by high MgO contents (generally >14 wt% anhydrous), anhydrous iron contents above 14 wt% FeO<sub>t</sub>, high TiO<sub>2</sub> (approximately 2.0 wt%), and high abundances of first-series transition metals (for >15 wt% MgO, Ni>500 ppm, Cr>600 ppm, Co>60 ppm and Sc>40 ppm). They also are distinguished by relatively high incompatible element concentrations such as Ta (0.8-4 ppm), Th (1-5 ppm), V (200-400 ppm), Zr (96-250 ppm) and LREE (La 10-35 ppm) and strongly negatively sloped chondrite-normalised REE patterns (Hanski & Smol'kin 1989, Fig. 11, 12 (Melezhik 1996, this volume). Their average sulphur content is 0.21 wt% and their δ<sup>34</sup>S values (Fig. 4(g) and (p)) range from -0.2‰ to +7.1‰ (Grinenko & Smol'kin 1991).

Ferropicritic volcanism occurs at several stratigraphic levels and in several forms at Pechenga. The oldest level, a 30 m thick sequence, was penetrated at the base of the Kolasjoki Volcanic Formation. Ferropicritic volcanites are most voluminous in the Productive and Pilgijärvi formations. The Lammas Member of the Productive Formation is represented by ferropicritic tuffs and tuffites with subordinate flows and 'ferropicritic black shales' (8-11 wt% MgO; 650-1600 ppm Cr; 270-850 ppm Ni) containing sulphide concretions and abundant calcite nodules (Melezhik



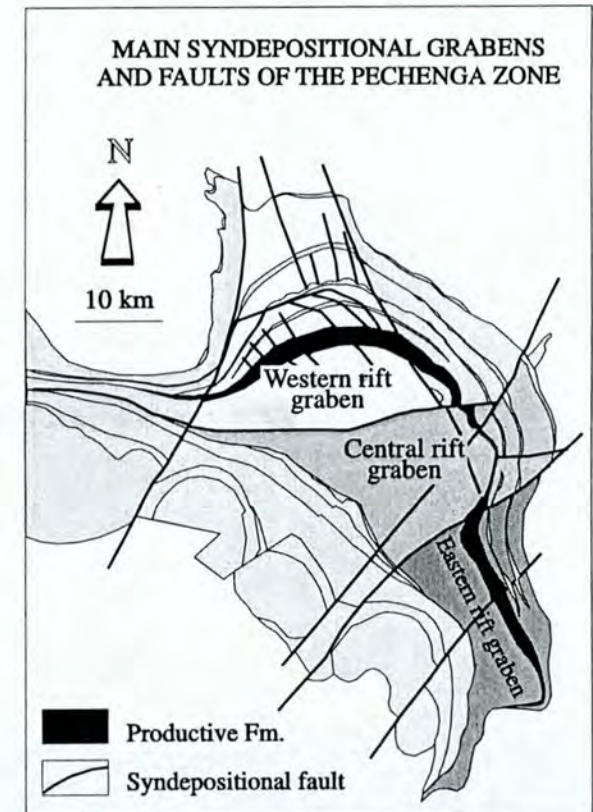
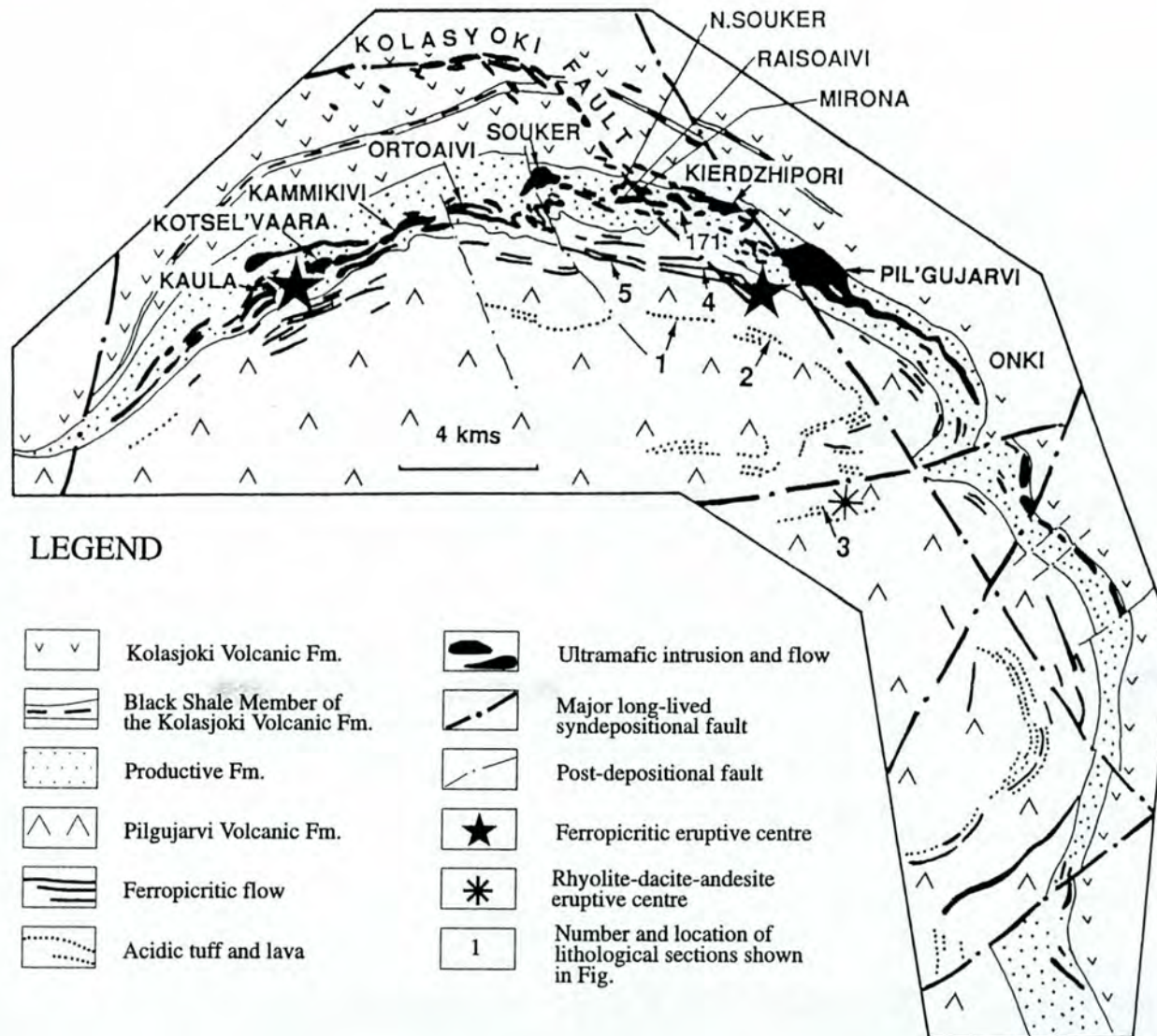


Fig. 2 Structural and stratigraphic locations of ultramafic intrusions, flows and other rocks related to ore-forming processes (Melezhik et al. 1994b)



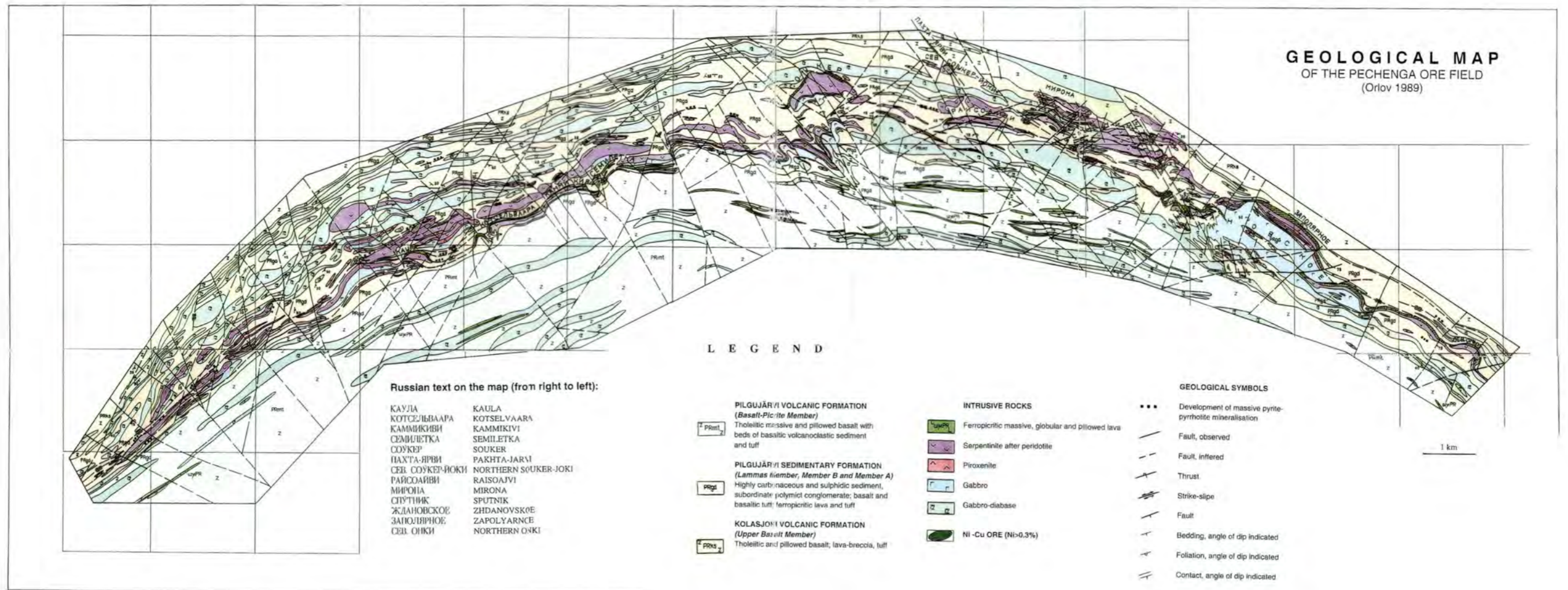


Fig. 3 Geological map of the Pechenga ore field.

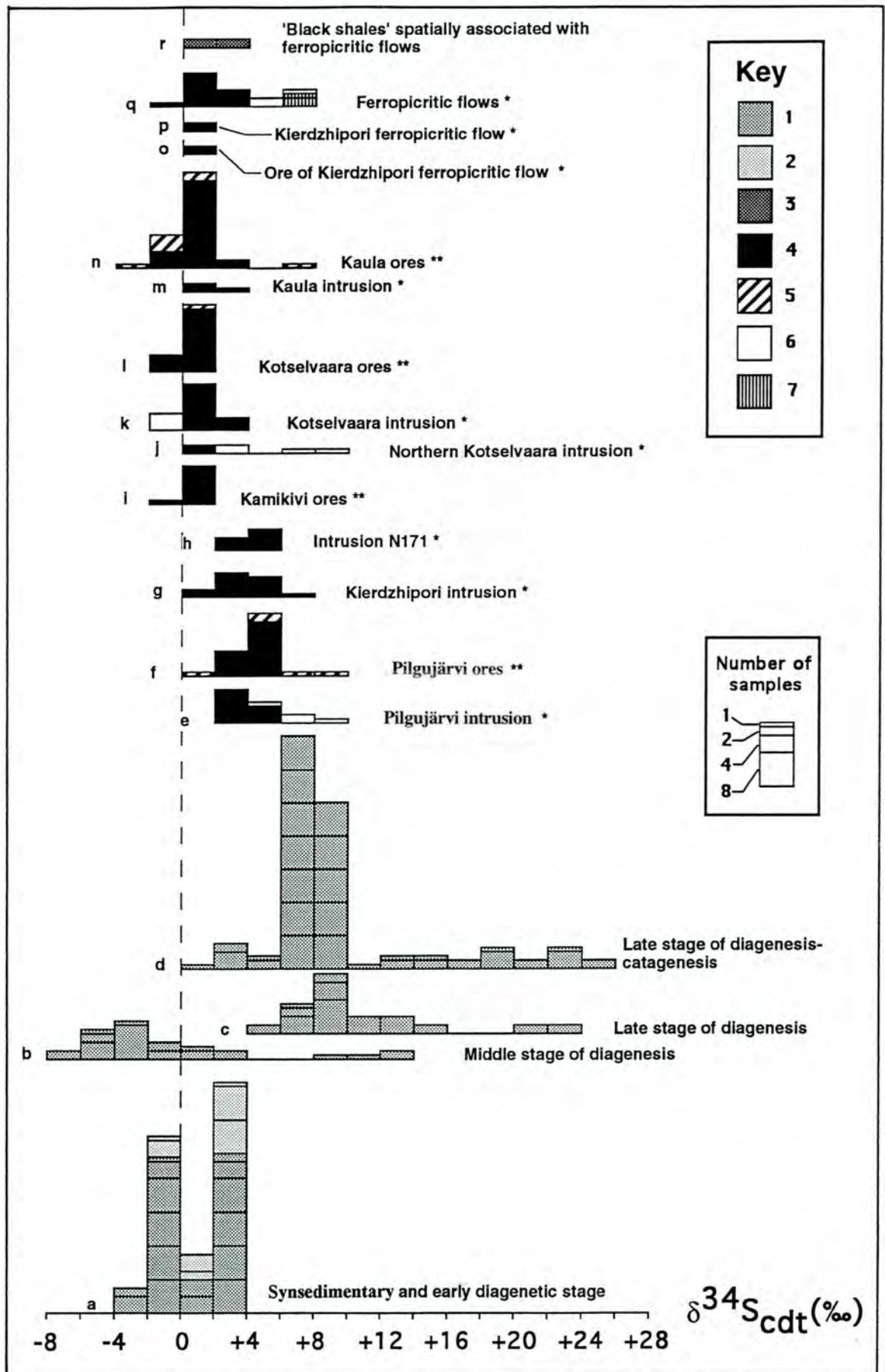




Fig. 4 (*facing page*) Isotope compositions of different genetic types of sulphides in the Productive Formation together with those of sulphur in; ultramafic-hosted Ni-Cu ores and disseminated sulphides of gabbro-wehrlite intrusions and ferropicritic flows, Pechenga (Melezhik et al. 1994b).

Key to numbered boxes with ornament: 1, sulphides of the Productive Formation; 2, synsedimentary and early diagenetic sulphides (Akhmedov & Krupenik 1990); 3, synsedimentary and early diagenetic sulphides from black shales associated with ferropicritic flows in the Pilgujärvi Volcanic Formation; 4, syngenetic disseminated sulphides in gabbro-wehrlite intrusions and ferropicritic flows and sulphides in disseminated, massive and brecciated ultramafic-hosted Ni-Cu ores; 5, metamorphic-metasomatic Ni-Cu ores hosted by the Productive Formation; 6, disseminated sulphides from low marginal zones of gabbro-wehrlite intrusions and ferropicritic flows; 7, disseminated sulphides from upper marginal zones of ferropicritic flows.

\*, Data from Grinenko and Smol'kin (1991); \*\*, Data from Grinenko et al. (1967). The Kotselvaara and Kaula intrusions are considered in this study as ferropicritic flows.

Table 1. Bulk composition of differentiated ultramafic intrusions and of ferropicrites (from Melezhik et al. 1994b).

	Differentiated intrusions					Ferropicrites					
	1	2	3	4	5	6	7	8	9	10	11
SiO <sub>2</sub>	41.88	41.14	43.03	45.13	38.53	43.86	43.71	45.97	44.96	46.29	43.11
TiO <sub>2</sub>	2.99	1.81	2.07	2.07	1.76	1.99	1.83	2.57	2.31	1.99	2.01
Al <sub>2</sub> O <sub>3</sub>	6.81	6.22	6.37	7.21	3.61	6.97	8.12	7.68	6.39	7.18	7.73
Fe <sub>2</sub> O <sub>3</sub>	3.33	7.33	n.d	n.d.	18.26	3.09	3.02	n.d.	n.d.	n.d.	17.63
FeO	12.83	9.96	17.85	16.77	n.d.	11.83	12.24	14.99	15.73	15.23	n.d.
MnO	0.18	0.21	0.219	0.22	0.21	0.17	0.18	0.21	0.21	0.23	0.21
MgO	15.61	19.33	22.61	18.66	23.07	14.79	15.28	17.39	19.92	18.67	15.04
CaO	10.68	6.53	5.95	8.96	4.09	11.35	9.06	10.51	9.47	9.16	6.17
Na <sub>2</sub> O	0.77	0.93	0.91	0.27	0.02	0.29	0.39	0.17	0.41	0.32	0.72
K <sub>2</sub> O	0.65	0.43	0.33	0.09	0.03	0.11	0.19	0.07	0.07	0.18	0.19
H <sub>2</sub> O <sup>+</sup>	n.d.	5.09	n.d.	n.d.	n.d.	4.69	4.76	n.d.	n.d.	n.d.	n.d.
P <sub>2</sub> O <sub>5</sub>	n.d.	n.d.	0.11	0.19	0.16	n.d.	0.31	0.24	0.22	0.32	0.17
S <sub>tot</sub>	0.37	0.31	n.d.	n.d.	0.04	0.04	0.11	n.d.	n.d.	n.d.	0.11
CO <sub>2</sub>	n.d.	0.36	n.d.	n.d.	n.d.	0.52	0.39	n.d.	n.d.	n.d.	n.d.
Cr(Cr <sub>2</sub> O <sub>3</sub> )	n.d.	n.d.	(0.36)	(0.28)	(0.22)	n.d.	0.094	(0.10)	(0.20)	(0.15)	(0.36)
Ni(NiO)	(0.06)	0.15	(0.21)	(0.15)	0.16	0.11	0.064	(0.10)	(0.11)	(0.27)	0.11
Cu(CuO)	n.d.	0.03	n.d.	n.d.	0.01	0.02	n.d.	n.d.	n.d.	n.d.	0.02
Co(Co)	n.d.	0.01	n.d.	n.d.	0.01	0.01	n.d.	n.d.	n.d.	n.d.	0.01
LOI	4.02	n.d.	n.d.	n.d.	9.24	n.d.	n.d.	n.d.	n.d.	6.31	5.68

1 - Average of Ni-bearing intrusions, Pechenga (Papushis 1952); 2 - weighted average of Ni bearing intrusions (n=88), Pechenga (Predovsky et al. 1971); 3 - weighted average of Ni-bearing intrusions (n=163), Pechenga (Brugmann et al. 1991); 4 - average of lower chilled margins of Ni-bearing intrusions, Pechenga (Brugmann et al., 1991); 5 - average of differentiated intrusions, Pasvik (n=33); 6 - average of Pechenga picrites (n=7) (Predovsky et al. 1971); 7 - average of Pechenga picrites (n=10) (Predovsky et al., 1987); 8 - average of lower chilled margin of picritic flow (n=4), Pechenga (Brugmann et al. 1991); 9 - weighted average of picritic flow (n=16), Pechenga (Brugmann et al. 1991); 10 - average of Pechenga picrites (n=68) (Brugmann et al. 1991); 11 - average of Pasvik ferropicrites (n=3).

LOI, loss of ignition.

n.d., not determined.

et al. 1988, 1994a). The total thickness of this member varies from zero near the Russian-Norwegian border zone, up to 50-250 m in the Western Rift Graben, to 600 m in the eastern flank (Eastern Rift Graben, Lammas area) where the rocks are mainly tuffites.

Younger ferropicrites of the Pilgijärvi Volcanic Formation (Fig. 2) are developed as massive, pillowed and lesser globular and spinifex-textured (Fig. 5, section 4 and 5) volcanic rocks (Zagorodny et al. 1964; Suslova 1979; Skufin & Fedotov 1989; Hanski & Smol'kin 1989; Hanski 1992) that occur as three to four, 20 to 50 m thick, flows in the three lowermost members of the Pilgijärvi Volcanic

Formation. The distribution of these flows is controlled by the main syndepositional faults (Fig. 2). Some of the flows display well-developed vertical zonation similar to that observed in komatiitic differentiated flows (Fig. 5, section 4). The uppermost ferropicritic flow is spatially associated with an acidic tuff horizon (Fig. 2), discussed below.

Two ferropicritic explosion centres, the Kaula and Kierdzhipori, are located in the Western Rift Graben (Fig. 2 and 6) near its major, bounding, syndepositional faults. The Kaula Centre (Fig. 6, section B) crops out in the quarry at Kotselvaara, and occurs within the Lammas Member of the Productive Formation. It is a 100 m thick body comprising basal fragment-supported explosion breccia with a ferropicritic lapilli tuff matrix (Table 2), which passes

gradually stratigraphically upwards through graded lapilli tuff into ferropicritic black shales. The basal explosion breccia is composed of angular fragments of black shales and diagenetic carbonate concretions of the Productive Formation, basalts, phosphorous-bearing limestone and partially melted and recrystallised cherts, which are chemically similar to rocks of the underlying Kuetsjärvi and Kolasjoki Sedimentary Formations of the NPG (Table 2).

The Kierdzhipori Centre (Fig. 6, section E) does not crop out and was discovered by drilling. It is a 600 m thick pile of eruptive ferropicrites (Table 2) which occupies the middle and upper parts of the Productive Formation (Skuf'in & Fedotov 1989, Fig. 2 and 6) and is interpreted to be a palaeovolcano.

### 3.3. Acidic Volcanism

Acidic volcanism occurs as a 5 to 40 m horizon of tuffs and local flows occurring as doublets and triplets separated by tholeiites, located ca. 800-1000 m above the upper contact of the Productive Formation (Fig. 2, 5). The sequences are distinguished by erosional surfaces between cycles, very intensive syndepositional folding, sedimentary dikes and well-developed current bedding (Melezhik 1992). Most tuff sequences show cyclic coarsening- or fining-upward development (Fig. 5, sections 1 and 2), with bases of massive lapilli tuff and lesser subaerial welded tuff with volcanic bombs. These gradually pass upwards through medium-grained crystalloclastic tuffs to either a thinly bedded and laminated or massive, microcrystalline tuff. Rhyolitic flow-breccia occurs rarely.

The acidic flows contain plentiful microgranophyre fragments, euhedral and corroded quartz crystals surrounded by devitrified glass and abundant small, partially melted fragments of granite (Predovsky et al. 1987; Zagorodny et al. 1964) and gneiss.

These volcanic rocks have unusual compositions (Zagorodny et al. 1964; Predovsky et al. 1974; Hanski 1992; Melezhik 1992). They are Zr-enriched (up to 895 ppm) ferrodacites to ferrorhyolites (Table 3) with highly variable  $\text{Na}_2\text{O}/\text{K}_2\text{O}$  ratios (0.01-7.0), attributable to magma contamination and heterogeneity.

A remnant of a dacite-rhyolite eruption centre at Luotn, ca. 6 km southeast of Pil'guyarvi (Fig. 2), is spatially associated with the eastern syndepositional bounding fault of the Western Rift Graben (Fig. 2). The Luotn Centre is represented by a hot- and cold-lahar rock assemblage (Fig. 5, section 3) containing 1 cm to 1 m diameter fragments of limestone, calcareous sandstone, basaltic ferropicrite, ferrobasalt, ferroandesite, tholeiitic basalt and  $\text{SiO}_2$ -

rich rock (Table 4), as well as 1 to 10 m blocks of flow-folded rhyolite and soft-sedimentary deformed, thinly bedded rhyolitic tuff.

### 3.4. Productive Formation

More than 90 percent of the gabbro-wehrlite intrusions and all the economic Ni-Cu deposits occur within the Productive Formation (Fig. 3). The density of intrusions is directly proportional to the thickness of the host sedimentary rocks (Gorbunov et al. 1985), with the highest density occurring within the thick Productive Formation sequence in the Western Rift Graben (Melezhik et al. 1994b). The bodies lie in the uppermost Lammas Member of the Productive Formation in the western part of this graben (Kaula, Kotselvaara, Kammikivi, West Ortoaivi - western group, Fig. 2), but transgress down through the stratigraphy towards the east where they lie in Productive Formation Members A and B (East Ortoaivi, Souker, North Souker; Sputnik/Kierdzhipori, Severny and Zhdanov in the Pilgujärvi intrusions; Onki - eastern group).

The Productive Formation consists of different types of sedimentary and sedimentary-volcanic rocks, all of which carry  $\text{C}_{\text{org}}$  and iron sulphides and are



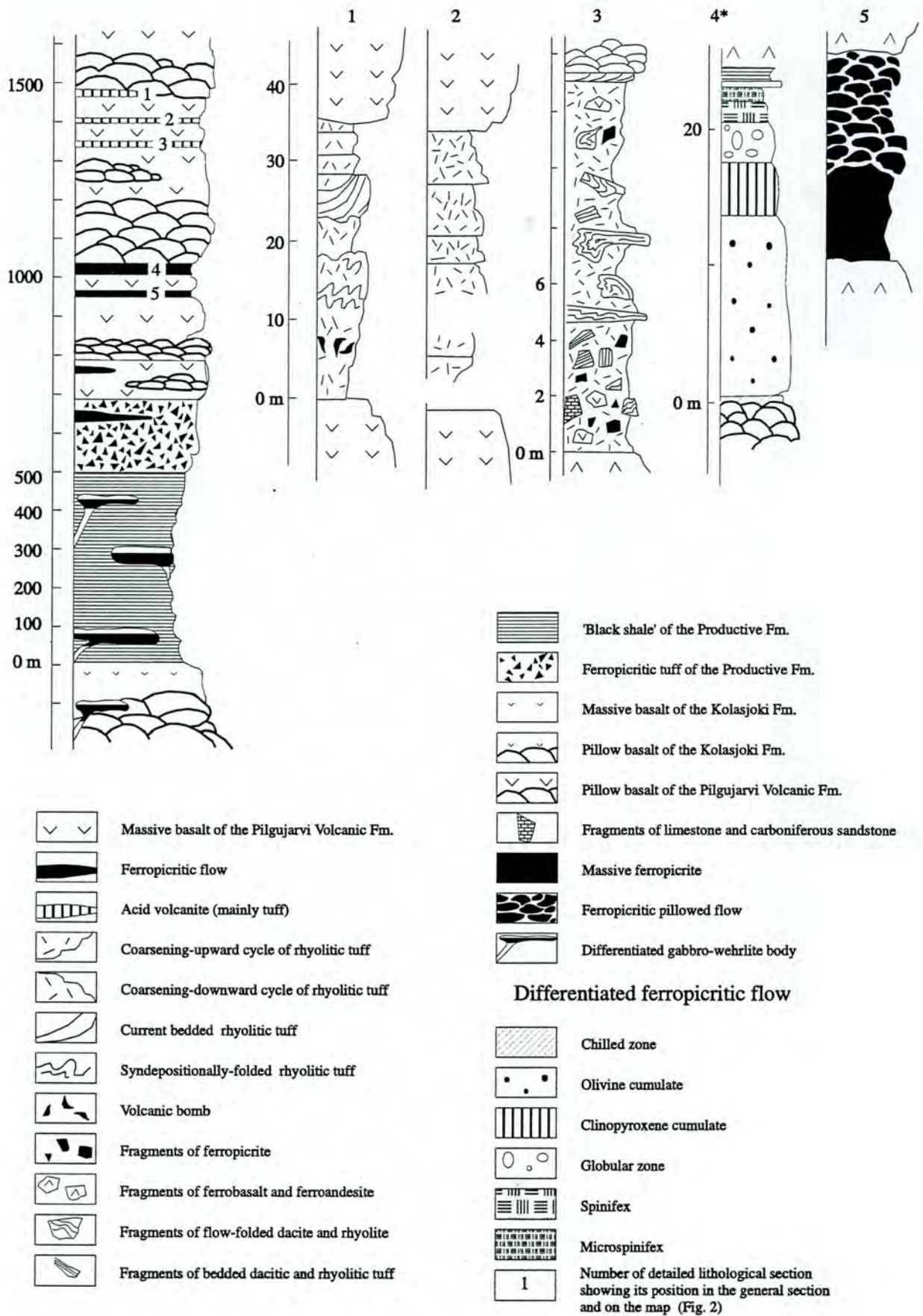


Fig. 5. Lithological sections of the 'Productive' Formation, acidic tuff horizons and ferropicritic lava flows. Locations of sections 1-5 is shown in Fig. 2. \*, Section 4 after Brüggmann et al. (1991).

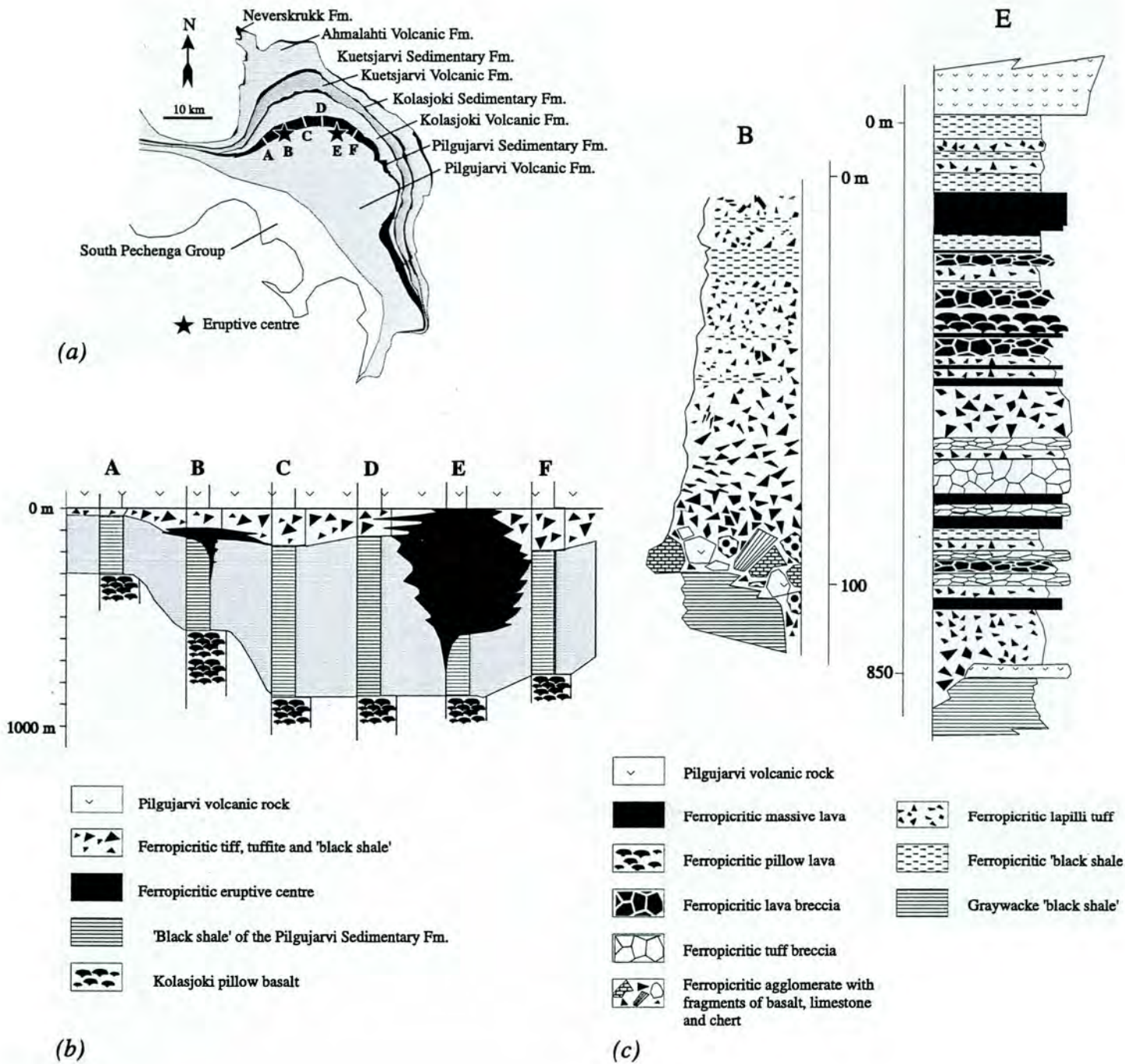


Fig. 6. Ferropicritic eruptive centres of the Pechenga Zone. (a) Locations of ferropicritic eruptive centres and lithological sections. (b) Longitudinal section (looking north) of the Pilgularvi Sedimentary Formation. (c) Lithological sections B and E of ferropicritic eruptive centres (section E modified from Skuf'in and Fedotov 1989).

Table 2. Whole-rock analyses of ferropicrites and fragments from ferropicritic explosion breccia, Kaula and Kierdzhipori Eruptive Centres, Pechenga (Melezhik et al. 1994b).

	Kaula Eruptive Centre								Kierdzhipori Eruptive Centre		
	Breccia matrix	Phosphorus limestones		Limestones		SiO <sub>2</sub> -rich rocks			Ferropicritic lava-breccia, pillowed and massive lava		
	PS-144	P-0093A	P-0093	P-0093B	P-0095L	P-0088	P-0089	P-0090A	2728/757	2728/734	2728/750
SiO <sub>2</sub>	38.96	57.94	39.23	38.26	22.67	89.42	88.14	87.31	43.81	40.61	44.02
TiO <sub>2</sub>	2.31	0.25	2.15	1.06	0.68	0.01	0.08	0.05	1.91	2.05	2.35
Al <sub>2</sub> O <sub>3</sub>	6.64	2.12	7.18	4.85	2.89	0.52	0.68	0.77	6.33	6.61	8.36
Fe <sub>2</sub> O <sub>3</sub>	17.28	4.76	3.86	5.69	2.94	2.55	0.84	0.07	3.66	3.81	3.07
FeO	n.d.	5.25	8.84	5.92	5.04	1.84	2.88	2.11	12.51	10.49	12.99
MnO	0.16	0.18	0.17	0.29	0.32	0.02	0.03	0.04	0.21	0.22	0.16
MgO	14.24	2.93	9.02	7.19	5.06	0.05	0.46	0.58	15.17	11.62	13.78
CaO	7.98	13.03	13.06	18.44	33.08	2.38	2.56	4.44	8.87	12.02	6.39
Na <sub>2</sub> O	-	0.16	0.07	0.19	0.14	0.02	0.02	0.03	0.16	0.15	0.13
K <sub>2</sub> O	0.51	0.33	0.12	0.45	0.28	0.02	0.02	0.05	0.23	0.12	0.14
H <sub>2</sub> O <sup>-</sup>	n.d.	0.31	0.48	0.75	0.36	0.09	0.12	0.17	n.d.	n.d.	n.d.
H <sub>2</sub> O <sup>+</sup>	n.d.	2.31	6.28	3.65	3.65	0.23	1.22	0.75	5.81	5.97	6.32
P <sub>2</sub> O <sub>5</sub>	0.23	4.28	2.61	0.13	0.09	0.49	0.07	-	0.21	0.18	0.25
S <sub>tot</sub>	0.22	2.21	0.98	0.19	0.07	1.49	0.83	0.14	0.62	5.42	0.94
CO <sub>2</sub>	n.d.	4.98	6.32	13.2	24.16	1.46	2.14	3.34	0.24	0.28	0.41
LOI	9.63	n.d.	n.d.	n.d.	n.d.	n.d.	n.d.	n.d.	n.d.	n.d.	n.d.
Total	98.21	99.96	99.67	100.13	99.75	99.95	99.62	99.73	100.11	99.55	99.31

LOI, loss of ignition.; n.d., not determined, *dashes*, below detection limit.

characterised by sulphur contents ranging from 0.04 to 19.5 wt%. Average sulphur concentrations are highest within the Western Rift Graben (4.5 wt%), decreasing eastwards to 0.5 wt% Melezhik et al. 1988).

The sedimentary rocks contain four temporal generations of pyrite (py) and two generations of pyrrhotite (po): py<sub>1</sub>-py<sub>2</sub>-po<sub>1</sub>-py<sub>3</sub>-po<sub>2</sub>-py<sub>4</sub> (Balabonin 1984; Melezhik et al. 1988), which can be distinguished on the basis of  $\delta^{34}\text{S}$  composition (Melezhik & Grinenko 1993; Melezhik et al. 1994b, Fig. 4a, b, c and d). Synsedimentary py<sub>1</sub> and early diagenetic py<sub>2</sub> (Fig. 4a) show very tight  $\delta^{34}\text{S}$  patterns, with two  $\delta^{34}\text{S}$  maxima between -2‰ and 0‰ and +2‰ and +4‰. The  $\delta^{34}\text{S}$  values for py<sub>3</sub> and po<sub>1</sub> of the middle stage of diagenesis (Fig. 4b) range from -8‰ to +14‰ with a maximum between -2‰ and -6‰. Late diagenetic (Fig. 3c) and catagenetic (Fig. 4d) stages produced py<sub>4</sub> and po<sub>2</sub> with similar  $\delta^{34}\text{S}$  values ranging from 0‰ to +28‰ with maxima between +8‰ and +10‰ and +6‰ and +10‰, respectively.

#### 4. Ore Deposits

All economically interesting ultramafite-hosted Ni-Cu deposits are located at Pechenga within the Western Rift Graben (Fig. 2) between the two main syndepositional faults near Kaula in the west and Pilgijärvi in the east (Fig. 2). In the west (Kaula, Kotselvaara, Kammikivi, Semiletka/West Ortoaivi, Fig. 2) the ores occur in one inter-stratal tectonic level within the ferropicritic tuffs of the Lammas Member of the Productive Formation. The deposits near the Kaula Eruptive Centre are the richest, characterised by mainly massive ores, but are also the smallest of the whole ore field. In the central and eastern areas, the ore-bearing massifs and deposits are distributed in two levels: within Member A of the Productive Formation (East Ortoaivi, North Souker and Mirona deposits), Member B of the Productive Formation (Raisoajvi, Souker deposits, intrusion 171) and both Members A and B (Sputnik/Kierdzhipori, Severny



Table 3. Whole-rock analyses of acidic tuffs, Pechenga and Pasvik (from Melezhik et al. 1994a).

	Dacite	Rhyolites								
	MZ-27♣	P-0063/0♣	87/3♣	P-0063A♣	87/82♣	MZ-29♣	MZ-25♣	MZ-26♣	PS-000*	NW00126*
SiO <sub>2</sub>	65.21	73.13	74.36	76.87	78.35	78.64	81.06	85.25	76.19	73.6
TiO <sub>2</sub>	0.41	0.34	0.19	0.89	0.28	0.26	0.33	0.21	0.54	0.6
Al <sub>2</sub> O <sub>3</sub>	13.68	10.48	11.17	6.31	8.68	8.01	6.71	5.39	10.88	10.9
Fe <sub>2</sub> O <sub>3</sub>	2.72	0.96	0.21	2.15	0.52	1.21	2.85	0.66	-	6.42
FeO	4.88	4.65	4.21	5.49	3.11	2.91	2.23	2.25	2.29	n.d.
MnO	0.11	0.09	0.03	0.11	0.03	0.05	0.05	0.03	0.02	0.09
MgO	1.22	0.95	1.42	0.97	0.56	0.21	0.23	0.15	0.47	0.85
CaO	0.62	0.81	0.61	1.01	0.38	2.32	0.59	3.33	1.51	1.2
Na <sub>2</sub> O	2.46	2.56	4.29	0.19	0.09	0.91	1.95	0.05	3.03	2.41
K <sub>2</sub> O	5.97	3.94	1.69	3.08	6.59	3.52	2.54	1.58	1.51	2.24
H <sub>2</sub> O <sup>-</sup>	0.12	0.23	n.d.	0.29		0.04	0.12	0.03	0.14	n.d.
H <sub>2</sub> O <sup>+</sup>	2.09	1.47	n.d.	1.97	0.09	1.13	0.75	0.95	0.46	n.d.
P <sub>2</sub> O <sub>5</sub>	0.09	0.05	0.02	0.04	0.49	0.05	0.07	0.02	0.03	0.04
S <sub>tot</sub>	-	0.05	0.11	0.23	0.09	-	0.23	-	0.72	n.d.
CO <sub>2</sub>	0.05	0.18	0.45	0.04	0.49	0.36	0.19	0.27	0.17	n.d.
LOI	n.d.	n.d.	n.d.	n.d.	n.d.	n.d.	n.d.	n.d.	n.d.	1.39
Total	99.63	99.93	100.09	99.65	100.63	99.65	99.81	100.17	99.43	100

♣Pechenga samples.

\*Pasvik samples.

LOI, loss of ignition.

n.d., not determined; *dashes*, below detection limit.

and Zhdanovskoe in the Pilgujärvi intrusions, Onki). The largest Pechenga deposits (Sputnik/Kierdzhipori, Severny and Zhdanovskoe) occur within the Pilgujärvi intrusion near the Kierdzhipori Eruptive Centre, and contain the bulk of the district's disseminated ores.

All commercial ores are associated with mafic-ultramafic bodies and located in their lowermost portion. Ore bodies are characterised by very uniform morphology. They are either lenses or beds. The ore bodies strike from 400 to 2000 m and dip from 300 to 3000 m although in the Zdanovskoe deposit commercial ores have been intersected at the depth of 3500 m and apparently continue to dip. The thickness of ore bodies ranges from 100 to 120 m.

The main ore-forming minerals are monoclinic and hexagonal pirrotite (60-70 wt. %), pentlandite, chalcopyrite and magnetite. The minor minerals are pyrite violarite, sphalerite, bornite, cubanite, mackinawite, valleriite and platinum group minerals (Distler et al. 1990). All the Pechenga ores were

subjected to metamorphic and metasomatic alterations which led to the development of 3 to 4 generations of the main ore minerals.

Gorbulov (1968) described four types of Ni-Cu ore: ultramafic-hosted massive, brecciated massive and disseminated sulphide Ni-Cu ores and 'black shale'-hosted stringer predominantly sulphide Cu ores.

Disseminated syngenetic ores are the most voluminous, 70-80% in volume. They associate with peridotite portion of the differentiated ultramafic bodies and differ in sulphide content and grain-size of sulphide minerals. The sulphide content gradually increase towards the lower contact of ultramafic bodies. Low-grade disseminated ores contain 6-15% of sulphides and 0.3-0.8 wt % Ni. Sulphide and Ni concentrations in densely disseminated ores range from 15 to 45% and from 1.5 to 3.8 wt. % respectively. The grain sizes of sulphides vary from 0.0n to 15 mm. The unaltered disseminated ores are characterised by the sideronitic texture.

Table 4. Whole-rock analyses of fragments from acidic tuffs, Pechenga (from Melezhik et al. 1994a).

	Basaltic ferropicrites			Basalt		Ferrobasalts			Ferroandesites			SiO <sub>2</sub> -rich rocks(?)	
	87/1	SK-1	87/1A	SK-2	87/41	87/66	87/78	SK-3	73/6-7	1204/1	SK-1	SK-2	
SiO <sub>2</sub>	40.21	40.69	41.01	48.83	49.01	49.26	50.97	58.58	58.62	60.23	84.75	90.42	
TiO <sub>2</sub>	0.11	0.19	0.27	3.18	1.61	1.56	1.31	1.82	0.77	1.72	0.45	0.25	
Al <sub>2</sub> O <sub>3</sub>	15.88	15.52	15.11	13.45	12.77	9.98	12.82	12.19	8.87	13.19	3.39	1.71	
Fe <sub>2</sub> O <sub>3</sub>	5.01	5.88	6.16	3.62	3.09	2.41	1.52	1.91	2.85	2.91	1.45	0.85	
FeO	17.76	16.97	16.18	7.55	11.91	11.13	11.16	8.68	6.37	7.77	2.33	2.77	
MnO	0.21	0.21	0.21	0.21	0.21	0.16	0.21	0.11	0.12	0.08	0.04	0.04	
MgO	8.31	8.34	8.38	2.12	6.01	6.12	6.05	3.71	4.56	2.61	1.01	0.97	
CaO	0.34	0.39	0.45	6.91	7.88	8.28	7.77	2.91	9.21	3.02	2.14	0.89	
Na <sub>2</sub> O	0.82	0.65	0.47	2.51	2.75	0.34	4.06	2.52	0.35	1.66	1.22	0.11	
K <sub>2</sub> O	1.93	2.11	2.27	4.14	0.21	0.59	0.49	2.12	0.07	2.82	0.57	0.02	
H <sub>2</sub> O-	0.57	0.42	0.31	0.43	0.15	0.24	0.19	0.31	0.12	0.21	0.11	0.14	
H <sub>2</sub> O+	-	8.31	8.48	3.44	3.67	4.24	2.21	3.92	3.81	3.34	1.31	1.21	
P <sub>2</sub> O <sub>5</sub>	0.01	0.03	0.04	0.48	0.21	0.41	0.13	0.07	-	0.16	0.11	-	
S <sub>tot</sub>	0.06	0.04	0.02	0.23	0.03	0.11	0.14	0.16	-	0.19	0.02	0.21	
CO <sub>2</sub>	0.31	0.22	0.15	2.93	-	3.21	0.35	0.95	4.21	0.14	1.11	0.43	
Total	100.03	99.97	99.61	100.03	100.47	99.34	99.31	99.96	99.93	100.01	100.01	100.02	

Dashes, below detection limit.

The richest Ni ores are the syngenetic massive ores. They together with brecciated massive ores do not exceed 5-30% in volume. Ultramafite-hosted breccia ores are spatially related to the massive ores, and together they form 0.5 to 11 m thick bodies occurring at the bases of the differentiated gabbro-wehrlite bodies. In some cases the massive and brecciated massive ores may be implaced in strike-slip zone within 'black shales'. Ore bodies are contiguous with, and extend up to 1000 m along strike from, ultramafic-hosted massive and breccia sulphide ore bodies.

Massive and brecciated massive ores contain 45-98% of sulphides. The Ni concentrations range from 2.5 to 12 wt. %. The breccia ores are composed of rounded fragments of serpentinite, densely disseminated ores and 'black shales' in a sulphide matrix identical to the massive ore.

In some places 'black shales' bordering on ultramafic bodies may be also mineralised This represents the fourth major ore type: the Productive Formation black shale-hosted, stringer, remobilised metasomatic-metamorphic ore. Ore bodies are contiguous with, and extend up to 400 m along strike

from, massive and breccia sulphide ore bodies. The shale-hosted ores are dominated by chalcopyrite, with grades up to 10 wt% Cu (Gorbunov et al. 1985).

All ore bodies contain all four ore types, although there are deposits which are only represented by the massive and/or massive brecciated ore types. The average nickel and copper concentrations gradually increase from the eastern group of deposits towards the western ones as indicated in Table 5.

Table 5. Westwards increase in the average nickel concentrations in ultramafic-hosted sulphide Ni-Cu ores.

Deposit	Ni, wt %
Sputnik-Kierdzhipori-Severny-Zdanovskoe	0.65
Semiletka	0.99
Kotselvaara-Kammikivi	1.23
Kaula	3.25

The average ratio of nickel, copper and cobalt in ultramafic-hosted sulphide Ni-Cu ores is

1:0.5:0.038. This entirely differs from that of 'black shale'-hosted ore which is 1:1.0:0.02.

$\delta^{34}\text{S}$  values of ores and their host intrusion/flows are comparable (Fig. 4e and f, 4k and l, 4m and n, 4o and 4p). The western group of deposits and their hosts are characterised by near chondritic  $\delta^{34}\text{S}$  values ranging from -3‰ to +6‰ with maxima between 0‰ and +2‰ (Fig. 4i, j, k, l, m and n, Grinenko & Smol'kin 1991). All of the eastern deposits and their hosts (Fig. 4e, f, g and h) are marked by heavier  $\delta^{34}\text{S}$  values (+1‰ to +8.5‰, Grinenko et al. 1967) and maxima between +2‰ and +6‰. There are no differences in  $\delta^{34}\text{S}$  composition between ore-bearing (Fig. 4e, k and m) and barren (Fig. 4g, h and j) intrusions of both groups.

There are no essential differences in  $\delta^{34}\text{S}$  values between ultramafite-hosted disseminated, massive and brecciated ores (Fig. 4, Grinenko et al 1967). They display narrow  $\delta^{34}\text{S}$  ranges: -4‰ to +4‰ in the western group (Fig. 4j, k and m), and 0‰ to +8‰ in the eastern group bodies (Fig. 4e, g and h, Grinenko & Smol'kin 1991). All ores in footwall sediments show a wider  $\delta^{34}\text{S}$  range from -6‰ to +10‰.

Until recently, Pechenga sulphide ore was thought to be associated only with the ultramafic part of differentiated gabbro-wehrlite intrusions (Gorbunov 1968; Zak et al. 1982). However, Korchagin (Gorbunov et al. 1989) discovered a 3.2 m thick, differentiated basaltic ferropicrite flow within the Lammas Member south of Kierdzhipori (Table 6), hosting 0.45 m of massive ore (2.14-4.87 wt% Ni, 0.96-2.04 wt% Cu, 0.05-0.11 wt% Co, 32.1-32.4 wt% S) overlain by 1 m of disseminated ore (0.57 wt% Ni, 0.25 wt% Cu, 0.025 wt% Co, 0.02 wt% Zn, 4.4 wt% S) (Fig. 7). Disseminated Ni-Cu ore at the base of a 40 m thick, differentiated ferropicritic flow or sill was also discovered at Kammikivi (Fig. 7, Hanski 1992). Both the Kierdzhipori and Kammikivi bodies are located within ferropicritic tuffs of the Lammas Member near the Kierdzhipori and Kaula ferropicritic explosion centres, respectively (Fig. 2). These ferropicritic flow-hosted ores (Fig. 4o) have similar  $\delta^{34}\text{S}$  signatures to the gabbro-wehrlite-hosted western group ores (Fig. 4i, l) and n), and to unmineralised Productive Formation and Pilgjarvi Formation-hosted ferropicrite flows (Fig. 4g, p and q) and gabbro-wehrlites (Fig. 4j, k and m).

## 5. Discussion

### 5.1. Host and associated rocks

Pechenga Ni-Cu ores are located mainly within the ultramafic portions of differentiated gabbro-wehrlite

intrusions, and less so at the bases of ferropicrite ultramafic volcanic flows. Strongly negatively-sloped chondrite-normalised REE patterns of these host rocks are identical to those of spatially-related rhyolitic tuffs, their ferrobasaltic fragments, and of other ferropicrites occurring at different stratigraphic levels in the Pilguärvi Sedimentary and Volcanic Formations (Fig. 12, Melezhik 1996, this volume), suggesting that all of these rocks originated from the same parental magma (eg. Hanski 1992).

Table 6. Whole-rock analyses of Ni-Cu-bearing ferropicritic flow, Kierdzhipori (Gorbunov et al. 1989).

	1	2	3
SiO <sub>2</sub>	53.65	28.51	47.73
TiO <sub>2</sub>	2.74	3.03	2.15
Al <sub>2</sub> O <sub>3</sub>	7.01	13.88	6.41
Fe <sub>2</sub> O <sub>3</sub>	6.31	4.73	4.29
FeO	5.88	13.71	12.59
MnO	0.11	0.14	0.09
MgO	7.89	14.97	8.08
CaO	6.22	6.67	5.98
Na <sub>2</sub> O	0.01	0.01	0.04
K <sub>2</sub> O	0.01	0.01	0.03
P <sub>2</sub> O <sub>5</sub>	0.16	0.26	0.19
S <sub>tot</sub>	1.42	0.77	4.43
CO <sub>2</sub>	3.19	3.15	3.21
Cr	0.06	0.05	0.29
Ni	0.02	0.02	0.57
Cu	0.01	0.02	0.25
Co	0.004	0.004	0.025
V	-	-	0.05
LOI	6.03	10.41	5.23
Total	100.02	99.95	99.42

1, Globules of gloular ferropicrites; 2, matrix of globular ferropicrites; 3, massive part of flow.

LOI, loss on ignition.

Dashes, below detection limit.

The ultramafic volcanic rocks have been classified chemically as 'ferropicrites' (Hanski & Smol'kin 1989; Hanski 1992), and have been shown to have similar geochemical characteristics as the gabbro-wehrlite bodies (Table 1). Ferropicrites, like komatiites, have high MgO contents, but unlike komatiites, they have high FeO<sub>i</sub> and TiO<sub>2</sub>, first-series transition metal and incompatible element



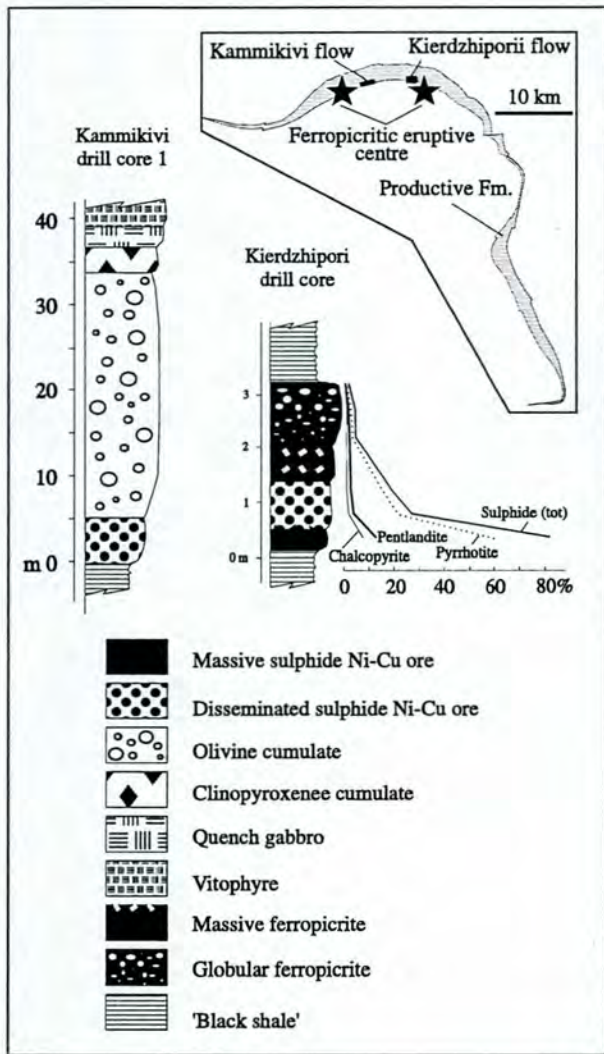


Fig. 7 Ni-Cu-bearing ferropicritic flows, Pechenga (Kammikivi flow after Hanski and Smol'kin 1990; Kierdzhipori flow after Gorbunov et al. 1989). *Inset*, location map.

concentrations and strongly negatively sloped chondrite-normalised REE patterns. Some of these contrasts are illustrated in Fig. 8, which compares Pechenga-Pasvik gabbro-wehrlites and ferropicrites with komatiitic, nickeliferous host rocks from the Lower Proterozoic Thompson area, Manitoba (Peredery 1979) and the Lower Proterozoic Cape Smith Belt, northern Quebec, Canada (Barnes et al. 1982).

Campbell et al. (1989) suggested that Archaean high-Mg komatiites were produced by melting in the high-temperature axis of a starting mantle plume and that their depleted geochemical and isotopic signatures implied that their related plumes would originate from a MORB-like mantle source. In the post-

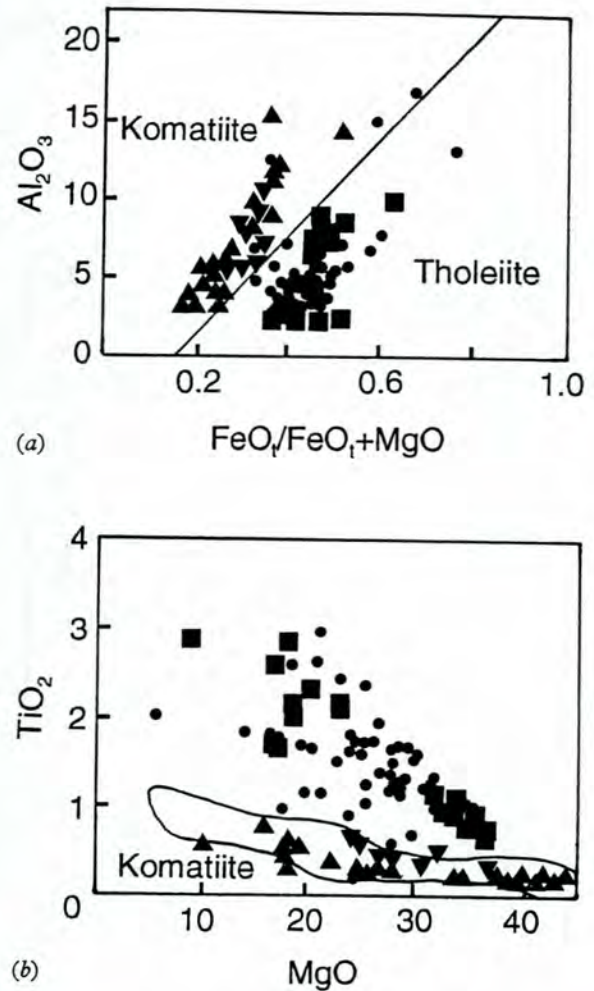


Fig. 8 Ultramafic rocks from Pasvik (*dots*), Pechenga (*squares*), Thompson (*triangles*) and Cape Smith (Raglan) (*inverted triangles*) plotted on diagrams of (a)  $\text{Al}_2\text{O}_3$  versus  $\text{FeO}_4/\text{FeO}_1 + \text{MgO}$  and (b)  $\text{TiO}_2$  versus  $\text{MgO}$  (from Melezhik et al 1994b).

Archaean, the source for mantle hotspots changed to more enriched OIB-source mantle, reflected in continental flood basalt provinces (Campbell & Griffiths 1992). Hofmann and White 1982) proposed that the OIB source could have been a component of a subducted oceanic slab. Campbell and Griffiths (1992) further refined and investigated these models, observing the change in the maximum MgO content of the komatiitic and picritic magmas from approximately 33 wt% in the Archaean to less than 22 wt% MgO in younger magmas.

The Pechenga-Pasvik ferropicrites and gabbro-wehrlites, though physically and geochemically similar to komatiites, are enriched in certain major and incompatible trace elements such as REE, suggesting that they may have originated from an enriched mantle source, possibly contaminated by

subducted lithosphere rather than OIB. Hanski (1992) attempted to apply the plume model of Campbell and Griffiths (1990) to the Pechenga ferropicrites but noted a number of inconsistencies in the available data and left the application to future research.

Barley and Groves (1992) showed that the major classes of metallic mineral deposits can be related to the timing of cyclic formation and breakup of the continents, as far back as at least 2700 Ma. The Pechenga ferropicrites, gabbro-wehrlites and related Ni ores formed during the 2000 Ma supercontinental rifting period (Barley & Groves 1992). Their enriched nature suggests that they may represent the earliest evidence of lithosphere subduction and recycling. However, depleted MORB-like komatiitic sources were still present at 2000 Ma, reflected in the Cape Smith and Thompson nickeliferous host rocks.

Campbell and Griffiths (1990, 1992) interpreted the absence of enriched or OIB-type plumes in the Archaean to reflect the length of time required for oceanic crust to be recycled through the mantle and provide source material for future plumes. In the Early Proterozoic, depleted komatiites such as those in the Manitoba and Cape Smith Belts were still forming, but in the Phanerozoic only one rare exception (Gorgona Island of Tertiary age) is known. Pechenga thus represents the oldest known example of the enriched OIB plume type.

## 5.2. Sulphur source

Although the mode of formation of the Ni-Cu ores of the gabbro-wehrlite intrusions has been ascribed to a magmatic immiscibility model (Gorbunov 1968; Väyrynen 1938) like the 'billiard ball' model proposed by Naldrett (1973), the sulphur source remains enigmatic. Grinenko et al. (1967) and Pushkarev et al. (1988) suggested, on the basis of sulphur and lead isotopic studies, a predominantly mantle sulphur source for the Ni-Cu sulphide ores, except for the deposits hosted by the Pilguyarvi intrusion which may have incorporated a component of crustal sulphur. Grinenko and Smol'kin (1991) considered that the ultramafic magmas were subjected to sulphur contamination in magma chambers located somewhere beneath the Pechenga rift. According to their model, sulphides in economically interesting deposits were the result of contamination by Archaean crustal material containing chondritic sulphur, whereas sulphides in barren intrusions, the Kierdzhipori and Pilguyarvi ore-bearing intrusions and ferropicritic flows were produced by contamination by sulphur derived from non-Pechenga Proterozoic rocks. Hanski (1992) concluded that the Kaula, Kotselvaara and Kammikivi ores were juvenile in origin, but the

Pilguyarvi intrusion and its ores were a product of assimilation of country rocks by the magma.

These models did not take into account the temporal  $\delta^{34}\text{S}$  evolution of sulphides in the Productive Formation (Fig. 4a, b, c and d) and cannot explain the widely varying published  $\delta^{34}\text{S}$  values of 'syngenetic' ore sulphides: +1‰ to +3‰ (Akhmedov & Krupenik 1990), +11‰ to +15‰ (Hanski 1992), -4‰ to +10‰ (Grinenko & Smol'kin 1991) and -8‰ to +28‰ (Melezhik & Grinenko 1993).

Background sulphur isotope compositions and sulphur contents for all species of ultramafic rock are  $-0.5 \pm 1.5\text{‰}$  and 0.05 to 0.15 wt% (Al'mukhamedov & Medvedev 1982). The widely varying  $\delta^{34}\text{S}$  compositions listed above, and above-background average sulphur contents of both ferropicritic flows (0.20 wt%) and intrusions (0.20 to 0.37 wt%) suggest that the ferropicritic magmas were subjected to sulphur contamination in amounts corresponding to 25 wt% (flows) and 25 to 60 wt% (intrusions), not taking into account the ore sulphur.

All economic deposits in the Western Rift Graben are hosted by the most sulphur-rich (4.5 wt%) Productive Formation sedimentary rocks, suggesting that Productive Formation sulphur may have been the ore sulphur source. If true, then the initial juvenile ultramafic magma sulphur ( $-0.5 \pm 1.5\text{‰}$   $\delta^{34}\text{S}$ ) would be affected by assimilation of Productive Formation sulphides. These could be syngenetic to early diagenetic (-4 to +4‰, Fig. 4a), middle diagenetic (-8 to +14‰, Fig. 4b), and/or late diagenetic/catagenetic (0 to +28‰, Fig. 4c and d) sulphides.

The ferropicritic flows (Fig. 4p and q) and their ores (Fig. 4o) show  $\delta^{34}\text{S}$  ranges similar to syngenetic and early diagenetic Productive Formation sulphides, which can be explained by the physical extrusion mechanism of the flows onto relatively unconsolidated sediments. Pilguyarvi Volcanic Formation-hosted ferropicritic flows (Fig. 4q) and spatially associated black shales (Fig. 4r) show similar features.

The placement of the intrusions into the consolidated sediments implies that if they assimilated sedimentary sulphur, they would have  $\delta^{34}\text{S}$  contents reflecting an average between all of the Productive Formation sulphide diagenetic stages (ie., between ca. +2 and +8‰).  $\delta^{34}\text{S}$  contents of the eastern group of intrusions and ores (Fig. 4e, f, g and h) show this range, but the western intrusions and ores (Fig. 4i, j, k, l, m and n) have  $\delta^{34}\text{S}$  ranges (-3 to +6‰) similar to the syngenetic and early diagenetic sulphides only (Fig. 4a).

The high sulphide concentrations in the western deposits cannot be explained by sulphide liquid segregation from a single intrusive body and thus require either an independent injection of sulphide liquid derived from a greater volume of magma (Gorbunov 1968), or a dynamic flow regime such as that described for Australian Kambalda-type Ni-Cu deposits (Barnes et al. 1988a, 1988b, 1988c; Groves & Lesher 1981; Lesher et al. 1984). The latter mechanism involves voluminous eruption of ultramafic magmas into rift-phase greenstone belts, forming large and channelised flows that assimilate varying amounts of sulphidic footwall rocks during emplacement. The Kierdzhipori ore-bearing, differentiated ferropicritic flow (Fig. 7) provides evidence to support such a model at Pechenga, and the model can be applied to all the western differentiated 'intrusions', which generally are difficult to distinguish from differentiated flows. Even though evidence of thermal erosion by ferropicritic flows has not yet been described at Pechenga, the dynamic flow regime model answers several questions regarding orebody origins: (1) the location of the 'intrusions' in the uppermost part of Productive Formation, (2) the temporal and spatial association of the 'intrusions' with major ferropicritic explosion events; (3) the most massive and richest ores occurring in these 'intrusions' and (4) the similarity of  $\delta^{34}\text{S}$  composition between the 'intrusions' and their ores and true ferropicritic flows and their ores.

Grinenko and Smol'kin (1991) noted increases in  $\delta^{34}\text{S}$  near the lower contacts of the Northern Kotselvaara ultramafic body (Fig. 4j), of the Pilgijärvi intrusion (Fig. 4e) and of the ferropicritic flows in the Pilgijärvi Volcanic Formation (Fig. 4q), and attributed these to contamination by the underlying sediments during extrusion or intrusion. They also documented increases in  $\delta^{34}\text{S}$  near the upper contacts of ferropicritic flows (Fig. 4q). These features cannot be explained only by contamination by the underlying sediments, as shown by black shales (0 to +2‰  $\delta^{34}\text{S}$ , Fig. 4r) associated with the Pilgijärvi Volcanic Formation ferropicritic flows (lower margins +4 to +6‰, Fig. 4q). Hanski (1992) suggested that the elevated  $\delta^{34}\text{S}$  contents in the marginal zones were formed during metamorphism. There is substantial evidence to support this: (1) the great  $\delta^{34}\text{S}$  range and isotopically heavy sulphur of the metamorphic-metasomatic Ni-Cu ores (Fig. 4e) and n); (2) the similarity of ferropicritic flow and intrusion marginal sulphides to those of (1), above; and (3) the variation in  $\delta^{34}\text{S}$  of the late diagenetic to catagenetic Productive Formation sulphides.

The sulphide characteristics of the Pechenga ore deposits and their hosts can thus be attributed to (1)

local contamination by different diagenetic Productive Formation sulphides, through assimilation both during intrusion and during dynamic volcanic flow and thermal erosion, and (2) metamorphism in the marginal zones of the host and barren bodies.

## 6. Ore Deposit Model

A model for the formation of the Pechenga Ni-Cu ore bodies is presented in Fig. 9. Four thick sedimentary-volcanic cycles were deposited from 2400 to 1970 Ma ago on consolidated Archaean basement in the intercontinental Western Rift (Fig. 2) of the Pechenga Rift Zone. The last magmatic event controlled by and occurring within this graben was the intrusion and violent extrusion of ferropicritic magmas from 1990 to 1970 Ma. These magmas migrated upwards through continental crust along deep-seated, graben-bounding, syn-sedimentary faults, and on emplacement or extrusion, assimilated more than 25 to 60 percent of their sulphur from  $C_{\text{org}}$ - and S-bearing Productive Formation black shales. Ferropicritic flows were contaminated by synsedimentary to early diagenetic sulphur from unconsolidated sediments of the Productive Formation with mean values between 0‰ and +2‰, and intrusions were contaminated by sulphides from consolidated black shales with average  $\delta^{34}\text{S}$  values between +4‰ and +6‰. Upon reaching the surface or near-surface, the magmas cooled and crystallised, with massive Ni-Cu sulphide ores coalescing at the bases of ultramafic bodies hosted within black shales and ferropicritic tuffs of the Productive Formation, and within the Kolasjoki Volcanic Formation along the Kolasjoki Fault, and disseminated ores forming stratigraphically above the massive ores. The ores are located both in the basal ultramafic portions of differentiated gabbro-wehrlite intrusions (eastern group) and in the basal portions of differentiated ferropicritic flows (western group).

The highest grade ores are located within the Western Rift Graben near the major transversal syn-sedimentary faults and two ferropicritic explosion centres at Kaula and Pilgijärvi. Ferropicritic magmatic activity also produced ferropicritic explosion material (Lammas Member), which overlies the Member A and B sediments of the Productive Formation, and which is most voluminous nearest the major syn-sedimentary faults and the economic Ni-Cu deposits at Kaula-Kotselvaara and Pilgijärvi (Fig. 2).

The final stage of ferropicritic volcanism was spatially and temporally associated with a short-term rhyolitic explosive event, which brought fragments of partially melted Archaean crustal material and



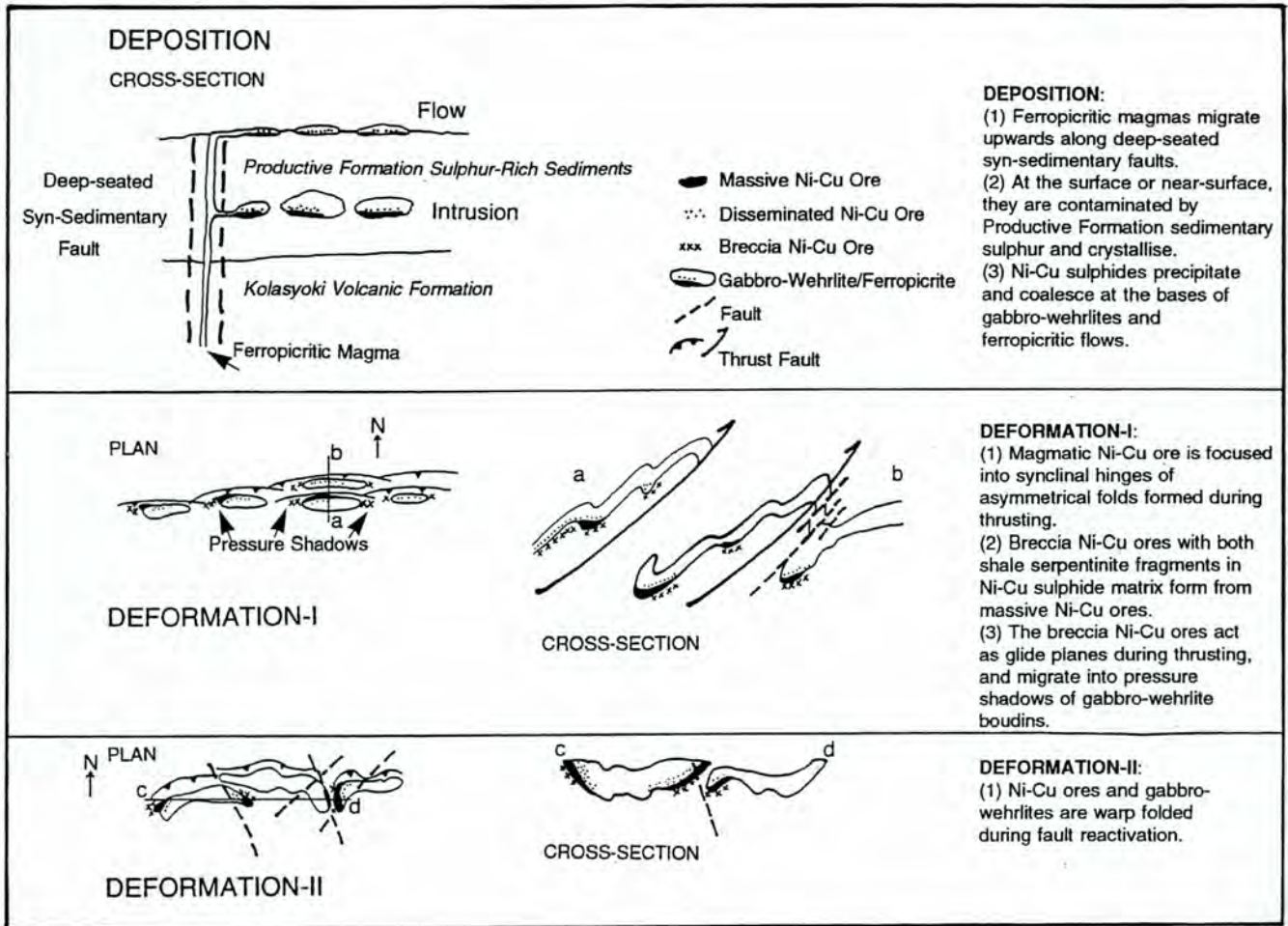


fig. 9 Schematic model of formation of Pechenga ultramafic-hosted sulphide Ni-Cu ore deposit (from Melezhik et al. 1994b).

remnants of ferropicrite-ferrobasalt-ferroandesite-ferrodacite-ferrorhyolite volcanic association up from great depths. These fragments provide further evidence for the existence of continental crust beneath the Pechenga rift at 1970 Ma ago and support the intercontinental rift Pechenga Group model presented in Melezhik et al. (1994a).

Primary deformation is represented by northward-verging thrusting, cleavage development, boudinage and north-verging asymmetrical folding with axial planes that dip to the south at 35° to 60° and resulted in the localisation of all economically interesting deposits to

the troughs of synclinal asymmetric folds (Gorbunov 1968). Breccia ores with round serpentinite fragments in a nickel-copper sulphide matrix formed from the massive ores and migrated subsequently into the pressure shadows of ultramafic boudins. Sulphides were also mobilised into adjacent sedimentary rocks along fault planes. Secondary deformation is characterised by open folding, as well as by boudinage caused by northeast-trending brittle-ductile shearing and faulting, on earlier syn-sedimentary fault systems (Hudson et al. 1992).

## References

- Akhmedov A. M. and Krupenik V. A. 1990: Turbidity regimes of the sedimentation and pyrite-forming processes in the Early Proterozoic Pechenga Basin. *Soviet Geol.*, 11, 51-60 (in Russian).
- Al'mukhamedov A. I. and Medvedev A. Ya. 1982: *Sulphur Geochemistry in Processes of the Basic Magma Evolution*. Moscow, Nauka (in Russian).
- Bakushkin Ye. M. *et al.* 1990: Mountain General'skaya. In: Mitrofanov. F. P. & Balashov Yu. A. (eds), *Geochronology and Genesis of the Layered Basic Intrusions, Volcanites and Granite-Gneisses of the Kola Peninsula*. Apatity, 14-15. (in Russian).
- Balabonin N. L. 1984: *Mineralogy and Geochemistry of the Iron Sulphide Deposits (North-West of the Kola Peninsula)*. Apatity. (in Russian).
- Barley M. E. and Groves D. I. 1992: Supercontinent cycles and the distribution of metal deposits through time. *Geology*, 20, 291-294.
- Barnes S. J. Coats G. J. A. and Naldrett A. J. 1982: Petrogenesis of a Proterozoic nickel-sulfide-komatiite association, the Katiniq Sill, Ungava, Quebec. *Econ. Geol.*, 77, 413-429.
- Barnes S. J. Gole M. J. and Hill R. E. T. 1988: The Agnew nickel deposit, Western Australia: Part I. Structure and stratigraphy. *Econ. Geol.*, 83, 524-537.
- Barnes S. J. Gole M. J. and Hill R. E. T. 1988: The Agnew nickel deposit, Western Australia: Part II. Sulfide geochemistry, with emphasis on the platinum-group elements. *Econ. Geol.*, 83, 537-550.
- Barnes S. J. Hill R. E. T. and Gole M. J. 1988: The Perserverance ultramafic complex, Western Australia: The product of a komatiite lava river. *J. Petrol.*, 29, 305-331.
- Boyd R. and Nixon F. 1985: Norwegian nickel deposits: a review. *Geol. Surv. Finland Bull.*, 333, 363-394.
- Brüggemann G. E. Hanski E. J. and Smolkin V. F. 1991: Geology and geochemistry of volcanic rocks and nickel-bearing intrusions of the Pechenga Complex, Kola Peninsula, USSR. In Naldrett A. J. (ed), *Ore Deposits Course*, University of Toronto, December 1991, Chapter 8.
- Campbell I. H. and Griffiths R. W. 1990: Implications of mantle plume structures for the evolution of flood basalts. *Earth Planet. Sci. Lett.*, 99, 79-93.
- Campbell I. H. and Griffiths R. W. 1992: The changing nature of mantle hotspots through time: implications for the chemical evolution of the mantle. *J. Geol.*, 92, 497-523.
- Campbell I. H. Griffiths R. and Hill R. I. 1989: Melting in an Archaean mantle plume: heads its basalts, tails its komatiites. *Nature*, 339, 697-699.
- Chadwick J. Russia's Pechenganikel. 1992: *Mining Mag.*, May, 270-274.
- Distler V. V. *et al.* 1990: Platinum-group elements in the copper-nickel ores of the Pechenga ore field. *Int. Geol. Rev.*, 32, 83.
- Eliseev N. A. *et al.* 1961: *Ultramafic and Mafic Intrusions of Pechenga*. Leningrad, the USSR Academy of the Sciences. (in Russian).
- Gorburnov G. I. 1968: *Geology and origin of the copper-nickel sulphide ore deposits of Pechenga (Petsamo)*. Moscow, Nedra, 352 pp. (in Russian).
- Gorburnov G. I. Korchagin A. U. and Mednikov A. I. 1989: Metalliferous picrites in Pechenga. *Trans. USSR Acad. Sci.*, 304, 1205-1208. (in Russian).
- Gorburnov G. I. *et al.* 1985: The Nickel Areas of the Kola Peninsula. *Geol. Surv. Finland Bull.*, 333, 41-121.
- Grinenko L. N. and Smol'kin V. F. 1991: Isotopic composition and content of sulphur in the ferropicrites and gabbro-wehrlites of the Pechenga zone. *Geochemistry*, 9, 1250-1261. (in Russian).
- Grinenko L. N. Grinenko V. A. and Lyakhnitskaya I. V. 1967: Isotopic composition of sulphides of the Kola Peninsula Ni-Cu deposits. *Geology of the Ore Deposits*, 4, 3-17. (in Russian).
- Groves D. I. and Lesher C. M. (eds) 1981: Regional geology and nickel deposits of the Norseman-Wiluna Greenstone Belt, Western Australia. Publication 7, University of Western Australia Department of Geology and Extension Service, Perth, 234 p.
- Hanski E. J. 1992: Petrology of the Pechenga ferropicrites and cogenetic, Ni-bearing gabbro-wehrlite intrusions, Kola Peninsula, Russia. *Geol. Surv. Finland Bull.*, 367.
- Hanski E. J. and Smolkin V. F. 1989: Pechenga ferropicrites and other Early Proterozoic picrites in the eastern part of the Baltic Shield. *Precambrian Res.*, 45, 3-82.
- Hanski E. J. and Smol'kin V. F. 1990: Thick, layered ferropicritic flows in the Pechenga area and their relation to associated Ni-Cu deposits. *Volcanological Congress*, 3-8. September, Mainz (FRG), Abstracts.
- Hanski E. *et al.* 1990: The age of the ferropicritic volcanics and comagmatic Ni-bearing intrusions at Pechenga, Kola Peninsula, USSR. *Bull. Geol. Soc. Finland*, 62, 123-133.
- Hofmann A. W. and White W. M. 1982: Mantle plumes from ancient ocean crust. *Earth Planet. Sci. Lett.*, 57, 421-436.
- Hudson K. A. Melezhik V. A. and Green A. H. Potential for Pechenga-type Ni-Cu deposits in Pasvik, northern Norway. Abstract *Geology in Europe and Beyond* Instn Min. Metall., April 22-23, 1992.
- Lesher C. M. Arndt N. T. and Groves D. I. 1984: Genesis of komatiite-associated nickel sulphide deposits at Kambalda, Western Australia: A distal volcanic model. In: Buchanan D. L. and Jones M. J. (eds), *Sulphide deposits in mafic and ultramafic rocks*. Proceedings of International Geological Correlation Program Projects 161 and 91, Third Nickel Sulphide Field Conference, Perth, Western Australia, Inst. Min. Metall., London, 70-80.
- Melezhik V. A. *Early Proterozoic Sedimentary and Sedimentary Rock-Forming Basins of the Baltic Shield (Problems of the Reconstructions of Postsedimentary Processes)*. Nauka, St. Petersburg, 1992. (in Russian).
- Melezhik V. A. 1996: General geology and evolutionary history of the Early Proterozoic Pechenga Greenstone Belt. In: Melezhik V.A. & Often M. (eds), *Field Trip Guidebook "The Geology and Ore Deposits of the Pechenga Greenstone Belt*. International Field Conference and Symposium, IGCP Project 336, Norway, Trondheim.

- Melezhik V. A. and Grinenko L. N. 1993: Depositional and diagenetic  $\delta^{34}\text{S}$  signatures in 2.0 Ga-old 'black shales': isotopic constraints for the sulphur source of ultramafic-hosted Ni-Cu sulphide ore, Pechenga, Russia. *1st International Symposium on Applied Isotope Geochemistry*, Institut for energiteknikk, 29. August - 3. September, 1993, Abstracts.
- Melezhik V. A. et al. 1988: *Carbonaceous Deposits of Early Stages of the Earth's Evolution (Geochemistry and Conditions of Accumulation on the Baltic Shield)*. Nauka, Leningrad. (in Russian).
- Melezhik, V.A., Hudson-Edwards, K.A., Green, A.H. & Grinenko, L.I. 1994b: The Pechenga area, Russia. Part 2: nickel-copper deposits and related rocks. *Inst. Mining. Metall., Section B, Applied Earth Science 103*, 146-161.
- Melezhik, V. A., Hudson-Edwards, K. A., Skuf'in, P. K. & Nilsson, L.-P. 1994: The Pechenga area, Russia. Part 1: geological setting and comparison with Pasvik, Norway. *Inst. Mining. Metall., Section B, Applied Earth Science 103*, 129-145.
- Naldrett A. J. 1973: Nickel sulphide deposits - their classification and genesis with special emphasis on deposits of volcanic association. *Can. Inst. Min. Metall. Bull.*, 66, 45-64.
- Papushis B. I. 1952: A differentiation of ultramafic and mafic intrusions of Pechenga. In *Ultramafic and Mafic Intrusions and Sulphide Nickel-Copper Deposits of Pechenga* Moscow, the USSR Academy of Sciences. (in Russian).
- Peredery W. V. 1979: Relationship of ultramafic amphibolites to metavolcanic rocks and serpentinites in the Thompson Belt, Manitoba. *Can. Mineral.*, 17, 187-200.
- Predovsky A. A. Zhangurov A. A. and Fedotov Zh. A. 1971: Evolution of the composition of mafic-ultramafic rocks and its relation to associated Ni-Cu ores in Pechenga. In: *Problems of Magmatism of the Baltic Shield*. Leningrad, Nauka, 166-176. (in Russian).
- Predovsky A. A. Fedotov Zh. A. and Akhmedov A. M. 1974: *Geochemistry of the Pechenga Complex*. Leningrad, Nauka. (in Russian).
- Pushkarev Yu. D. et al. 1988: Pb-isotope geochemistry and the generation of nickel-bearing basic-ultramafic rocks in the Kola Peninsula. In: Shukolukov Yu. A. (ed), *Isotope Geology and Processes of Ore Formation*. Leningrad, Nauka, 150-166. (in Russian).
- Rusanov S. M. 1981: Tholeiite-komatiite formation of the Pechenga Complex. *Soviet Geol.*, 2, 98-112. (in Russian).
- Skuf'in P. K. and Fedotov Zh. A. 1989: Picritic pillow lavas in early Precambrian volcanic section of the Pechenga Zone. *Rep. USSR Acad. Sci.*, 306, 956-962. (in Russian).
- Strishkov V.V. 1989: The nickel and cobalt industry of the U.S.S.R. - problems, issues and outlook. Unpublished report, USSR Acad. Sci.
- Suslova S. N. 1979: Petrochemical characteristics of komatiites from Precambrian volcanic complexes in the Kola Peninsula, *Int. Geol. Rev.*, 21, 654-664.
- Väyrynen H. 1938: Petrologie des Nickelerzfeldes Kaulatunturi-Kammikivittunturi in Petsamo. *Bull. Comm. Geol. Finlande*, 116. (in German).
- Zagorodny V. G. Mirskaya D. D. and Suslova S. N. 1964: *Geology of the Pechenga Sedimentary-Volcanogenic Series*. Leningrad, Nauka. (in Russian).
- Zak S. I. et al. 1982: *Geology, Magmatism and Ore Formation in the Pechenga Ore Field*. Leningrad, Nedra. (in Russian).



**EARLY PROTEROZOIC LAYERED MAFIC-ULTRAMAFIC MASSIF OF MT. GENERAL'SKAYA.**

V.A. Telnov, A.N. Bolshakov, V.V. Distler, D.M. Tourvovtsev & V.A. Melezhik

**1. Introduction**

A layered mafic-ultramafic rock massif on Mt. General'skaya is located 10 km east of Zapolyarny in the Murmansk region. The massif is just within a contact between Early Proterozoic sedimentary-volcanic rocks of the Pechenga supergroup on the one hand, and Archean gneisses on the other.

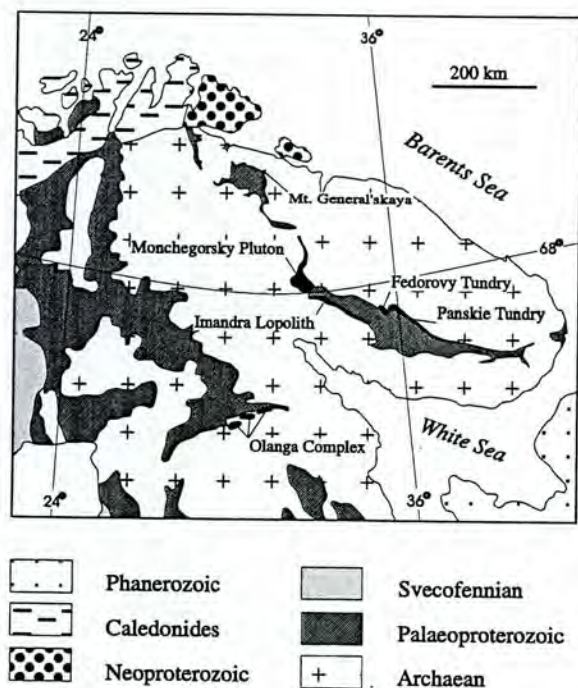


Fig. 1 Generalised geological map showing the location of the Early Proterozoic layered intrusions of the Kola region.

Geological examination of the Mt. General'skaya massif dates back to 1969, when prospecting for nickel-copper ores began. At that time sulphide-rich layers with a maximum thickness of 20 m were discovered. Concentration of nickel and copper in

them ranges from 0.2 to 0.4 wt. % with concentrations in some samples up to 1.5-2.0 wt. %. In a few samples, concentrations of platinum group elements (PGE) were found to be remarkably high, 12-18 ppm.

In 1994 the Pechenga geological prospecting group of the "PechengaNickel" Concern resumed its activities in surveying deep-seated horizons of the Mt. General'skaya massif in respect to it nickel and PGE ore potentiality.

Geological study of the target area is still going on and the information presented in this paper should, therefore, be regarded as preliminary.

**2. Morphology and structure of the Mt. General'skaya massif**

That part of the Mt. General'skaya massif which crops out at the present erosional surface looks like an elongated triangular (Fig. 2) that trends towards northeast with its long axis of 4 km. The southwestern side of the massif is around 3 km wide.

The massif's footwall, when shown in a longitudinal profile, has its contact dipping southwards at about 30° (Fig. 4), while the hanging wall's contact flattens out towards the southeast, eventually becoming horizontal (see drill hole 3463). Correspondingly, the massif's thickness increases from several hundreds to 1,000 m. Considering this, and the fact that the intrusive body's geometry in a cross-section turns to be nearly that of a sill, one is inclined to think of the massif as an apophysis of a large pluton overlain by the Petsamo Supergroup.

The massif is discordant in relation to the Archean gneisses. The structure of the Mt. General'skaya intrusion can be described as pronounced layering. The layering is nearly conformable to outward boundaries of the massif. A trachtyoid texture is recorded in its lower zone, where it conforms to the layering. The age of the massif is 2.505±1.6 Ma (U-Pb, baddeleyite, Amelin et al., 1995).

The rocks of the massif are cut in many places by diabase dykes which vary in thickness from 0.3-0.5 m to 3.7 m. Dykes dip at high angles of 70-80°, and their orientation is not yet clear.

**3. General petrographic description of the main rock types**

The petrographic description presented below is based on drill hole 3463, in which the most complete layering with the total thickness of 1,000 m was documented. A



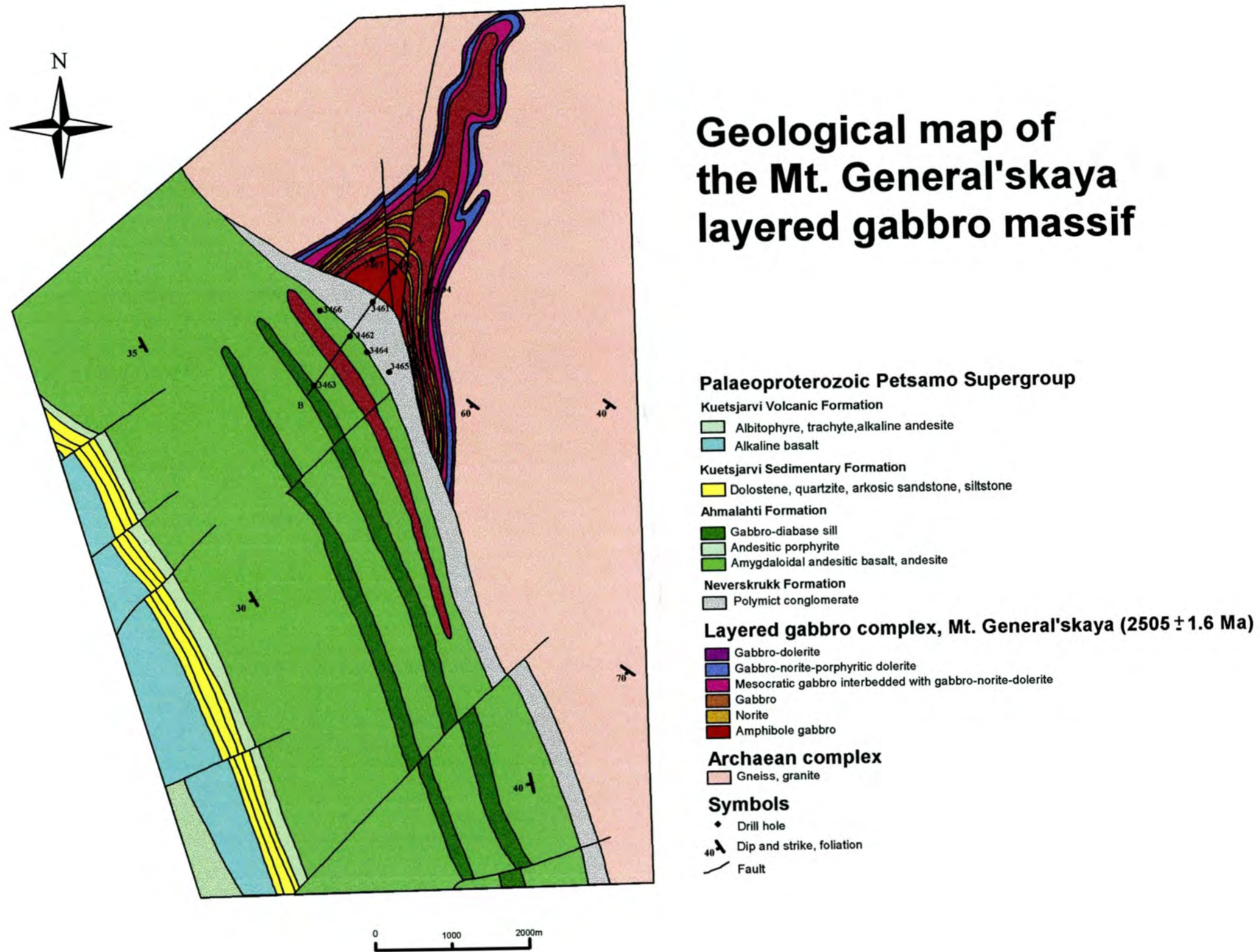


Fig. 2 Geological map of the Mt. General'skaya massif.



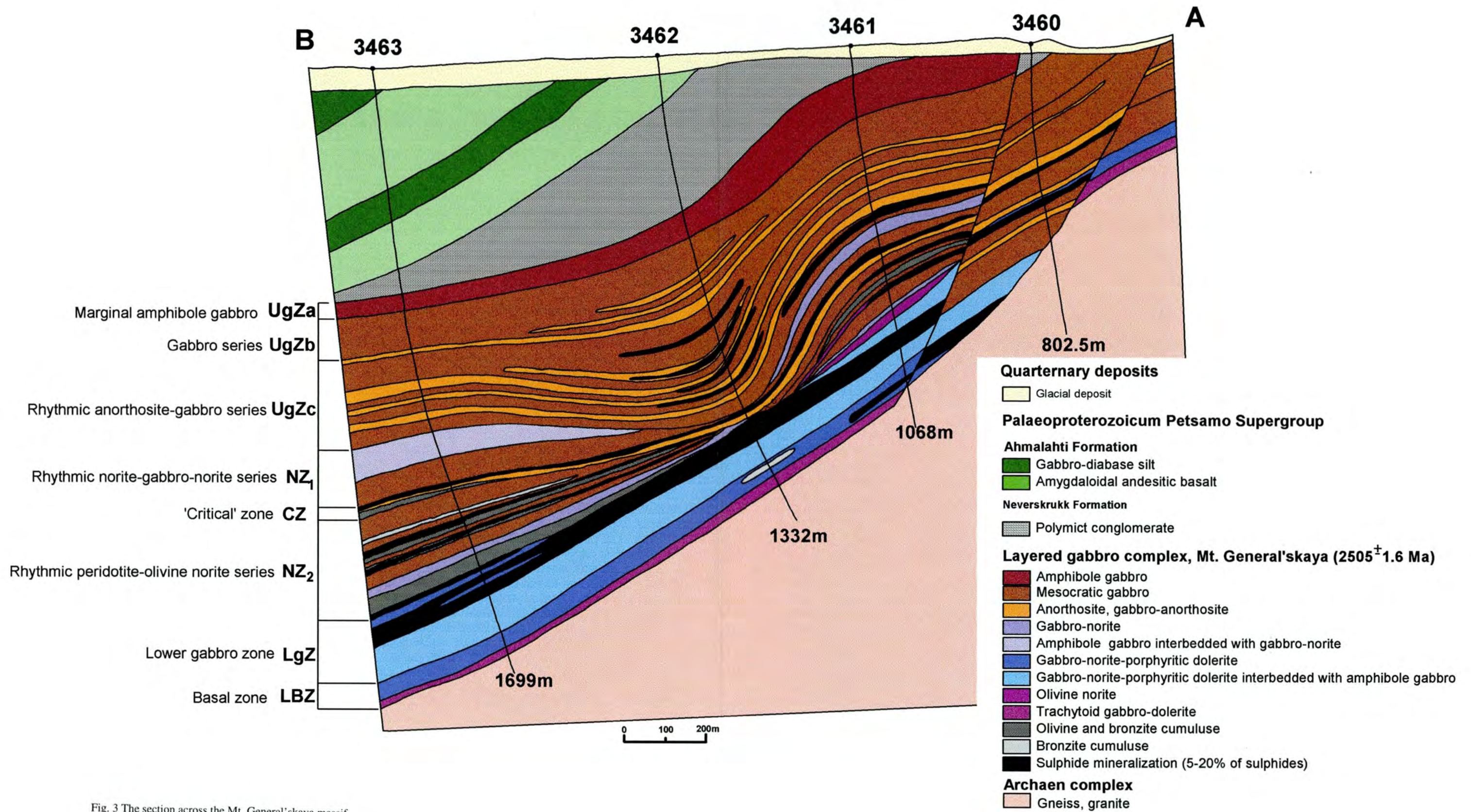


Fig. 3 The section across the Mt. General'skaya massif.



number of different zones have been defined in this drill hole. The zones are the largest units of the layering (Table 1). As based on cumulus mineralogy all zones are divided into series which in

turn are divided into cyclic rhythms. The latter consist of a number of horizons that are made up of different rock types.

Table 1. Stratification of the Mt. Generalskaya massif.

Zone and its index	Series	Index	Principal cumulus association
Upper gabbro, <b>UgZ</b>	Marginal amphibole gabbro Gabbro	<b>UgZ<sub>1</sub></b> <b>UgZ<sub>1</sub></b>	<b>pC</b> <b>pC</b> <b>aC</b> <b>p(pig?)C</b>
	Rhythmic anorthosite-gabbro-norite gabbro	<b>UgZ<sub>3</sub></b>	<b>pC</b> <b>pbC</b>
Rhythmic peridotite-norite, <b>NZ</b>	Rhythmic norite-norite gabbro	<b>NZ<sub>1</sub></b>	<b>bC</b> <b>bpC</b> <b>poC</b>
	'Critical' zone Rhythmic peridotite-olivine-norite olivine	<b>CZ</b> <b>NZ<sub>2</sub></b>	<b>pC</b> <b>oC</b> <b>obC</b> <b>pbC</b>
Lower gabbro, <b>LgZ</b>			<b>pC</b> <b>pbC</b> <b>bC</b>
Basal zone, <b>BZ</b>			<b>pC</b>

Cumulus associations: **pC**, plagioclase; **aC**, augite; **p(pig?)C**, plagioclase-pigeonite (?); **pbC**, plagioclase-orthopyroxene; **bC**, orthopyroxene; **bpC**, orthopyroxene-plagioclase; **poC**, plagioclase-olivine; **oC**, olivine.

*The upper gabbro zone (UgZ)* is identified in an upper section of the massif. Its maximum thickness is 550 m in drill hole 3462. A cross-section of the zone reveals three series (top to bottom): marginal amphibole gabbro (thickness 50-100 m), gabbro series (100-120 m), and anorthosite-gabbro-norite rhythmic series (up to 350-370 m).

*The marginal amphibole gabbro series* composes a top endocontact zone of the massif. It is a medium-grained rock with a massive texture and gabbroic/gabbroic-ophitic structure. Rock-forming principal minerals include plagioclase (40-70%), amphibole (35-50%), and subordinate phlogopite, quartz, sphene and apatite. The plagioclase ( $An_{47-65}$ ) is severely saussuritized and prehnitized. The amphiboles show a dual origin: they are primarily magmatic and pseudomorphous after clinopyroxene.

*The gabbro series* comprises coarse-to-medium-grained mesocratic gabbros which have gabbroic and gabbroic-ophitic textures, showing in places poikilitic-ophitic features. The rocks form a

plagioclase cumulate with the intercumulus clinopyroxene; where there is a gabbroic texture, however, the clinopyroxene-plagioclase relation changes to cotectic. The plagioclase ( $An_{62-69}$ ) makes up that rock cumulus which is in the form of prismatic and tabular crystals displaying an obvious marginal zonation. The clinopyroxene is totally amphibolized. The rocks contain a small amount of orthopyroxene (under 5%) and secondary minerals (serpentine, talc). Secondary intercumulus minerals are phlogopite, quartz and apatite. In the gabbros, some spaces are composed of the clinopyroxenites that are supposed to mark the basement of particular rhythms in the gabbro series section.

*The rhythmic anorthosite-gabbro-norite gabbro series.* These rocks form a major portion of the top gabbro zone. The series' top edge boundary is identified by a thick (5-10 m) layer of anorthosites and leucogabbroids that come into view and which are clearly visible in the top sections. Each rhythm features a regular composition: its top portion comprises anorthosite, leucogabbro and

leucogabbro-norite; the middle portion contains gabbro and norite-gabbro; at the bottom of the rhythms, melanogabbro-norite is recorded.

The anorthosites (bytownites) make up a plagioclase adcumulus. They are characterized by panidiomorphic-granular texture and taxitic structure, and comprise a cumulus plagioclase (over 90%) and intercumulus ortho- and clinopyroxene, phlogopite, sphene and sulphides. In cores of zoned crystals, the plagioclase corresponds to bytownite  $An_{68-72}$  and its marginal zone is by 5-6 numbers more acid. The leucogabbro and leucogabbro-norite contain more mafic minerals (up to 35%), but the structural relations of the rock-forming minerals remain the same.

The gabbro-norites and gabbros are remarkable for the poikilitic and poikilitic-ophitic structure and ataxic fabric in connection with segregated microareas of anorthosites (bytownite  $An_{66-69}$ ). Close to the bottom of some rhythms, at the boundary with the melanogabbro-norites, idiomorphic cumulus bronzite appears and the rock becomes porphyreous.

The melanogabbro-norites are characterised by a relatively low plagioclase content (under 35%) and contain largely cumulus bronzite.

**Peridotite-norite zone (NZ)** has a thickness of from 330-390 m which drastically decreases in the marginal segments of the massif. The zone comprises three series: the upper (rhythmic norite-gabbro-norite) and the lower series (rhythmic peridotite-olivine-norite), while a critical zone runs in between them.

The gabbro consists of medium-grained rocks with ophitic and poikilitic-ophitic structures. These rocks are made of cumulus plagioclase (40-50%) and intercumulus clinopyroxene (35-45%), as well as orthopyroxene (under 5%), phlogopite and oxides. The gabbro-norites and norites are the most abundant rocks of the upper series. They are coarse- to medium-grained, with gabbroic-ophitic, poikilitic and gabbroic structure variations. The bytownite (40-55%) fills the cumulus of the rocks, where it forms up prismatic and tabular crystals with polysynthetic and regular twins and fringe zones that make up at least 30% of the crystals' area. The diopside-augite of the intercumulus appears in the form of the grains and poikilocrysts which are xenomorphous in respect to the plagioclase. The diopside-augite is distinguished by exsolution texture, with the orthopyroxene plates coming out, makes the diopside-augite quite different from the pyroxenes. The bronzite is represented by

idiomorphic short-prismatic or isometric crystals 1-3 mm in size occasionally containing minute poikilitic ingrowths of plagioclase. Findings of light-brown hornblende (less than 1%), phlogopite, oxides and apatite have been recorded in the intercumulus.

The olivine norites and olivine gabbro-norites vary in thickness from few to about 20 meters, and their maximum thickness of 20-22 m is pinpointed at the bottom of NZ-zone. The rocks are equigranular, coarse- and medium-grained. Their mode demonstrates widely variable amounts of plagioclase (20-70%), olivine (5-45%), orthopyroxene (10-40%) and clinopyroxene (0-15%), as well as minor concentrations of accessory hornblende (under 5%), phlogopite (under 1%), secondary minerals (under 10%), oxides and sulphides. The poikilitic structure prevails, but there are also poikilitic-ophitic, ophitic, hypidiomorphic-granular, coronitic and porphyreous structures. The olivine clearly stands out in the rock cumulus, for it appears as ruggedly isomorphic grains (1-2 mm, occasionally up to 3 mm). The cumulus olivine possesses a persistent composition,  $Fo_{70-76}$ . The plagioclase is identified in the form of subidiomorphic prismatic zoned crystals (0.8-1.2 mm). A central portion of the cumulus plagioclase grains is azonal or slightly zonal, forming some 50-60% of the crystal surface area. Its composition makes it similar to bytownite ( $An_{69-74}$ ) and changes little through the NZ-zone section. The fringe zones of the crystals betray a very distinct zonation and they are more acidic in composition,  $An_{59}$ . Even more acidic are large (2-4 mm) isometric-tabular crystals of the nonzoned intercumulus plagioclase which induced the porphyreous structure of the rock. The pyroxenes represent intercumulus stages. The bronzite with a mode comprising  $Ca_{3.5}Mg_{71.78}Fe_{17.25}$  forms xenomorphous oikocrysts (up to 5-7 mm) with poikilitic inclusions of olivine and plagioclase. Unlike the orthopyroxene, the diopside-augite with a mode of  $Ca_{37.45}Mg_{45.51}Fe_{8.12}$  is more variable through the NZ-zone section and is in equilibrium with the former. The diopside-augite is encountered as roughly xenomorphous grains and oikocrysts (0.5-4 mm) that contain plagioclase and olivine.

The peridotites are recorded at the bottom of a few rhythms, within the rhythmic peridotite-olivine-norite series. Their layers are up to 4-6 m thick. In terms of their mode, these rocks correspond to harzburgites. They consist of olivine (40-60%), orthopyroxene (35-50%), clinopyroxene (under 10%), hornblende (2-4%), phlogopite and plagioclase (under 5%). Poikilitic structure is most commonly found in the harzburgites. The olivine in

the peridotite is remarkable for its most high magnesium content,  $FO_{77-78}$ .

The plagioclase ( $An_{66-70}$ ) is spotted as zoned prismatic grains in the cumulus. The hornblende produces separate bodies or discontinuous coronitic reaction rims around the olivine and at its boundary with the plagioclase. The secondary minerals comprise the products which resulted from transformations of the mafic minerals. The olivine is replaced by antigorite, chrysotile, and magnetite, as well as by the talc, carbonate and brucite that originated later. The orthopyroxene is serpentinized and amphibolized, while the clinopyroxene and hornblende are replaced by chlorite. Saussurite and hydrogarnet appear instead of plagioclase.

**The critical zone (CZ)** of the intrusive is about 10 meters thick and is traced at a more or less same stratigraphic level in several drill holes. A peculiar thing about this critical zone is its taxitic look which is due to irregular combination of coarse- and micro-grained rocks. The zone comprises plagioclase adcumulate, coarse-to-medium-grained cotectic orthopyroxene-plagioclase growths, and micro-grained plagioclase segregations with a flow texture.

The anorthosite (plagioclase adcumulate) makes up isolated areas and microsegregations of the cumulus plagioclase. The plagioclase is notable for the variability of its forms (long- and short-prismatic, tabular) and size (from hundred fractions of one millimeter to 2-4 mm). Its texture is panidiomorphic-granular, its composition corresponds to a bytownite ( $An_{63-75}$ ). A central portion of the zoned crystals and their periphery were found to have the composition of  $An_{69-75}$  and  $An_{63-66}$  respectively.

The leucogabbro-norites and leuconorites possess a considerable amount (65-90%) of cumulus plagioclase in the form of microanorthosite segregations and also intercumulus clino- and orthopyroxene.

The melanogabbro-norites compose individual areas amidst the gabbroids, and they are characterized by a presence of large poikilitic crystals of the intercumulus bronzite which comprises cumulus olivine and plagioclase. The primary minerals are not observed in these rocks.

**The lower gabbro zone (LgZ)** is easily identified when the olivine cumulus disappears and is replaced by bronzite, plagioclase-bronzite and plagioclase cumulus associations. Rocks of this zone are a maximum of 190 m thick.

The lower gabbro zone is made up of chiefly mesocratic gabbro-norites and gabbros which alternate with gabbro-norites or quartz-bearing and micropegmatic gabbros and anorthosites. A certain regularity is observed in the way these rocks are distributed in a section of the lower gabbro zone, some of the rhythms being 20 to 30 meters thick. The top of the rhythms in most cases consists of leucogabbro or mesocratic gabbros, occasionally with anorthosites that contain cumulus plagioclase but lack orthopyroxene. Towards a basement of such rhythms more and more of the cumulus bronzite appears in the form of porphyreous gabbro-norites, which percentage in melanogabbro-norites and orthopyroxenites may be as much as 70-90%.

**Basal zone (LBZ)** is discriminated in the lower marginal portion of the massif. Its thickness is about 65 m and it comprises gabbro-norites and gabbros with a fine-grained fabric on the one hand, and porphyreous and trachytoid structure on the other.

A lower subzone of the basal zone, which is about 10 to 15 meters thick, directly touches the Archaean gneisses. The subzone's section includes trachytoid microdolerites and hornblende microgabbros. The rocks consist of plagioclase (40-60%), amphibole (30-50%), phlogopite (up to 5%), sphene (up to 1%), and quartz. The cumulus plagioclase  $An_{53-56}$ , which shows a partial marginal zonation, is remarkable for its very obvious orientation of fine (0.2-0.8 mm) long-prismatic crystals. Light-brown cumulus hornblende produces porphyreous segregations (1.5-2 mm). Clinopyroxene is replaced in these rocks by yellowish-green actinolite, phlogopite and titanite. An intercumulus occasionally contains quartz as well.

Above this, a section of trachytoid gabbroids is gradually replaced by marginal porphyreous gabbro-norites and gabbros of a top subzone. The trachytoid structure of these rocks disappears. The thickness of the horizon varies from 40 to 50 meters. The porphyreous gabbro-norites and gabbros have cumulus bronzite as a component (0-10%) in the form of large (2-3 mm) short-tabular insets, and also sporadic prisms of augite (0-5%) with noticeable ordinary twins. Both sorts of pyroxene are seen against a fine-grained ground mass of plagioclase and augite that make up a cumulus.

Rocks of the basal zone also contain xenoliths of country rocks including quartz-biotite schists, microquartzites, biotite-plagioclase-actinolite schists and gneisses.



## Whole-rock chemistry

29 samples from drill hole 3463 were analysed for major and trace elements by conventional wet-chemistry methods, and 98 samples from drill hole 3461 were analysed by ICPMS for 66 elements. Analyses of main rock types from drill hole 3463 are shown in Table 2 and Fig.4. The contents of Fe, Mn, Mg, Cr, Ti, V, Ni, Cu, Ag and Pd versus depth of drill hole 3461 are shown on Fig. 5. The whole-rock geochemistry reflects that the cryptic mineralogical variations are only moderately pronounced. Generally, there is a decrease in Fe, Mg, Cr, Ti and Mn from the bottom to the top, and Ni, Cu, Ag and Pd irregularly increase downwards through the intrusion (Fig.5). The fine-grained marginal gabbro (samples 22, 23, Table 2) is characterised by low  $TiO_2$  (=0.56-0.63) and  $K_2O$  (0.44-0.55) and relatively high MgO (10.6-10.8). All rock types are characterised by the same REE-patterns (Fig.6). The rocks are slightly enriched in LREE, indicating some contamination by a continental crustal source. The rocks are marked by a slightly decreased (negative)  $\epsilon Nd(T)$  value of  $2.3 \pm 0.4$  (Balashov et al. 1990), which is distinguished by only relatively small differences from mean mantle value.

Table 2 shows the chemical composition of rocks from the Mt. General'skaya massif.

## 5. Chemical composition of rock-forming minerals

The Mt. General'skaya massif is remarkable for a few petrological features that prove it to be a specific type of rhythmically layered intrusive. One of its most important peculiarities is that the largest portion is made of rocks containing a cumulus plagioclase. An exception to this are peridotite horizons and those bronzite-rich rocks where plagioclase represents a typical intercumulus stage.

The second peculiar thing about the massif is that while it demonstrates a complete pattern of stratification throughout its cross-section, i.e. from anorthosite to peridotite, the rock-forming minerals vary only slightly in their chemical composition (Table 3). This means that a complete layering of the massif, in terms of stages, is accompanied by less developed cryptic layering.

Finally, there is one more essential petrological feature in the massif's appearance, and this is an obvious discontinuity in the way the minerals tend to vary in their composition within the zones and cyclic rhythms (Fig. 7). These peculiarities with

respect to each of the rock-forming minerals are described below.

*Plagioclase.* Variations in composition of the cumulus plagioclase range, on the whole, within 52%-75% An (Fig. 7). Judging by the tendencies in the plagioclase composition's alterations one can distinguish at least 4 large discontinuous areas that correspond to the major zones of the intrusive. In the upper gabbro zone (UgZ<sub>1,3</sub>) the mode of the central portion of zonal plagioclases covers a span of 66%-72% An and 66%-52% An within the confines of those zones where an adcumulus growing-up of the crystals takes place. The second macrorhythm (NZ<sub>1,2</sub>), which is accompanied by a presence of monomineral bronzite cumulate, is characterized by a sudden change in a basification of a plagioclase cumulus 68%-75% An and by a 62%-68% An mode recorded in the crystal's fringe zones.

The critical zone turns out to be a particular area in the plagioclase's mode. Within this zone, the mineral's mode, in fact, runs the gamut of variations in composition of the plagioclase 66%-75% An, as is the case throughout this section of the intrusive. At the critical horizon, the plagioclase's mode jumps to the more silicic area, and basification gradually increases up to the NZ<sub>2</sub> - LgZ boundary.

The third microrhythm corresponds to the lower gabbro zone where the plagioclase's mode also changes to the more silicic area of 62%-70% An in the centers of crystals and to 52% An in the zones of adcumulus growing.

Finally, in the 4th discontinuous zone, that is marked as BZ, the mineral's mode ranges as much as 47%-51% An, and there are cases when oligoclase of 20% An is encountered in the intercumulus.

*Olivine.* When cumulus olivine appears, it is a clear sign of a UgZ - NZ petrological boundary. The total variation range for the olivine in NZ-zone is estimated at Fo<sub>69</sub>-Fo<sub>78</sub>. Several cyclic rhythms are identified, showing

Table 2. Chemical composition of rocks from the Mt. General'skaya massif, drill hole 3463.

Sample nn	SiO <sub>2</sub>	TiO <sub>2</sub>	Al <sub>2</sub> O <sub>3</sub>	Fe <sub>2</sub> O <sub>3</sub>	FeO	MnO	CaO	MgO	K <sub>2</sub> O	Na <sub>2</sub> O	SO <sub>3</sub>	P <sub>2</sub> O <sub>5</sub>	NiO	CuO	CoO	Cr <sub>2</sub> O <sub>3</sub>	V <sub>2</sub> O <sub>5</sub>	LOI	Total	H <sub>2</sub> O
27	52.99	0.30	17.10	1.14	6.37	0.13	10.1	6.71	0.53	2.75	0.23	0.11	0.025	0.016	0.005	0.008	0.019	1.47	100.60	0.21
28	51.80	0.28	17.23	1.00	5.53	0.13	11.52	8.68	0.36	2.17	<0.05	0.06	0.028	0.007	0.005	0.01	0.019	1.16	99.99	0.23
1	49.76	0.31	17.18	1.14	5.61	0.15	12.10	8.02	0.45	2.47	<0.05	0.05	0.028	0.011	0.005	0.008	0.017	2.41	99.72	0.21
2	52.92	1.21	13.85	3.68	8.41	0.21	8.06	4.23	3.54	2.56	0.22	0.13	0.013	0.012	0.005	0.01	0.029	0.78	99.87	0.23
29	56.11	0.65	15.16	1.33	6.18	0.10	4.27	7.77	2.76	2.89	0.08	0.15	0.018	0.004	<0.005	0.01	0.02	2.49	100.00	0.41
24	50.52	0.27	15.1	1.83	5.45	0.16	8.32	10.64	0.40	1.85	0.13	0.05	0.034	<0.004	0.006	0.011	0.02	2.00	100.02	0.34
25	51.39	0.25	15.25	1.23	6.08	0.15	10.53	10.69	0.48	1.87	<0.05	0.04	0.035	0.004	0.006	0.01	0.023	8.00	100.04	0.25
26	50.75	0.27	14.02	2.91	4.57	0.15	11.18	10.81	0.53	1.87	1.04	0.05	0.038	0.006	0.006	0.013	0.006	1.9	100.12	0.33
3	51.35	0.33	16.21	0.95	5.75	0.14	11.59	9.02	0.70	2.24	<0.05	0.06	0.03	0.007	0.005	0.01	0.019	1.51	99.92	0.17
4	50.82	0.24	14.87	0.94	5.87	0.14	10.58	11.32	0.60	1.97	0.24	0.06	0.035	0.005	0.006	0.01	0.018	2.08	99.8	0.18
5	50.21	0.23	17.92	0.65	5.28	0.12	11.52	9.54	0.32	2.10	<0.05	0.06	0.03	0.006	0.005	0.016	0.014	1.81	99.83	0.28
6	46.14	0.21	16.2	1.12	6.75	0.14	8.78	14.07	0.40	1.67	<0.05	0.05	0.073	<0.004	0.009	0.009	0.007	4.14	99.77	0.45
7	43.93	0.22	12.42	2.13	8.49	0.16	6.70	19.91	0.36	1.19	0.13	0.05	0.12	0.007	0.008	0.007	0.006	3.85	99.70	0.46
8	47.11	0.26	17.46	1.13	6.65	0.12	9.14	11.84	0.36	2.05	<0.05	0.07	0.077	0.006	0.015	<0.005	0.005	3.34	99.63	0.33
9	48.33	0.27	15.92	0.75	6.51	0.14	9.32	13.45	0.35	1.79	<0.05	0.07	0.084	0.014	0.008	0.011	0.008	2.60	99.63	0.21
10	48.09	0.21	21.27	0.82	4.75	0.10	11.45	7.35	0.55	2.51	0.51	0.05	0.013	0.14	0.007	0.01	0.01	1.92	99.76	0.18
11	44.94	0.21	17.30	1.80	6.67	0.12	8.85	12.29	0.38	1.81	1.49	0.07	0.3	0.27	0.014	0.014	0.01	3.70	100.24	0.25
12	47.17	0.17	23.77	1.23	4.38	0.08	12.28	5.51	0.36	2.30	1.08	0.06	0.21	0.24	0.007	0.007	0.031	1.45	100.34	0.2
13	47.89	0.26	14.22	1.05	7.93	0.16	7.99	15.01	0.31	1.47	<0.05	0.05	0.086	0.008	0.009	0.013	0.013	3.06	99.53	0.38
14	42.87	0.20	11.21	3.40	7.72	0.18	5.04	21.05	0.36	0.69	0.86	0.06	0.27	0.15	0.015	0.014	0.017	5.97	100.08	0.6
15	42.51	0.23	7.04	5.06	7.76	0.19	3.53	26.70	0.09	0.22	0.34	0.06	0.21	0.05	0.018	0.013	0.014	5.8	99.84	0.37
16	45.88	0.29	14.63	2.64	6.51	0.15	7.99	15.92	0.30	1.69	0.39	0.07	0.14	0.08	0.009	0.022	0.016	2.85	99.64	0.3
17	48.27	0.28	15.76	2.43	6.51	0.15	9.29	13.92	0.48	1.66	<0.05	0.08	0.098	0.007	0.009	0.014	0.075	0.72	99.75	0.19
18	47.53	0.27	7.07	4.69	3.87	0.38	15.77	15.07	0.46	0.82	0.73	0.13	0.12	0.014	0.008	0.075	0.023	2.76	99.79	0.23
19	50.94	0.42	16.06	1.82	6.46	0.15	10.87	8.82	0.48	2.17	0.38	0.1	0.067	0.05	0.007	0.024	0.026	0.87	99.71	0.17
20	48.95	0.37	16.95	1.32	5.38	0.14	10.44	9.92	0.52	2.09	0.27	0.09	0.087	0.027	0.007	0.05	0.024	2.08	99.72	0.26
21	50.76	0.47	15.4	3.93	4.94	0.16	10.87	8.93	0.62	2.12	0.15	0.09	0.039	0.019	0.006	0.042	0.031	1.41	99.99	0.19
22	52.53	0.63	15.37	2.47	6.58	0.16	10.80	7.76	0.55	2.12	0.05	0.1	0.029	0.012	0.006	0.029	0.039	0.90	100.14	0.18
23	52.11	0.56	15.00	3.31	5.53	0.16	10.63	8.44	0.44	2.55	0.08	0.1	0.033	0.015	0.006	0.033	0.034	1.00	100.03	0.23

LOI, loss of ignition.

Analyses were performed in the Chemical-Technological Laboratory of the Kola Inform-Laboratory Centre, Muransk region, Russia.

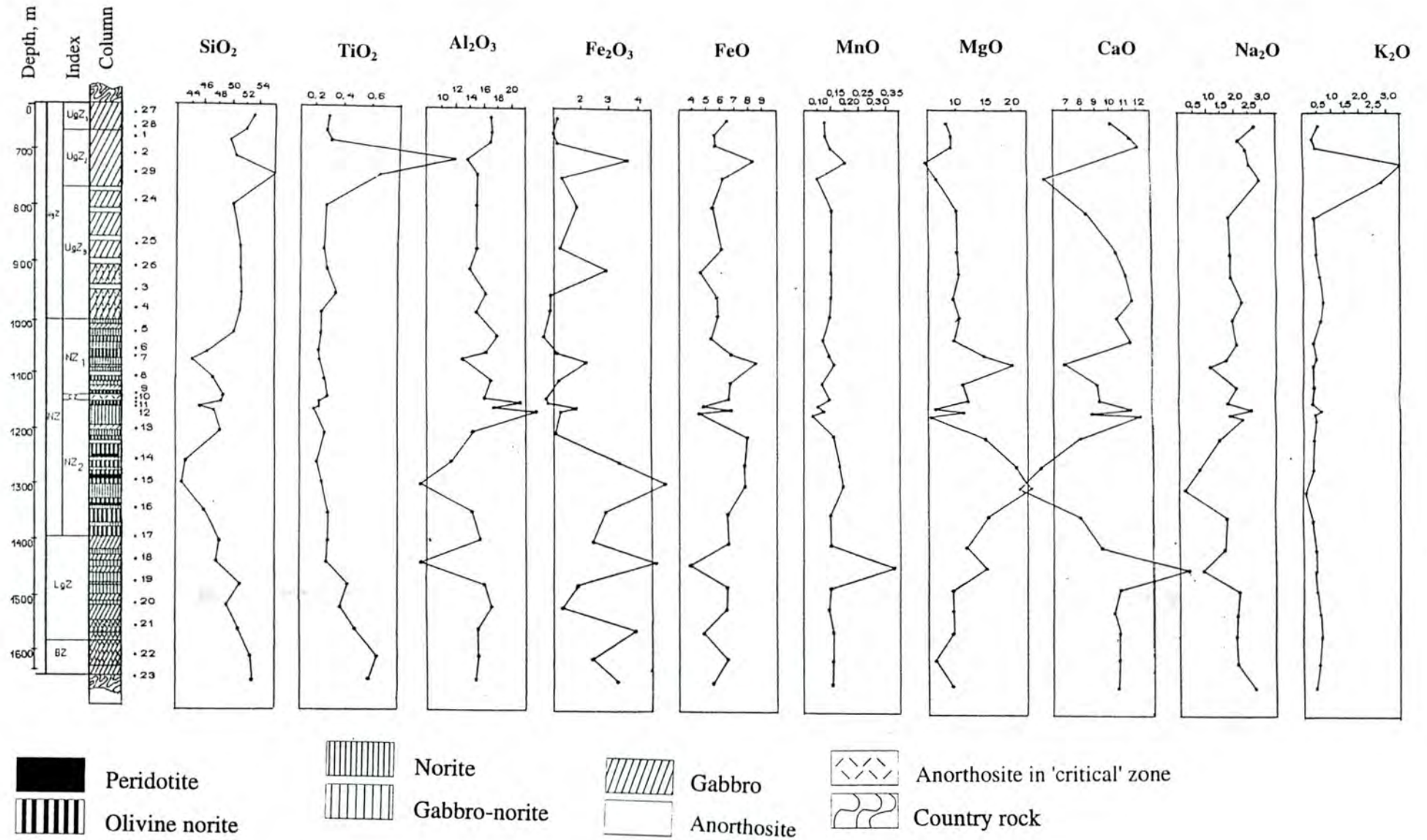


Fig. 4 Stratigraphic geochemical sections of the General'skaya layered gabbro massif based on drill hole 3463.



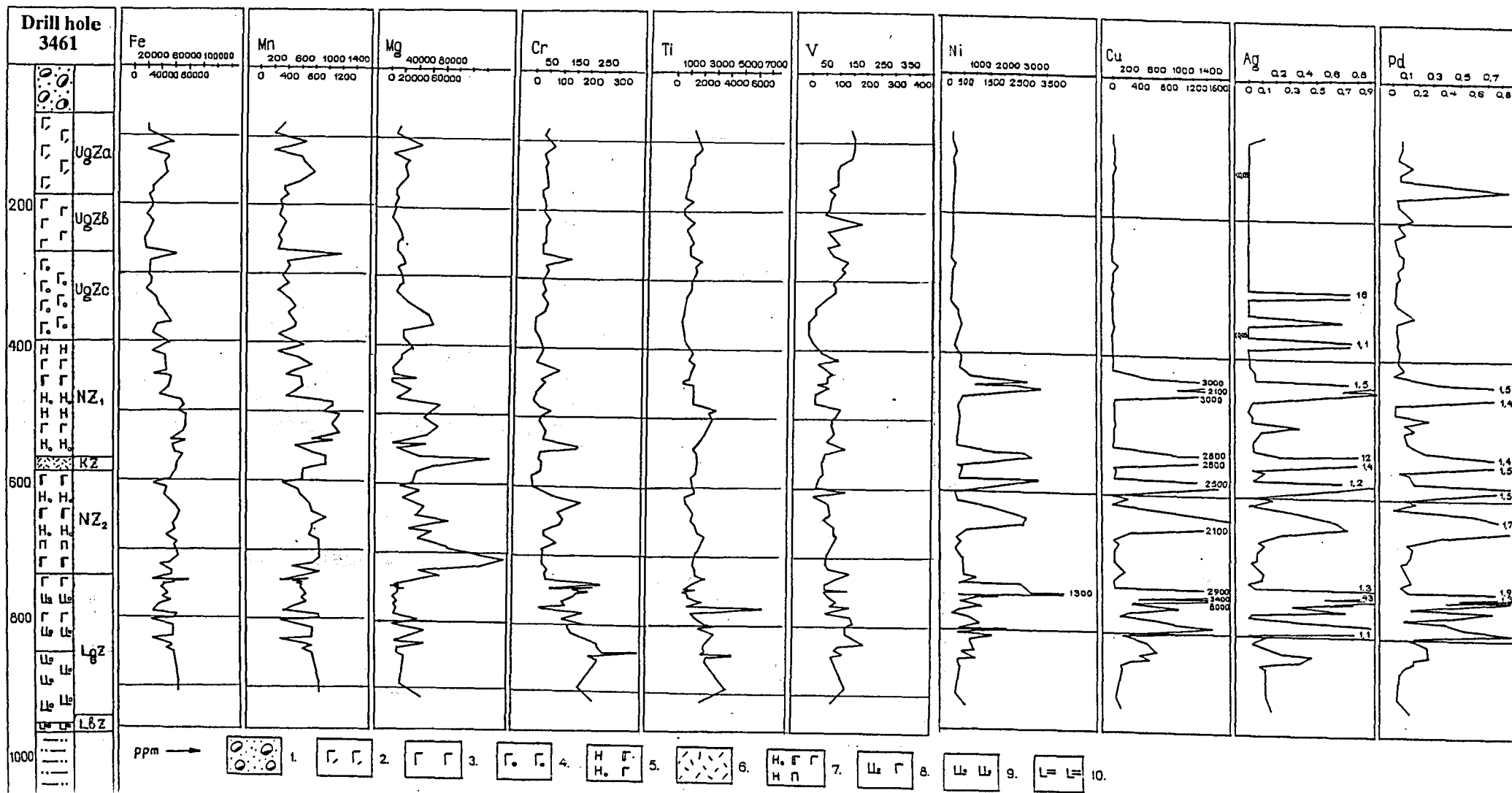


Fig. 5 Stratigraphic geochemical sections of the General'skaya layered gabbro massif based on drill hole 3461.

1, Quaternary deposits; 2, amphibole gabbro; 3, gabbro; 4, interbedded anorthosite, leuco- meso and melanogabbro; 5, alternate rhythms of norite, gabbro-norite, olivine norite and gabbro; 6, 'critical' zone consisting of anorthosite and leucogabbro; 7, interbedded olivine gabbro-norite, gabbro-norite, gabbro, norite and peridotite; 8, interbedded gabbro-norite-dolerite and porphyritic fine- to coarse-grained gabbro; 9, porphyritic gabbro-norite-dolerite; 10, trachytic microdolerite.

Table 3. Chemical composition of rock-forming minerals from the Mt. General'skaya massif.

	1		2			
	Ol	Pl	Ol	Pl	Opx	Cpx
SiO <sub>2</sub>	37.73	52.21	37.99	50.53	55.61	53.86
TiO <sub>2</sub>	0.02	0.07	0.02	n.d.	0.12	0.52
Al <sub>2</sub> O <sub>3</sub>	0.09	29.77	-	31.04	1.57	2.38
Cr <sub>2</sub> O <sub>3</sub>	0.01	0.03	0.03	n.d.	0.15	0.1
FeO	19.9	0.41	24.66	0.44	13.56	6.38
MnO	0.31	0.01	0.3	n.d.	0.36	0.19
MgO	40.65	0.32	36.39	0.27	26.06	15.82
CaO	0.11	13.64	0.17	14.12	2.55	21.35
Na <sub>2</sub> O	n.d.	3.79	n.d.	3.55	0.13	0.53
K <sub>2</sub> O	n.d.	0.08	n.d.	0.06	0.01	0.01
Total	98.82	100.33	99.84	100.01	100.12	101.14

	2		3			4	
	Phl	Opx	Pl	Cpx	Phl	Opx	
SiO <sub>2</sub>	40.06	52.98	49.95	52.57	37.22	55.81	
TiO <sub>2</sub>	2.69	0.17	n.d.	0.33	4.15	0.05	
Al <sub>2</sub> O <sub>3</sub>	17.05	1.49	30.76	2.06	16.14	1.44	
Cr <sub>2</sub> O <sub>3</sub>	0.19	-	n.d.	0.01	-	-	
FeO	10.59	15.73	0.64	7.35	13.33	14.13	
MnO	0.06	0.34	n.d.	0.22	0.04	0.15	
MgO	16.85	26.23	0.12	16.5	15.72	25.3	
CaO	0.81	2.27	13.84	21.42	0.43	2.45	
Na <sub>2</sub> O	0.47	0.12	3.72	0.36	0.69	0.08	
K <sub>2</sub> O	9.01	0.01	0.05	0.01	7.95	0.02	
Total	97.78	99.34	99.08	100.83	95.67	99.43	

	4		5		
	Pl	Cxp	Pl	Opx	Cpx
SiO <sub>2</sub>	50.63	52.89	51.19	57.53	51.47
TiO <sub>2</sub>	0.07	0.31	0.07	0.07	0.6
Al <sub>2</sub> O <sub>3</sub>	30.05	1.69	28.61	1.02	2.74
Cr <sub>2</sub> O <sub>3</sub>	0.01	0.01	0.06	0.06	0.1
FeO	0.8	6.11	0.48	15.61	8.7
MnO	0.04	0.2	-	0.45	0.27
MgO	0.28	15.82	0.2	22.59	13.55
CaO	14.09	21.81	14.65	0.85	20.58
Na <sub>2</sub> O	3.45	0.38	3.86	0.15	0.53
K <sub>2</sub> O	0.07	0.01	0.01	0.02	0.01
Total	99.49	99.23	99.13	98.35	98.55

\*, including 0.22 wt. % NiO in olivine; \*\*, including 0.28 wt. % NiO in olivine.

n.d., not determined; dashes, below detection limit.

1, harzburgite (sample 3463/1291); 2, olivine norite (sample 3462/1237.5); 3, norite (sample 3463/1223.9); 4, gabbro-norite (sample 3463/1017.5); 5, porphyritic gabbro-norite from lower gabbro zone (sample 3463/1480.7).

regular variations in the amount of magnesian olivine. The general regular feature is such that the highest magnesium content, which corresponds to Fo<sub>78</sub> values, is common in the horizons most rich in olivine, whereas the minimum of Fo<sub>69</sub> corresponds to leucocratic norites. As for other transitional varieties of olivine norites, complementing the anorthosite-norite-peridotite or anorthosite-olivine-norite cyclic rhythms,

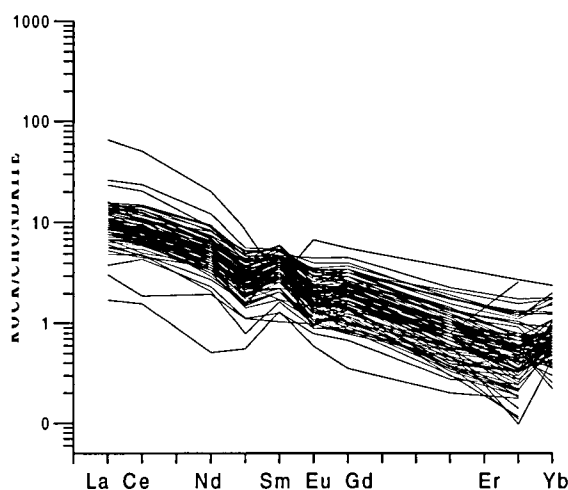


Fig. 6 Chondrite-normalised rare-earth element diagram for rocks of the Mt. General'skaya massif.

magnesium content in olivine does not change that much (Fo<sub>72-75</sub>), but it always increases in areas with more olivine. Nickel, olivine's typical component, betrays the variations of concentrations in the range of 0.22-0.36 wt. %, which is normal for olivine with such magnesium content.

**Orthopyroxene.** A high-grade amphibolite metamorphism of the massif's endogenic contact zones prevents a close look into peculiarities of orthopyroxene mode variations. The most comprehensive data gives an idea of the peridotite-norite zone. Basic variations of the mineral's composition within this zone are observed in a proportion of enstatite (En) and ferrosilite (Fs) minerals, while wollastonite (Wo) mineral's proportional share being constant (1-6 mole percent). An overall variation range of the enstatite end member spans En<sub>71-82</sub>, whereas for ferrosilite, Fs<sub>17-25</sub>, the magnitude of X<sub>Mg</sub> varies from 69 to 82 mole percent. Likewise, for olivine, orthopyroxene's mineral modes are stratified both within and between the cyclic rhythms, the general tendency being that the magnesium content increases in proportion to an enlargement of the total

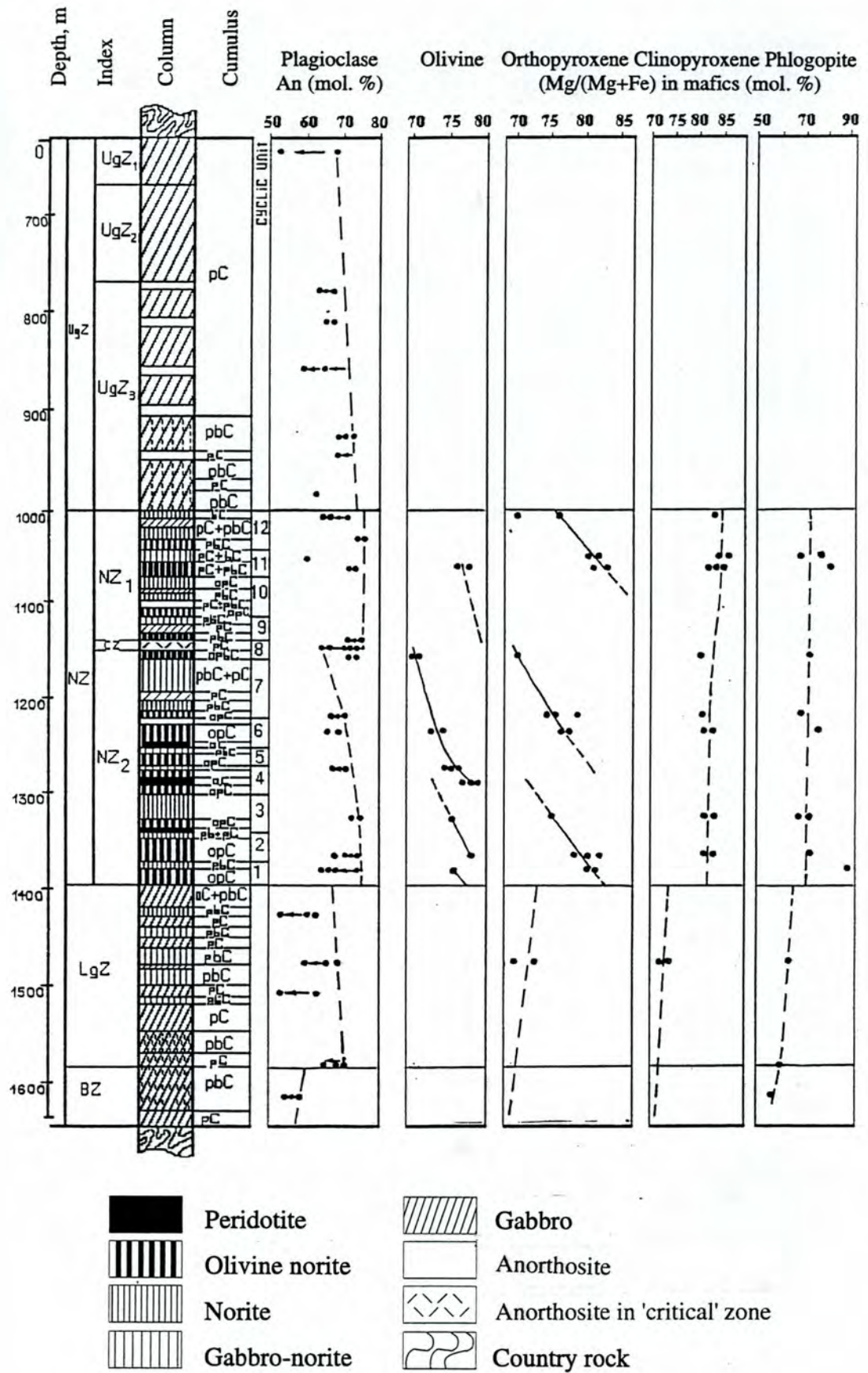


Fig. 7 Composition of the main rock-forming minerals versus depth, drill hole 3463



mineral substance. Within a cyclic rhythm, the orthopyroxene shows the minimum magnesium content in leucocratic norites, while the highest magnesium content is in the horizon most lavishly enriched with orthopyroxene. Transition to the next macrorhythm is accompanied by a remarkable reduction in magnesium content. As in the case of olivine, the modes of orthopyroxene behave most typically within the critical zone, as it is their particular petrological horizon.

Thus, it is in this zone that the least magnesian modes of the common minerals appear. A high upper bound to alumina content is also typical of orthopyroxene.

In the lower gabbro zone, the iron content of the mineral rises dramatically to  $Fs_{28-30}$ , and this tendency to become more and more ferriferrous marks a transition to the basal zone.

*Clinopyroxene.* An intercumulus origin of the clinopyroxene gave rise to other regularities in its mode variations, different than those of typical cumulus stages. No cyclic variation of the clinopyroxene's modes was recorded within or between the cyclic rhythms. Within the confines of NZ-zone, a gradual change in the mineral's mode was marked not only by concentrations of iron and magnesium, but also by variations in calcium content. With ferrosilite (Fs) and enstatite (En) minerals within the confines of the peridotite-norite zone ranging from 8 to 12 and from 45 to 51 mole percent respectively, wollastonite (Wo) varies from  $Wo_{37}$  to  $Wo_{45}$ , while total iron content (f) is 14% to 20% and it quite clearly tends to increase towards the basement of NZ-zone. That the clinopyroxene becomes strongly ferriferrous is a noteworthy specific feature of the lower gabbro zone (f = 27%-28% for  $Fs_{15-17}$ ), and there is a general tendency of the iron content still to increase within the basal zone. Like in orthopyroxene, alumina concentration in clinopyroxene hardly correlates with a large-scale range of iron enrichment (Fig. 8).

*Phlogopite.* This represents an intercumulus stage and is not common in the rocks of the massif. Its magnesium content in the peridotite-norite zone varies in a range of 66-86 mole percent. The rocks of the lower gabbro and basal zones become more ferriferrous and here a biotite with 55-63 molecular proportion of magnesium is more common.

An intercumulus paragenetic equilibrium association of biotite and clinopyroxene, which is widespread in the massif's rocks and is most common within an interval including the peridotite-norite,

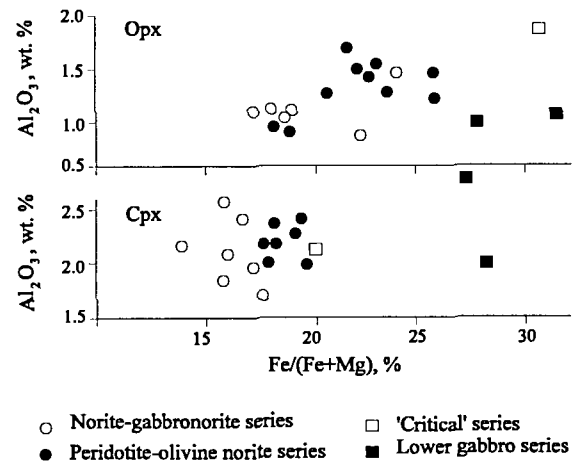


Fig. 8 Composition of ortho- and clinopyroxenes.

lower gabbro and basal zones, enables us to estimate, to a certain extent, the temperature conditions of the rock-forming process, using a biotite-clinopyroxene geothermometer conceptually based on a distribution of magnesium and iron in coexisting biotite and pyroxene, with distribution dependent on PT-conditions. As shown in the  $X_{Mg}^{Bi}-X_{Mg}^{Cpx}$  diagram (Fig. 9), the rocks of the peridotite-norite zone undergo crystallization at the highest temperature ( $850^{\circ}-900^{\circ}$ ) conditions, and at the same time the melt crystallization temperature towards the marginal zones drops slightly. Generally speaking, this data represents the actual values of the ultramafic magma crystallization temperatures fairly well, and it correlates well with the available data on  $Phl-Cpx$  equilibrium proportions for other massifs (e.g. Talnakhsky).

### Sulphide mineralisation

Sulphide mineralization is encountered in rocks throughout the whole cross-section of the Mt. Generalskaya massif. The percentage of chalcophile metals is under 0.5% of the rocks' volume and it is only in few horizons that nickel concentration range is 0.65%-2.0% Ni and that of copper is 0.60%-1.5%. Nickel prevails over copper, and the nickel to copper proportion is usually 1:2, seldom less than 0.8 or greater than 3. When concentrations of nonferrous metals are low, the sulphides produce fine (1-2 mm) angular or lentiform elongated isolated bodies, or segregations, with a nearly parallel trend. Such orientation is influenced by sulphide elongation along the grains of non-metallic minerals that substitute primary silicates.

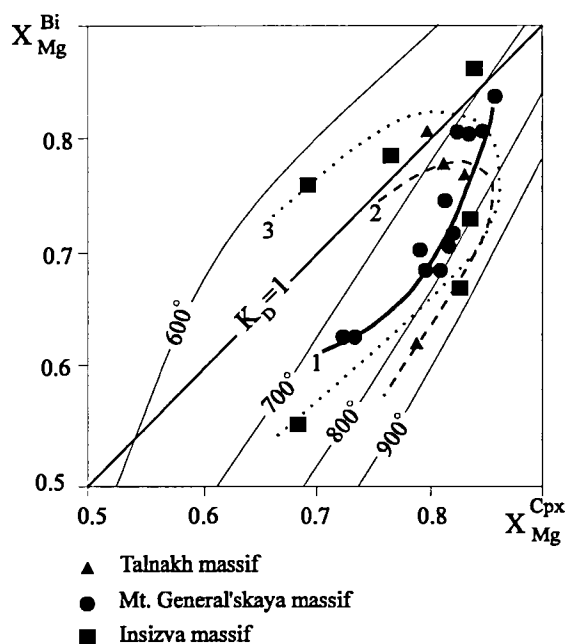


Fig. 9 Mineral equilibrium temperature of coeval clinopyroxene and biotite (phlogopite) from ultramafic rocks of the Mt. General'skaya massif.

As soon as the concentrations of nonferrous metals go up, in addition to the isolated particles of sulphides mentioned above, fairly large (up to 2 mm) phenocrysts and schlieren of irregular shape appear. More often than not in peripheral parts, the large sulphide phenocrysts, or insets, are accompanied by fine angular segregations with higher chalcopryrite concentrations than in the master insets. What is typical of the Mt. General'skaya mineralization pattern is that these insets show persistent mineral composition both vertically and laterally. Basically, the mineralization comprises a pyrrhotite +pentlandite+chalcopryrite association, occasionally there is pentlandite+chalcopryrite, whereas a millerite+chalcopryrite+pyrite paragenesis is found at a wedge-out of ore bodies (drill hole 3460).

When it comes to a predominantly pyrrhotite mineralization, then the chalcopryrite normally forms either a rim around the sulphide insets or single fine grains. The pyrrhotite, on the other hand, forms large outstanding grains, usually with regular and smooth edges. The pyrrhotite comes in two modifications, i.e. monoclinical and hexagonal. Nickel content in pyrrhotite ranges from 0.18 to 0.61 mass percent (Table 4). The monoclinical pyrrhotite in pyrrhotite twins is usually more rich in nickel. The pentlandite findings are recorded most commonly as large (up to 3 mm) isometric porphyraceous single bodies. Flame-like and tabular, or bladed, pentlandites are encountered in a far lower amount and their fine segregations are localized either in cracks or at the edges of

pyrrhotite grains. The pentlandite is classified as a nickel-enriched variety, with nickel concentration varying from 36 to 38 wt. %, which is the highest concentration of nickel in the pentlandite with a pyrrhotite+pentlandite paragenesis and rather high iron content in pyrrhotite. It should be noted that the segregations of the flame-like pentlandite in pyrrhotite is not infrequently more rich in iron than that of the porphyraceous pentlandite (Table 4). Cobalt concentration in pentlandite is estimated at 0.30-2.40 mass percent (Table 4). When the pentlandite appears in the essentially chalcopryrite stringers it is represented by a cobalt-bearing variety (sample 3463/1554.9). In the mineralization of this kind, pyrrhotite and even sphalerite are both loaded with a higher concentration of cobalt (Table 4).

The pyrite is considered to be a persistent mineral, its amount sometimes coming up to 20% of all the sulphides' volume. In these sulphides, it yields irregular grains, myrmekitic aggregates and fine (microns) hair-like veinlets. The pyrite in the silicates forms sieve-like monocrystals and rims, enclosing the silicate grains. The pyrite in the sulphides always contains some cobalt (1 to 3.8 mass percent) and an insignificant amount of nickel (0.19 wt. % at most, see Table 4). In low sections of the intrusive, the nickel concentrations are as high as 6.3 wt. % (Table 4). The pyrite segregations in silicates have practically no cobalt or nickel.

Within the wedge-out interval, the mineralized horizons are represented by a millerite+chalcopryrite+pyrite association. The millerite forms contact segregations sizing up to 0.3 mm. The pyrite, again, is contaminated with cobalt (Table 4). These three principal sulphides are accompanied by thiospinels containing nickel, iron and cobalt.

Common accessory minerals comprise sphalerite, mackinawite and argentopentlandite, their concentrations increasing in the chalcopryrite paragenesis. Iron concentration in sphalerite is something around 7 wt. %, cadmium is 0.9-1. wt. %. Manganese admixture is in insignificant amount of 0.02-0.05 wt. % (Table 4).

Structural and textural features of the ore minerals indicate that the sulphides formed during the late magmatic stage of the massif-forming process. The fact that the pentlandite of the porphyraceous segregations contains much nickel, when there is a high iron content in the accompanying pyrrhotite, and that the flame-like pentlandite is also rich in iron, leads us to assume that the mineralization

Table 4. Chemical composition of sulphides from the Mt. General'skay massif.

Sample nn	Mineral	Ni	Fe	Cu	Co	S	Total
3460/308.4	Millerite	64.61	1.02	0.03	-	35.38	101.9
	Violarite	42.11	23.58	0.41	0.04	32.09	98.23
	Pyrite	-	45.31	-	1.71	53.57	100.59
	Chalcopyrite	-	30.12	34.9	-	35.14	100.16
	Pentlandite	37.50	28.73	0.01	0.30	33.94	100.48
3460/457.7	Pyrite	0.03	44.41	-	2.55	53.60	2.55
	Chalcopyrite	0.02	30.44	35.14	-	34.52	100.12
	Pentlandite	24.00	38.79	0.07	0.02	35.44	98.32
	Pyrrhotite (hexagonal)	0.18	61.23	0.02	-	39.50	100.93
	Pyrrhotite (monoclinal)	0.43	61.35	-	-	39.05	100.83
3460/540.4	Pentlandite I	38.04	27.06	0.02	1.76	33.75	100.63
	Pentlandite II	34.88	29.89	0.03	1.32	34.14	100.26
	Pyrrhotite	0.50	62.16	-	0.03	39.93	101.62
3460/541.9	Pentlandite I	35.84	27.80	0.02	2.39	34.62	100.67
	Pentlandite II	29.54	34.63	0.04	0.35	35.37	100.3
	Pyrrhotite	0.42	61.42	-	-	38.79	100.65
3461/887.7	Pentlandite I	36.32	29.64	0.07	0.62	33.62	100.27
	Pyrrhotite	0.22	61.74	0.01	-	39.09	101.06
	Pyrite	-	42.96	0.01	3.81	53.65	100.43
	Pentlandite	35.95	31.9	0.17	0.21	32.96	101.19
	Pentlandite	19.51	34.66	0.23	-	31.53	100.13
3462/821.2	Pentlandite	35.14	30.11	-	1.12	33.95	100.32
	Sphalerite	8.00	53.05	0.27	-	37.12	98.44
	Sphalerite	0.20	7.15	0.13	0.05	33.67	100.55
3463/1146.3	Pentlandite I	34.16	28.93	0.07	1.17	33.4	99.71
	Pyrrhotite	0.43	58.80	-	-	38.94	98.17
	Pyrite inclusions in silicates	0.04	44.90	-	-	53.36	98.30
	Pyrite inclusions in sulphides	0.15	44.48	-	2.03	53.45	100.11
3463/1148.5a	Pentlandite I	36.38	28.69	0.05	0.77	34.75	100.63
	Pyrrhotite	0.40	58.93	0.02	-	40.45	99.85
3463/1148.5b	Pentlandite	37.15	28.90	0.07	0.6	32.95	99.67
	Pyrrhotite	0.55	61.29	0.01	-	39.80	101.66
	Pyrite	0.03	45.95	-	1.11	54.92	102.01
3463/1159.2	Pentlandite I	36.50	29.59	0.04	0.44	34.24	100.81
	Pentlandite II	36.50	29.10	0.05	0.49	33.22	99.45
	Pyrrhotite	0.30	60.11	-	-	39.16	99.57
	Pyrite	0.19	46.38	0.05	0.98	54.15	101.75
3463/1154.4	Pentlandite I	37.35	27.80	0.03	1.10	34.58	100.86
	Pentlandite II	37.28	27.89	0.06	1.05	34.97	101.25
	Pyrrhotite	0.72	61.34	0.02	-	39.24	101.35
3463/1244.5	Pentlandite I	36.22	29.29	0.05	1.03	33.33	99.92
	Pyrrhotite	0.19	60.39	0.03	-	39.72	100.34
	Chalcopyrite	0.04	29.89	34.75	-	34.43	99.11
3463/1249.5	Pentlandite	36.60	29.01	0.05	0.83	33.36	99.85
	Pyrrhotite	0.30	60.18	-	0.02	39.50	102.00
3463/1250.5	Pentlandite	36.95	29.24	0.07	0.71	34.15	101.12
	Pyrrhotite	0.42	60.40	-	-	38.70	99.52
	Chalcopyrite	-	31.13	34.22	-	34.90	100.25
3463/1292	Pentlandite I	36.66	29.85	0.07	0.47	33.41	100.46
	Pentlandite I	36.02	28.95	0.05	0.70	33.46	99.18



3463/1292	Pyrrhotite	0.24	60.97	0.03	-	38.93	100.17
	Pyrite	-	43.72	0.02	2.50	53.37	99.61
3463/1420	Pentlandite I	34.98	30.17	0.09	1.02	33.17	99.43
	Pyrrhotite	0.04	61.52	0.05	-	38.16	99.77
3463/1421.2	Pentlandite I	36.16	29.41	0.04	1.14	33.27	100.02
	Pentlandite II	29.35	35.63	0.05	0.53	34.63	100.20
	Pyrrhotite	0.43	61.07	-	-	39.08	100.58
3463/1431.8	Pentlandite I	36.85	28.65	0.05	0.76	33.69	100
	Pentlandite II	37.26	28.75	0.01	0.06	33.90	99.98
	Pyrrhotite	0.43	59.97	-	-	38.63	99.03
	Pyrite	0.01	44.75	-	2.09	53.47	100.32
3463/1449.3	Pentlandite I	36.41	29.59	0.10	1.52	33.33	100.95
	Pentlandite II	25.2	39.15	0.04	0.78	35.68	100.85
	Pyrrhotite	0.47	60.33	-	-	38.51	99.31
3463/1482.9	Pentlandite I	36.14	29.10	0.03	0.41	34.31	99.99
	Pentlandite II	35.75	29.22	0.05	0.22	34.41	99.65
	Pyrrhotite	0.44	60.71	-	-	39.18	100.33
	Pyrite	-	45.44	-	1.49	53.44	100.37
3463/1493.5	Pentlandite	36.24	27.87	0.04	2.20	33.9	100.25
	Pyrrhotite	0.61	60.50	-	0.01	39.49	100.61
3463/1509.6	Pentlandite I	36.09	28.53	0.04	1.45	34.06	100.17
	Pentlandite II	36.46	28.15	0.06	1.48	33.37	99.52
	Pyrrhotite	0.44	60.23	-	-	38.73	99.40
3463/1514.9	Pentlandite I	36.63	28.58	0.04	1	32.74	98.99
	Pyrrhotite	0.51	61.40	-	-	39.10	101.90
	Chalcopyrite	0.05	30.97	34.94	-	34.17	100.09
3463/1554.9	Co-pentlandite	30.99	23.76	0.03	12.38	33.15	100.31
	Co-pentlandite	32.05	23.40	0.12	11.12	33.51	100.20
	Pyrrhotite	0.33	62.06	-	0.12	38.33	100.84
	Pyrrhotite	0.83	60.02	0.05	0.19	39.14	100.28
	Chalcopyrite	0.04	31.06	34.93	-	34.3	100.33
	Sphalerite	0.01	6.83	0.08	0.17	33.32	99.56
3463/1564.7	Pentlandite	36.21	28.27	0.11	1.39	34.09	100.07
	Chalcopyrite	-	31.27	34.25	-	35.06	100.68
	Pyrite	6.33	39.96	0.06	0.22	54.05	100.62

*Dashes, below detection limit*

process developed over a long period. During this process, as much nickel as possible localized in the porphyraceous pentlandite while peritectic point reactions were going between a crystallizing sulphide melt and residual sulphide liquid.

### Platinum mineralisation

A low-sulphide platinum mineralization, a particular type of platinum ore type that is characteristic of rhythmically layered intrusives, has not been encountered in the Mt. General'skaya massif so far. The platinum mineralization associates with magmatic sulphides only. The way these sulphides are distributed, and the amount in which they have accumulated, influenced a

distribution pattern and concentration of platinum group elements (PGE).

Correlation coefficients for concentrations of sulphur, nickel and copper on the one hand, and PGE total on the other, are estimated at no less than 0.8 for some drill holes and as 0.89 for the whole set of analytical data.

In compliance with the aforementioned regularities in a sulphide distribution pattern, the platinum mineralization is localized within several horizons ranging in thickness from one to ten meters. The highest concentrations of total metals in particular samples come to 3.5 ppm, yet in most of the samples  $PGE_{tot}$  is not greater than 1 ppm. Of all the platinum metals it is palladium that prevails, while the palladium to platinum ratio is close to 10:1. A

remarkable feature of the massif is its relatively high concentration of rare platinoids in PGE<sub>tot</sub>. Thus, in single samples, the concentrations of rhodium, iridium and osmium in amounts of up to 0.1 ppm are recorded, whereas platinum content in the same samples ranges from 0.05 to 0.10 ppm.

The principal holders of platinoids are the sulphoarsenites of nickel, cobalt and iron, and the platinoid minerals themselves. And the contribution of PGE's solid solutions in the sulphides, when compared with an overall balance of these elements, is rather insignificant.

The sulphoarsenites form fine (2-100 microns) numerous isometric grains with crystallographic limits. The sulphoarsenites contain the xenoliths of the enclosing sulphides. The sulphoarsenites are

represented largely by nickel-enriched cobalt, far less by cobalt gersdorffite, with a wide range of nickel and cobalt concentrations and less variable iron concentrations (Table 5). The mineral-forming metal concentrations vary within single grains. There are cases when nickeline grains are encountered in a central portion of the sulphoarsenite segregations.

The sulphoarsenites always contain quite noticeable concentrations of PGEs, especially rhodium and palladium (Table 6). The iridium and ruthenium concentrations therein do not exceed 0.19 wt. %, and that of osmium comes to 1.50 wt. %. Palladium, too, produces its own minerals of a merenskyite-melonite series, and there palladium and nickel concentrations are estimated at 14-28 and 0- wt. % respectively (Table 5). Atomic ratio numbers of

Table 5. Chemical composition of Pd-Pt-Bi minerals from the Mt. General'skay massif.

Sample nn	Mineral	Pd	Pt	Ni	Te	Bi	Sb	Total
3466/888.10	Merenskyite	26.56	0.38	-	54.07	18.20	0.20	99.40
"	"	27.06	0.14	-	54.73	18.61	0.19	100.80
3463/1249.6	"	26.76	0.42	-	50.55	22.60	0.33	100.66
3463/1493.5	"	26.17	0.75	0.07	50.40	22.31	0.24	99.94
3463/1292.0	"	26.83	0.05	0.08	59.33	12.53	0.20	99.02
3461/887.6	"	25.57	0.51	0.54	57.9	14.20	0.42	99.14
3462/987.0	"	25.04	0.16	1.17	62.79	9.18	0.65	98.99
"	"	26.15	0.54	1.20	62.84	8.99	0.66	100.38
3461/787.2	"	24.58	0.12	1.47	58.46	15.51	0.48	100.62
3461/887.7	"	24.66	0.47	1.83	58.36	14.86	0.44	100.01
3463/1430.0	"	24.84	0.33	1.91	65.78	7.79	0.34	100.95
3463/1425.4	Ni-merenskyite	20.97	0.40	4.18	66.34	8.51	0.25	100.65
3463/1449.3	"	17.42	-	6.56	68.76	6.35	0.40	99.49
3463/1431.8	Pd-melonite	14.64	0.32	8.66	71.68	5.03	0.35	100.68
3463/1244.0	"	14.58	0.57	8.77	69.71	6.42	0.46	100.51
3461/887.7	Kotulskite	41.86	0.17	-	37.84	19.89	0.30	100.06

Dashes, below detection limit.

Analyses were performed at ZNIGRI using a microprobe 'Camebax' by M. Botova

nickel and palladium are in a 0-1.1 range interval. Bismuth turns out to be a champion (up to 22.6 wt. % concentration in these minerals), and there is always some mix of platinum (up to 0.75 wt. %) and antimony (0.19-0.66 wt. %). The minerals give shape to fine (5-200 microns), rounded, ellipsoid, occasionally irregular bodies which are observed in pyrrhotite, pentlandite, chalcopyrite, and the contacts of sulphide and silicate grains. More often than not, palladium-bearing minerals are found in intergrowths together with the sulphoarsenites of cobalt, nickel and iron. A kotulskyite is spotted very seldom, occurring in fine (few microns)

segregations where it is intergrown with the abovedescribed minerals.

A sperrylite is a main reservoir for a platinum: it is in the form of elongated metacrysts, no larger than 100 microns in size, and it is always contaminated with rhodium (up to 1 wt. %).

The PGE's distribution in the sulphides (pentlandite and pyrite) is most irregular. Both analyzed minerals contain platinum, palladium, osmium, and iridium, each element in amount of maximum 0.2 wt. %.

Table 6. Chemical composition of As-Sb-S minerals from the Mt. General'skay massif.

Sample nn	Mineral	Co	Ni	Fe	Pt	Pd	Rh	Jr	Ru	Os	As	Sb	S	Total
3463/1554.9	Cobaltine	25.43	7.00	3.65	-	0.3	-	-	-	-	43.4	-	21.05	100.83
3461/887.7	"	21.23	5.82	9.16	0.14	0.29	1.25	-	-	-	39.74	-	22.47	100.15
3463/1249.6	"	19.34	10.34	6.41	0.17	0.12	-	-	-	0.20	43.99	0.01	19.43	100.01
3463/1153.2	"	18.96	10.91	5.75	-	0.25	-	-	-	-	43.11	-	21.17	100.15
3461/887.7	"	18.55	9.98	4.83	0.21	0.55	-	-	-	-	45.04	-	20.73	100.21
3463/1435.6	"	18.08	10.18	5.89	0.30	0.39	2.36	0.15	0.11	1.50	41.59	0.01	18.78	99.34
3463/1154.4	"	17.58	12.77	4.23	0.10	1.46	-	-	-	-	44.45	-	18.60	99.19
3463/1449.3	"	17.81	10.58	5.59	0.27	0.57	1.34	-	-	-	43.44	-	19.56	99.16
3463/1154.4	"	17.33	12.29	5.82	0.15	0.71	-	-	-	-	42.97	0.02	19.40	98.67
3462/987.0	"	15.59	13.01	5.21	0.37	1.55	-	0.13	-	0.68	44.27	-	28.02	100.85
3461/887	Gersdorffite	7.41	16.84	4.72	0.15	2.56	3.43	0.19	-	0.11	49.02	0.01	19.54	98.98
3463/1153.2	Nickeline	0.14	44.16	0.20	0.01	0.13	0.03	0.04	-	-	55.51	-	0.08	100.30

*Dashes*, below detection limit.

Analyses were performed at ZNIGRI using a microprobe 'Camebax' by M. Botova



## References

Amelin, Yu.V., Heaman, L.M. & Semenov, V.S. 1995: U-Pb geochronology of layered mafic intrusions in the eastern Baltic Shield: implications for the timing and duration of Palaeoproterozoic continental rifting. *Precambrian Research*, 75, 31-46

Balashov, Yu.A., Bayanova, T.B. & Mitrofanov, F.P. 1990: The Imandra Lopolith. In: Mitrofanov, F.P. & Balashov, Yu.A. (eds), *Geochronology and Genesis of Layered Basic Intrusions of the Kola Peninsula*. Apatity, Russia, pp. 24-30.

## EXCURSION ITINERARY

### An overview

The Early Proterozoic supracrustal rocks of the Petsamo Supergroup and their associated intrusive mafic-ultramafic complexes are excellently exposed in the vicinities of Zapolyarny and Nickel. Much of this area was the focus of exploration and prospecting for ultramafic-hosted sulphide Ni-Cu ores and therefore was intensively drilled and mapped during the last few decades. As a result of this prospecting work a number of new deposits have been discovered in the central Pechenga area, namely between Nickel and Zapolyarny.

The area is heavily polluted by the smelter in Nickel. The pollution impact in this area has resulted in vegetation damage, primarily to the north and north-east of Nickel. This in turn led to removal (by wind and fire) of dead vegetation and rapid erosion of soil. The final result is a completely bare landscape where the level of bed-rock exposure reaches 70-100%. What a geologists' dream!

Seventeen localities will be examined in the course of a three-day excursion. All localities are shown on the Russian topographic map as well as on the inset of the simplified geological map (Fig. 1). The localities are also listed in the stratigraphic column (Fig. 2).

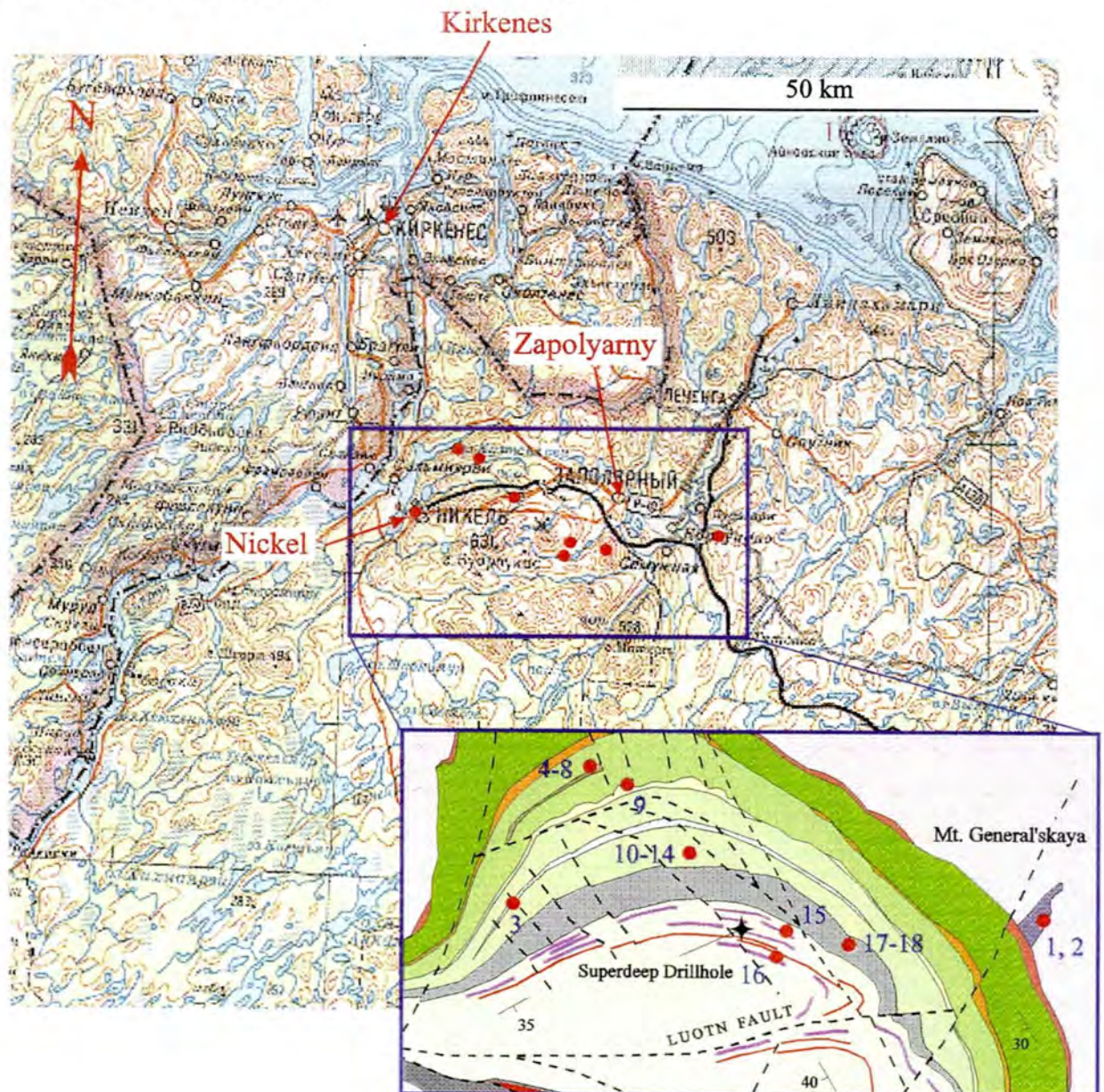


Fig. 1 Outline topographic and geological maps showing the excursion localities. For legend of the geological map see Fig. 2 in Melezhih 1996 (this volume).



ARCHAEAN			Stop nn	
EARLY PROTEROZOIC THRUST				
PETSAMO SUPER-GROUP	?	Tal'ya Fm.		
		L. Pestchanoe Fm.		
		Kasesjoki Fm.	Siltstone Mem.	
			Conglomerate Mem.	
	MID PETSAMO OROGENIC UNCONFORMITY			
	South Pechenga Group	Kaplya Fm.		
		Mennel' Fm.		
		Bragino Fm.		
		TECTONIC CONTACT		
		Kallojavr Fm.		
	PORITASH FAULT			
	PETSAMO SUPER-GROUP	Pilgujarvi Volc. Fm.	Suppavara Mem.	
			Upper Basalt Mem.	
			Middle Basalt Mem.	
Rhyolite Mem.			16	
Lower Basalt Mem.				
Basalt-Picrite Mem.			15	
Pilgujarvi Sed. Fm. (Productive Fm.)		Lammas Mem.	14	
		B Mem.	17, 18	
		A Mem.		
WEATHERING CRUST				
Kolasjoki Vol. Fm.		Upper Basalt Mem.	10-13	
		Black Shale Mem.		
		Lower Basalt Mem.		
North Pechenga Group		Kolasjoki Sed. Fm.	Black Shale Mem.	
	Dolostone Mem.			
		Red Bed Mem.	9	
DISCONFORMITY			9	
Kuetsjarvi Volc. Fm.	Basalt Mem.			
	Trachyandesite Mem.			
	Conglomerate Mem.	5-8		
	DISCONFORMITY	5		
	Trachyandesite Mem.	4		
Kuetsjarvi Sed. Fm.	Basalt Mem.			
	Dolostone Mem.			
	Quartzite Mem.			
DISCONFORMITY				
	Ahmlahti Volc. Fm.			
	Ahmlahti Sed. Fm.			
REGOLITH				
FIRST-ORDER UNCONFORMITY			1, 2, 3	
ARCHAEAN				

Fig. 2 Stratigraphic column showing the stratigraphic location of excursion stops.



## The Kola Superdeep Drillhole

*The guide is Dr. D.M.Guberman, Kola Superdeep Drillhole GeoLaboratory.*



**Superdeep Drillhole. 9 km south-west of Zapolyarny at 30°10'E 69°25'N (Fig. 1).**

**The 7,000 m thick sequence of the Early Proterozoic Petsamo Supergroup followed by 5, 256 m of Archaean supracrustal and igneous rocks.**

The Kola Superdeep Drillhole is still by far the deepest in the world (Fig. 3). The drilling started in May 1970 and stopped in 1995 after a number of unsuccessful attempts to pass a boundary depth of 12, 256 m which has been already reached in 1987.

The goals of this drilling program were: (a) to obtain direct information regarding the chemical composition and material properties of the upper and middle continental crust, and (b) to modernise existing equipment and technology for ultradeep scientific drilling. Since 1995, when drilling was stopped, the Kola Superdeep Drillhole has been reorganised into a GeoLaboratory for geochemical and petrophysical comparison of surface and deep-seated bed-rocks in the vicinity of the drilling site.

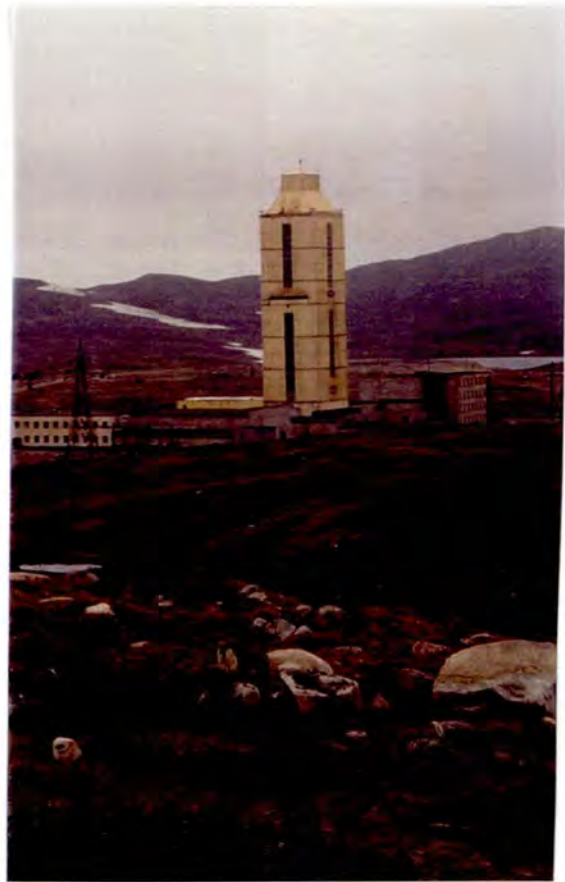


Fig. 3 Kola Superdeep Drillhole. Derrick housing.

## North-eastern Pechenga Greenstone Belt

*The guide is Dr. V.A.Tel'nov, Pechenga Exploration Expedition.*





**Locality 1, 2. Road Zapolyarny-Luostari, road-cut at 31°05'45"E 69°25'44"N.**

**Layered gabbro massif of Mt. General'skaya (Fig. 1).**

This route takes us from the town of Zapolyarny to Luostari, along the Kirkenes- Murmansk road and a local dirt road from Zapolyarny to Luostari. Gabbros outcrop west and south of the dirt road and are exposed best on Mt. General'skaya. The low-grade sulphide mineralisation in the lower gabbro zone may be seen in outcrops and in large blocks on the south-western and north-western cliffs of Mt. General'skaya

Rocks of the rhythmic peridotite-norite zone are exposed on the north-eastern slope of the Mt. General'skaya. Coarse-grained gabbros, gabbro-norites and piroxenites with disseminated sulphides may be observed.

**Locality 3. Drill-core storage, the town of Nickel. Core material from drill hole 3463 at 31°02'52"E 69°23'17"N.**

**Complete section of the layered gabbro massif of Mt. General'skaya.**

The most complete sequence of the layered gabbro complex was drilled by drill hole 3463 (Fig. 4).

The lowest fine-grained gabbro is a 10 to 15 meters thick layer which directly touches the Archaean gneisses. Rocks of the basal zone contain xenoliths of country rocks including quartz-biotite schists, microquartzites, biotite-plagioclase-actinolite schists and gneisses.

*The basal zone* has a total thickness about 80 m and comprises trachytoid, porphyritic and fine-grained gabbro-norites and gabbros.

The trachytoid gabbros consist of plagioclase (40-60%), amphibole (30-50%), phlogopite (up to 5%), sphene (up to 1%), and quartz. The cumulus plagioclase An<sub>53-56</sub> is remarkable for a very obvious orientation of fine (0.2-0.8 mm) long-prismatic crystals. A light-brown cumulus hornblende produces porphyroeous segregations (1.5-2 mm). A clinopyroxene is replaced in these rocks by a yellowish-green actinolite, phlogopite and titanite.

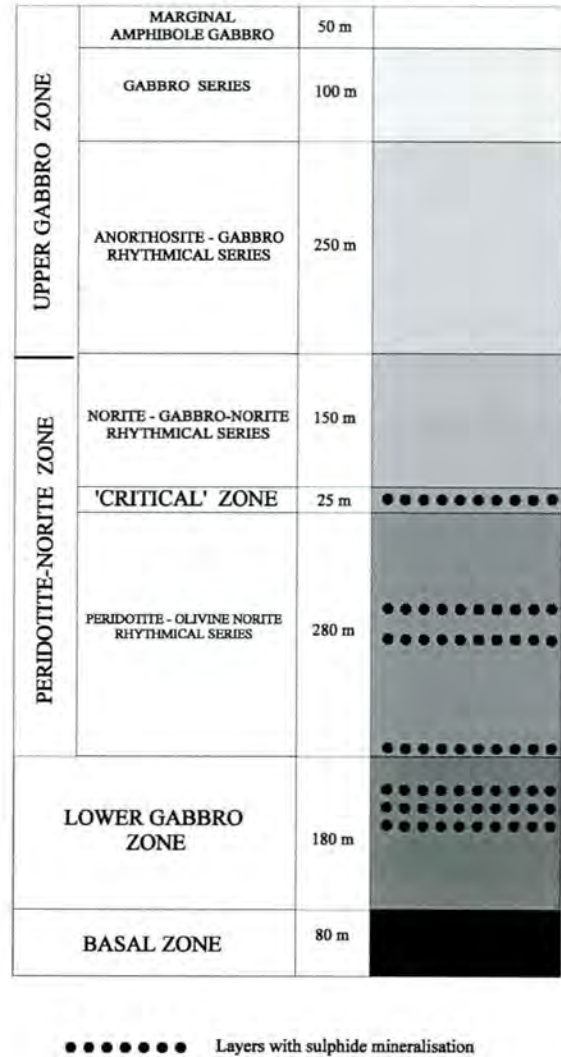


Fig. 4 Lithological sequence of the Mt. General'skaya layered gabbro complex, drill hole 3463.

An intercumulus occasionally contains quartz as well.

Higher in the basal zone the trachytoid gabbroids are gradually replaced by porphyritic gabbro-norites and gabbros. The trachytoid structure of these rocks disappears. These rocks have cumulus bronzite as a component (0-10%) in the form of large (2-3 mm) short-tabular insets, and also sporadic prisms of augite (0-5%).

*Lower gabbro zone* rocks, a 180 m thick unit of mesocratic gabbro-norites and gabbros alternating with gabbro-norites or quartz-bearing and micropegmatitic gabbros and anorthosites, contain no olivine cumulus. The latter is replaced by bronzite, plagioclase-bronzite and plagioclase cumulus associations.

**The peridotite-norite zone** has a thickness of 305 m and comprises three units: the upper rhythmic norite-gabbro-norite and lower peridotite-olivine-norite series with a critical zone between them.

The gabbro consists of medium-grained rocks with ophitic and poikilitic-ophitic structures. These rocks are made of cumulus plagioclase (40-50%) and intercumulus clinopyroxene (35-45%), as well as of orthopyroxene (under 5%), phlogopite and oxides.

The gabbro-norites and norites are the most abundant rocks of the upper series. They are coarse-to medium-grained, with gabbroic-ophitic, poikilitic and gabbroic structure variations. The bytownite (40-55%) fills the cumulus of the rocks. The diopside-augite of the intercumulus appears in the form of grains and poikilocrysts which are xenomorphous with respect to the plagioclase. The bronzite is represented by idiomorphic short-prismatic or isometric crystals sizing 1-3 mm. The intercumulus minerals are light-brown hornblende (less than 1%), phlogopite, oxides and apatite.

The coarse- and medium-grained, poikilitic and ophitic olivine norites and olivine gabbro-norites vary in thickness from a few to about 20 meters, and their maximum thickness of 20-22 m is at the bottom of the zone. The rocks consists of widely variable amounts of plagioclase (20-70%), olivine (5-45%), orthopyroxene (10-40%) and clinopyroxene (0-15%), as well as minor hornblende (under 5%), phlogopite (under 1%), oxides and sulphides. The cumulus olivine has a persistent composition, Fo<sub>70-76</sub>. The cumulus plagioclase is bytownite (An<sub>69-74</sub>) which is identified in the form of subidiomorphic prismatic crystals (0.8-1.2 mm). The pyroxenes represent intercumulus stages. The bronzite, Ca<sub>3-5</sub>Mg<sub>71-78</sub>Fe<sub>17-25</sub>, forms xenomorphic oikocrysts (up to 5-7 mm). The diopside-augite, Ca<sub>37-45</sub>Mg<sub>45-51</sub>Fe<sub>8-12</sub>, is more variable through the zone section

The poikilitic peridotites (harzburgites), in 4 to 6 m thick layers, are developed at the bottom of a few rhythms, within the rhythmic peridotite-olivine-norite series. The harzburgites consist of olivine (40-60%), orthopyroxene (35-50%), clinopyroxene (under 10%), hornblende (2-4%), phlogopite and plagioclase (under 5%). The is remarkable for its most high magnesium content, Fo<sub>77-78</sub>.

The plagioclase (An<sub>66-70</sub>) developed as zoned prismatic grains in the cumulus. The hornblende produces separate grains or discontinuous coronitic reaction rims around the olivine and at its contact with the plagioclase.

**The critical zone** of the intrusive is a 25 m thick unit of taxitic rocks with irregular combination of coarse- and fine-grained anorthosite, leuco- and melanogabbro-norites. The rocks comprises plagioclase adcumulate, coarse-to-medium-grained cotectic orthopyroxene-plagioclase growths, and micro-grained plagioclase segregations with a flow texture.

**The upper gabbro zone**, a 250 m thick unit, is identified in an upper section of the massif. A cross-section of the zone reveals three series (top to bottom): marginal amphibole gabbro (50 m), gabbro series (100 m), and anorthosite-gabbro-norite rhythmic series (250 m).

**The marginal amphibole gabbro series** rocks, medium-grained, massive, ophitic gabbros make up the top endocontact zone of the massif. Principle rock-forming minerals include plagioclase (40-70%) and amphibole (35-50%) with subordinate phlogopite, quartz, sphene and apatite. The plagioclase (An<sub>47-65</sub>) is severely saussuritized and prehnitized. The amphiboles are represented by both primarily magmatic and pseudomorphous after clinopyroxene.

**The gabbro series** comprises coarse-to-medium-grained, mesocratic, ophitic and gabbros, which have gabbroic and poikilitic gabbros. The rocks consist of prismatic and tabular crystals of plagioclase (An<sub>62-69</sub>) cumulate with the intercumulus amphibolized clinopyroxene.

**The rhythmic anorthosite-gabbro-norite gabbro series** forms a major portion of the upper gabbro zone. The top edge boundary is marked by a 5 to 10 m thick layer of anorthosites and leucogabbroids. Each rhythm has a regular composition: its top portion comprises anorthosite, leucogabbro and leucogabbro-norite; a middle portion contains gabbro and norite-gabbro; at the bottom of the rhythms we find melanogabbro-norite.



## The central Pechenga Greenstone Belt

The guide is Dr. V.A.Melezhik, Geological Survey of Norway.



**Locality 4. The Western Orshoivi, well exposed area at 30°18'50"E 69°28'20"N.**

**The succession of alkaline andesites, dacites and albitophyres of the Trachyandesite Member, the Kuetsjärvi Volcanic Formation (Fig. 1, 2, 5).**

This route takes us from Nickel along an extremely bad dirt road to the western part of Luchlompollo and then by hiking (1h. 40 min one way) to the mountain of Western Orshoivi (Fig. 5).

The Trachyandesite Member of the Kuetsjärvi Volcanic Formation is a sequence of up to 400 m of alkaline andesites, dacites, and rhyolite that is present throughout the Pechenga-Pasvik palaeorift. Lying conformably on the Lower Basal Member it serves as a very valuable stratigraphic marker. The

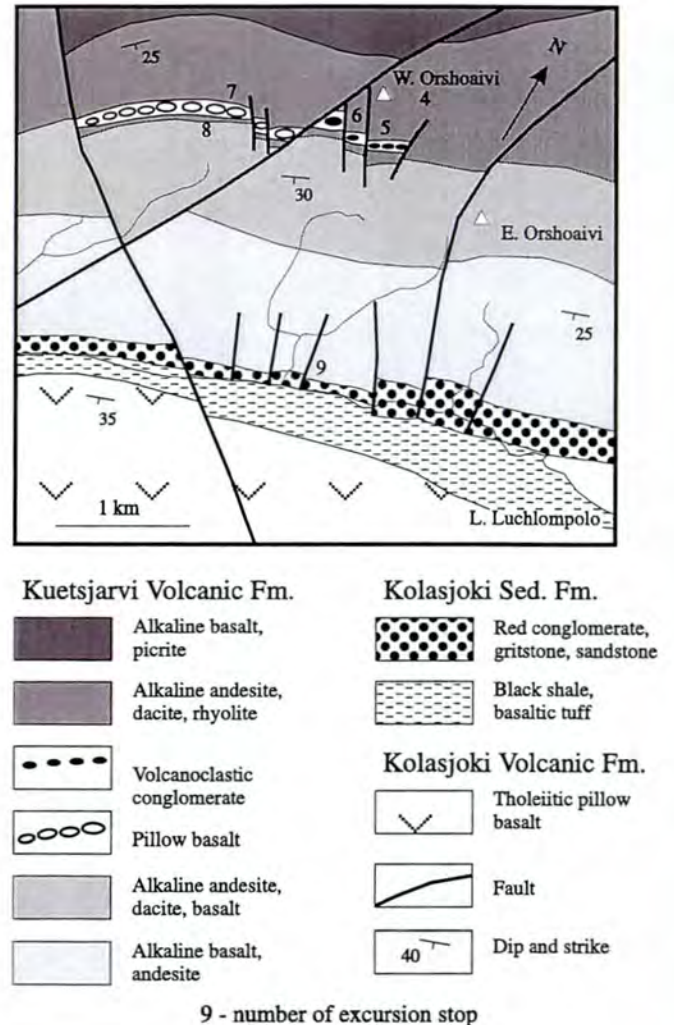


Fig. 5 Geological map of the Orshoivi area.

rocks of this unit contain ubiquitous vesicles and large amount of quartz, albite and hematite-filled amygdules (Fig. 6). The unit consists of a number of flows separated in places by thin layers of interflow breccia. The base of the flow unit may be rather massive and weakly vesicular while the middle part is represented by fluidal lava with spectacular flow-folded structures. Individual flows have grey or dark grey lower parts and red or brownish upper parts. Reddening is much more marked at the top of the flow unit. Contraction, exfoliation and reddening penetrating joints gave rise to polygonal structure at the top of some flow units (Fig. 7). The structure is of some palaeoenvironmental significance because the reddening is interpreted as being caused by surface oxidation. Oxidation of the upper parts of the lava flows on extrusion is a



common phenomenon affecting lava extruded in subaerial environments beneath oxygeniferous atmosphere. The reddening of the tops of the flows

is evidence that such an atmosphere existed when the Trachyandesite Member of the Kuetsjärvi Volcanic Formation was extruded.



Fig. 6 The amygdaloidal dacite, the Trachyandesite Member of the Kuetsjärvi Volcanic Formation. The bar-scale is 10 cm.



Fig. 7 The top of the dacitic lava-flow marked by the polygonal structure and reddening penetrating joints.

**Locality 5. The Western Orshoavi, well exposed area at 30°18'40"E 69°28'00"N.**

**The Conglomerate Member of the Kuetsjärvi Volcanic Formation (Fig. 2, 5). Contact between trachyandesite unit and volcanoclastic conglomerates. The complete sequence of the Conglomerate Member.**

The Conglomerate Member is a sequence of up to 80 m of polymict volcanoclastic conglomerates, siltstones, mudstones and pillow basalts.

Conglomerates rest unconformably on an uneven surface of alkaline andesites and mark a short-term nondepositional break. The conglomerate unit at locality 5 is made of pebble-supported polymict volcanoclastic conglomerates consisting of well rounded, poorly sorted pebbles and boulders (Fig. 8) which derive from the underlying volcanic sequence. Volcanic bombs may also be present. The unit is clearly layered and it composed of a number of 1 to 2m thick layers of conglomerates which are distinguished by clast size. In the upper most parts of the conglomerate sequence, a 0.5 m thick layer of black magnetite and hematite-rich siltstone is present.





Fig. 8. The volcanoclastic polymict pebble-supported conglomerate composed of pebbles of alkaline andesites and dacites derived from the Trachyandesite Member of the Kuetsjärvi Volcanic Formation.

The conglomerate member is of palaeotectonic significance because it indicates deposition in a water environment. The rocks of this unit are the only ones which were deposited in an ephemeral shallow water rift lake, while the rest of the Kuetsjärvi Volcanic Formation rocks are entirely subaerial. This lake developed only in the central part of the Western Rift Graben and it was apparently bounded by syndepositional faults.

**Locality 6. The Western Orshoavi, well exposed area at 30°18'10"E 69°28'00"N.**

**The Conglomerate Member of the Kuetsjärvi Volcanic Formation (Fig. 2, 5), mudstones with large boulders of dacite interpreted as a mud flow.**

The conglomerate sequence is replaced westwards by the black mudstones containing large boulders of dacites which are chaotically organised in the massive mud matrix (Fig. 9). These rocks are interpreted to represent a mass flow which was apparently provoked by an earthquake.



Fig. 9 Mud-supported volcanoclastic conglomerate.



**Locality 7. The Western Orshoavi, well exposed area at 30°17'30"E 69°27'30"N.**

**The Conglomerate Member of the Kuetsjärvi Volcanic Formation (Fig. 2, 5), the succession of pillow basalts.**

Further west from locality 6 the shallow water conglomerate- mud-flow association is gradually wedged-out and replaced by a 1 to 6 m thick layer of pillow basalts. The pillow basalts were emplaced on a surface of soft, unconsolidated, black, mud supported conglomerates (mud flow). The

mudstones are strongly deformed by lava flow and fill the spaces between the pillows in the footfall of the lava flow. The large, slumped pillows (Fig. 10) clearly indicate an eastern source for the unit. The pillow basalts, together with the underlying mud-supported and pebble-supported conglomerates, are considered to have formed within a restricted ephemeral lake. As it has been already discussed (locality 5) this lake developed only in the central part of the Western Rift Graben of the Pechenga intracontinental rift, the remainder of which was characterised by essentially subaerial volcanism.



Fig. 10. Slumped pillow in basalts of the Conglomerate Member of the Kuetsjärvi Volcanic Formation.

**Locality 8. The Western Orshoavi, well exposed area at 30°16'50"E 69°27'30"N.**

**The Upper Trachyandesite Member of the Kuetsjärvi Volcanic Formation (Fig. 2, 5), basalts with columnar joints.**

Immediately above the pillow lava unit another thin basalt flow occurs. This exposes an excellent development of columnar joints (Fig. 11) and manifests that an ephemeral lake filled completely and disappeared. From locality 8 further up to the top of the Kuetsjärvi Volcanic Formation, the



volcanic rocks possess only structural features which reflect deposition of the rocks in a

subaerial environment.



Fig. 11 The alkaline basalts with columnar joints. The hammer in the centre is 60 cm in length.

### **Locality 9. The Lake Luchlompolo, road cut section, small quarry and trenches at 30°19'40"E 69°26'50"N.**

#### **The contact between the Kuetsjärvi Volcanic Formation and Kolasjoki Sedimentary Formation (Fig. 1, 2, 5)**

At several localities near Luchlompolo, the Kuetsjärvi volcanites immediately adjacent to the Kolasjoki Sedimentary Formation show signs of subaerial weathering. The weathered rocks, represented by altered, patchy black-and-pink basalts, were only preserved in the palaeotopographic heights and were entirely removed by pre-Kolasjoki erosion in the palaeovalleys (Fig. 12). The parent materials for the palaeosols are alkaline basaltic lavas with columnar joints. The columns gradually become subdivided into small, rounded patches with highly oxidised, concentric boundaries on spheroidally weathered black-and-pink rocks. The

development of corestones appears to be directly related to the geometry of original columnar structure. The effects of weathering penetrated along the margins of the columns, causing weathering to proceed more rapidly along the outer margins of the columns. The spheroidal weathering produced corestones with black, hematite-rich, rims and pink cores and eventually developed a distinctive patchy structure which is locally called 'leopard' structure (Fig. 13).

The Kolasjoki Sedimentary Formation at Luchlompolo is a 60 to 100 m thick sequence of typical red beds. The formation starts with alluvial units which are violet, fine-grained, cross-bedded, ripple-marked sandstones containing a number of small pockets of pebbles. Black heavy minerals are common in coarse and fine-grained rocks. Synsedimentary folding, brecciation and various collapse-structures are very prominent at the Luchlompolo locality. All these are related to a syndepositional faulting and development of small-scale transversal graben (palaeovalleys).



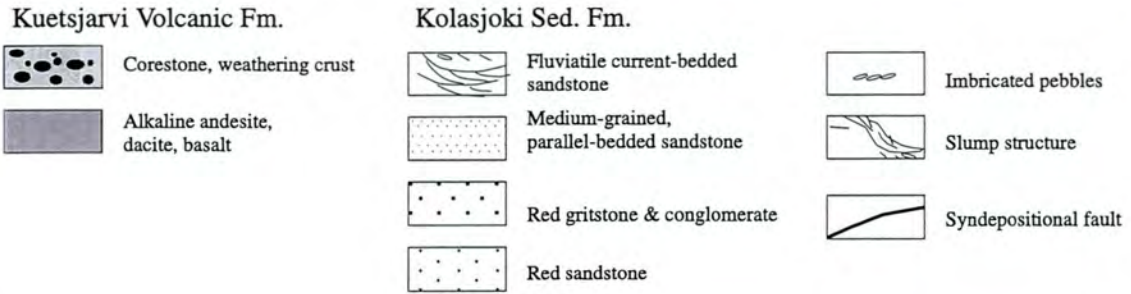
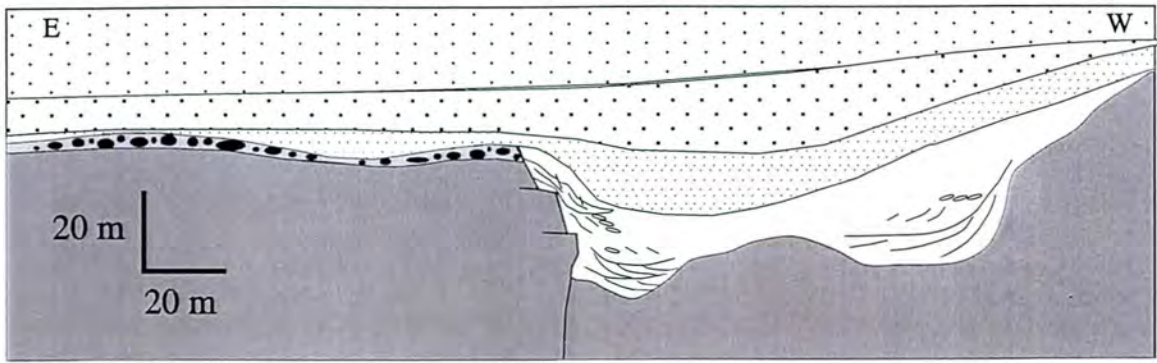


Fig. 12 Diagrammatic field sketch illustrating the palaeovalley filled inwith fluviatile sediments. 2 km west of Luchlompolo.

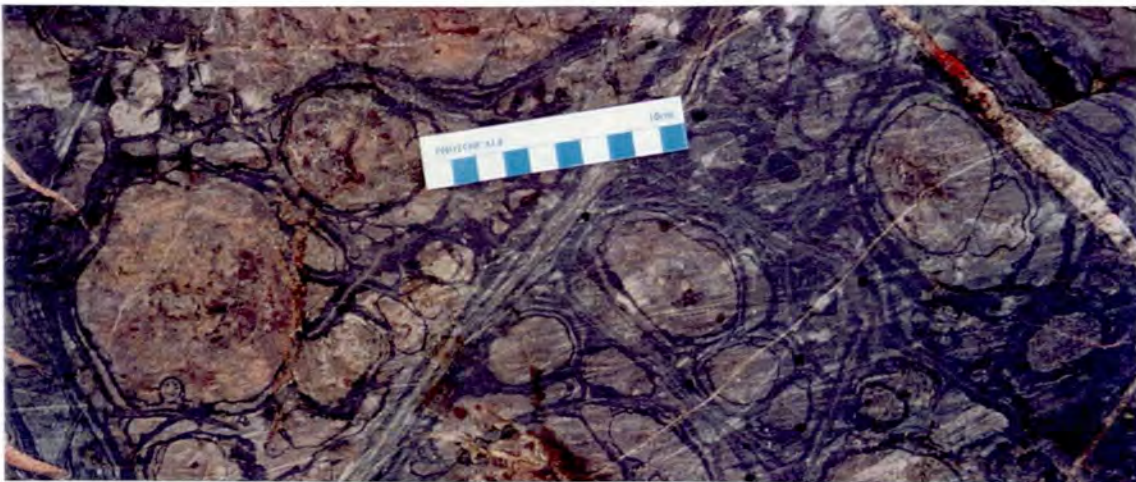


Fig. 13. The weathered, patchy black-and pink basalts beneath the Kolasjoki sediments. The corestones have black, hematite-rich rims and pink or brown cores which gives rise to a distinctive patchy structure locally called 'leopard'.



Fig. 14 Polymict conglomerate consisting of pebbles and amygdules derived from the Kuetsjärvi volcanites.



The alluvial unit at Luchlompolo fills a palaeovalley and logs of these sediments indicates that many of them were formed in river to delta environments. Evidence of former topography is seen where subvertical surfaces, up to 20 m high, have been buried by horizontal or gently dipping sediments (Fig. 12). Primary imbrication of pebbles indicates that stream-flow was generally north to south.

The sediments filling the palaeovalley are followed by a 30-60 m thick unit of brown and red polymict conglomerates, grit and coarse-grained sandstones. The sandstone-grit-conglomerate unit horizontally covers uneven palaeosurfaces and palaeovalleys filled in with fluvial deposits. This unit was not affected by syndepositional faulting and folding.

The rocks are composed of well rounded and sorted pebbles and grains of underlying Kuetsjärvi volcanites (Fig. 14). Some layers of coarse-grained sandstones consist of largely quartz and red albite amygdules. The 1-to 2 cm thick layers consisting of magnetite and hematite are common.

**Locality 10. The road cut and a number of natural exposures, 8 km west of Zapolyarny (Fig. 1, 2)**

**The Kolasjoki Volcanic Formation, middle part of the sequence, gabbro-diabase sill.**

The Kolasjoki Volcanic Formation is rather monotonous succession consisting of three main rock types: tholeiitic pillow basalts, tholeiitic lava-breccias and numerous gabbro-diabase sills which partly comagmatic and coeval with the Kolasjoki and partly with Pilgijärvi tholeiites.

A number of 2 to 10 m thick gabbro-diabase sills are exposed at Locality 10. They are composed of massive rocks containing sporadic epidote bulbs and tubes.

**Locality 11. Large block, 8 km west of Zapolyarny (Fig. 1, 2)**

**The Kolasjoki Volcanic Formation, middle part of the sequence, gabbro-diabase sill with columnar joints.**

When sills were placed near the surface they had columnar joints (Fig. 15).



Fig. 15 The large locally-arrived block of an extrusive gabbro-diabase with the columnar joints.



**Locality 12. A number of natural exposures, 8 km west of Zapolyarny (Fig. 1, 2)**

**The Kolasjoki Volcanic Formation, middle part of the sequence, pillow basalts.**

A very typical representative of the Kolasjoki pillow basalts is seen at Locality 12. Several lava flows, 1 to 3 m thick, with pillow structure are present. The pillows are well developed, only slightly deformed. They contain pipe vesicles which indicate a source of the flow. The top of the flow can be easily identified (Fig. 16).



Fig. 16. The 3 m thick flow of tholeiitic basalts with pillow structure. The hammer is 60 cm in length.

**Locality 13. A number of natural exposures, 8 km west of Zapolyarny (Fig. 1, 2)**

**The Kolasjoki Volcanic Formation, middle part of the sequence, tholeiitic lava-breccia.**

Lava-breccia are very abundant at Locality 13. In places, lava-breccia can be present at the top of the lava flow. Flow-top breccia consists of rounded and angular fragments sandwiched between a green vesicular flow top and an overlying sparsely vesicular flow base. Fig. 17 indicates a 3 m thick layer consisting of only lava-breccia.



Fig. 17 The tholeiitic lava-breccia at Locality 13.



**Locality 14. A spoil bank of the Zdanovsky quarry, 7.5 km west of Zapolyarny (Fig. 1, 2)**

**The Pilgujärvi Sedimentary Formation, representative rock types of the formation.**

There are certain obstacles to observing the rocks of the Productive Formation in natural situations because they are very rare. Admission to the abandoned quarries is forbidden as they have not been maintain for a number of years and therefore are dangerous. Active mines dealing with the mining of sulphide-bearing ultramafic rocks change every day and can hardly be used for the observation of the Productive formation rocks. An excellent opportunity for examining the whole assemblage of rocks may be provided by vast spoil banks developed in the vicinities of active mines. One of these, 7.5 km west of Zapolyarny, is the target of our excursion.

The Pilgujärvi Sedimentary Formation, also known as the 'Productive Formation', is the host formation for all the ultramafic intrusions and flows with economic sulphide Ni-Cu deposits. This makes the 'Productive' Formation rocks a key element in understanding of the ore-forming processes. The Productive Formation consists of different types of sedimentary and sedimentary-volcanic rocks, all of which carry  $C_{org}$  and iron sulphides. Among these rocks are: (a) horizontally laminated, arkosic and graywacke sandstones and siltstones with subordinate polymict conglomerate lenses; (b) highly carbonaceous and sulphidic graywacke and Bouma cycle (Fig. 18); (c) finely laminated rhythmites with pyritic layers and concretions (Fig. 19). The rocks expose an excellent development of current-bedded and syndimentary folded structures, eroded layers, sedimentary breccias and dikes, and abundant diagenetic carbonate concretions and lenses.

Two alluvial fan systems are developed in the Productive Formation. The rocks of the Kierdzhipori alluvial fan are

abundant in the spoil bank at Locality 14. These are phosphorous-bearing (up to 5 wt.  $P_2O_5$ ), polymictic, current-bedded, fine-grained arkosic breccia, conglomerates, gritstones and sandstones. The rocks are very rich in pyrite.



Fig. 18 The Bouma cycles in the highly carbonaceous and sulphidic graywacke sand- to siltstone. The bar-scale is 45 cm.

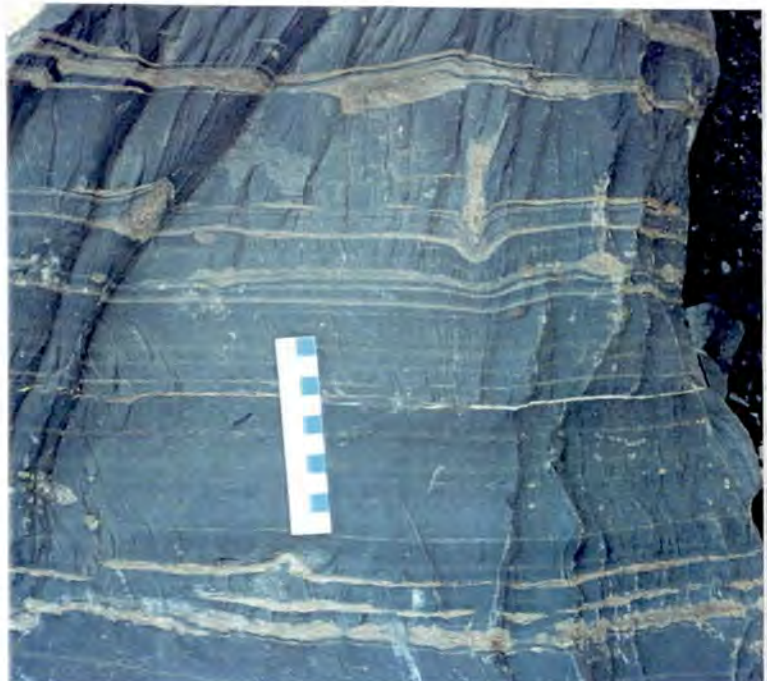


Fig. 19 Thinly bedded and laminated organic carbon-rich mudstone with diagenetic layers of pyrite. Note the latest development of pyrite along  $S_2$  cleavage. The bar-scale is 10 cm.



**Locality 15. A small exposure on the north-east side of the Mt. Rappesoarvi, 500 m west of the road from Zapolyarny to the Superdeep Drillhole at 30°39'30"E 69°24'00"N (Fig. 1, 2).**

**The Pilgujärvi Volcanic Formation, Basalt-Picrite Member, globular and pillow ferropicritic lava.**

The different modes of ferropicritic volcanism occurred during the deposition of the Basalt-Picrite Member. Massive, pillowed and globular ferropicritic lavas are common features of the member. Ferropicritic pillow lavas are found mainly in the central part of the of the Pechenga Zone (Fig. 1). Pillows display slightly flattened forms and range in size from 10 to 100 cm. Figure 20 shows an example of poorly developed pillow structure in the ferropicritic lava at Locality 15. The internal structure of the pillows is concentrically zoned due to the presence of marginally glass-rich chilled rims with amygdules. The inner part is olivine-porphyrific rock.

A specific feature of the ferropicritic lavas and some sills and dikes is the presence of well-developed globular structures. Globules range from 0.1 to 10 cm in size. The globular ferropicritic lavas can be seen at the same place as the pillow lava. Figure 21 shows an example of a globular lava at locality 15. This is adjacent to lava with pillow structure. The globules, 0.5 to 5 cm in size, are clearly distinguishable from their matrix due to their light colours when weathered.

The phenocryst and microcryst phases (olivine, clinopyroxene, kaersutite, magnetite and ilmenite) are the same in both the globules and the matrix. The only mineralogical difference is in the fine-grained mesostasis which is chlorite-rich in the matrix and alkali feldspar-rich in the globules (Hanski 1992). Characteristic features of globules are their frequent coalescence of with sharp cusps retained at the point of contact with coalescing globules. In some cases, the globules appear to have accumulated and formed layers up to 1.5 m thick. Hanski (1992) described how globule-forming material fringes the cooling cracks and also forms a band right at the contact with country rock.. All these observation provide good evidence of nonmagmatic but superimposed metasomatic origin for the globular structure.



Fig. 20 Well-developed pillow structure, Mt. Rappesoarvi, Locality 15. The bar-scale is 10 cm.





Fig. 21 Globular ferropicritic lava, Mt. Rappesoavi, Locality 15. The bar-scale is 10 cm.

**Locality 16. An excavation on the north-eastern slope of the Mt. Vilgiskoddeoivi, 100m south-west of the road from Zapolyarny to the Superdeep Drillhole at 30°37'40"E 69°23'00"N (Fig. 1, 2).**

**The Pilgujärvi Volcanic Formation, Rhyolite & Lower Basalt members, rhyolitic tuffs, massive and pillow tholeiitic lavas.**

Acidic volcanism occurs as a 5 to 40 m horizon of tuffs and local flows occurring as doublets and triplets separated by tholeiites, located ca. 800-1000 m above the upper contact of the Productive Formation. At Locality 16 the sequence is 35 m thick. It is distinguished by erosional surfaces between cycles, and the sequence shows cyclic coarsening- or fining-upward development (Fig 22)

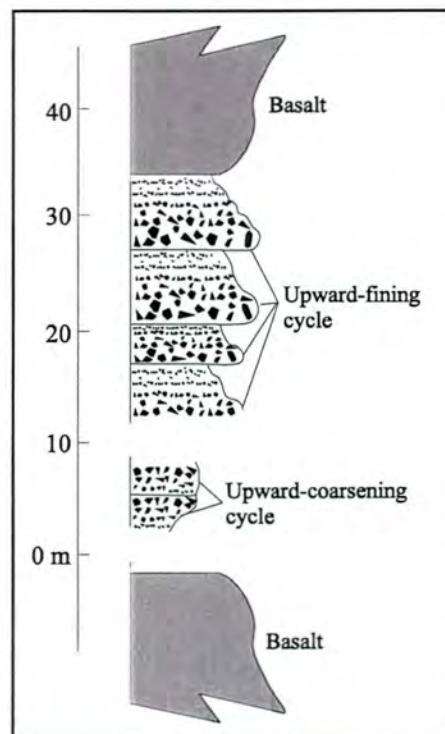


Fig. 22. Field sketch illustrating the cyclic build-up of the rhyolite tuffs. The sequence how it appears at the Mt. Vilgiskoddeoivi, Locality 16.



with bases of massive lapilli tuff and lesser subaerial welded tuff with volcanic bombs. These gradually pass upwards through medium-grained crystalloclastic tuffs to either a thinly bedded and laminated or a massive, microcrystalline tuff.

The acidic flows contain plentiful microgranophyre fragments, euhedral and corroded quartz crystals surrounded by devitrified glass and abundant small, partially melted fragments of gneiss.

These volcanic rocks have unusually high SiO<sub>2</sub> content with the range from 73 to 85 wt. %. They are Zr-enriched (up to 895 ppm) rocks with highly variable Na<sub>2</sub>O/K<sub>2</sub>O ratios (0.01-2.5), attributable to magma contamination and heterogeneity.

The Zapadny (Western), Zentral'ny (Central) and Severny (Northern) Ni-Cu mines.

*The guide is Mr. S.V. Sokolov, PechengaNickel Combine.*



**Locality 17. The Zapadny (Western) and Zentral'ny (Central) open pit Ni-Cu mines at 30°44'45"E 69°23'20"N (Fig. 1, 2).**

**The Pilgujärvi differentiated intrusion, ultramafic-hosted massive, brecciated massive, disseminated sulphide Ni-Cu ores.**

The Pilgujärvi differentiated intrusion will be examined in the largest open pit Ni-Cu mine in the area, 3.5 km long, 350 m deep (photo on the cover page).

The Pilgujärvi differentiated intrusion is located in the eastern part of the Ore Field, close to the lowermost part of the Productive Formation. It is the largest mafic-ultramafic intrusion in the Pechenga Zone. The intrusion was investigated by Smol'kin (1977). The comprehensive study was performed by Hanski (1992). The information presented in this section is largely based on Hanski's study (Hanski 1992).

Geological maps of the Pilgujärvi intrusion and its vertical section are shown in Figures 23 and 24 respectively. The intrusion constitutes two parts separated by a 'layer' of the Productive Formation 'black shales'. The southern part is dominated by gabbroic rocks while the northern branch contains a wide range of rock types. The ten ore deposits are distinguished in the northern part of the intrusion, namely from west to east: (1) Verkhnee (Upper deposit), (2) Tundrovoe (Tundra), (3) Sed'moe (Seventh), (4) Yugo-Zapadnoe (South-western), (5) Zapadnoe (Western), (6) Zentral'noe (Central), (7) Vostochnoe (Eastern), (8) Yugo-Vostochnoe (South-eastern), (9) Bystrinskoe (no English equivalent), (10) Zapolyarninskoe (Trans-Arctic). The Sed'moe (Seventh), Yugo-Zapadnoe (South-western) and Zapadnoe (Western) deposits are mined from the Zapadny (Western) open pit Ni-Cu mine, while the Zentral'noe (Central), Vostochnoe (Eastern) and Yugo-Vostochnoe (South-eastern) are exploited from the Zentral'ny (Central) open pit Ni-Cu mine. The Zapolyarninskoe (Trans-Arctic) deposit is mined from the underground Severny (Northern) Ni-Cu mine. The location of the Zapadnoe (Western), Zentral'noe (Central), Vostochnoe (Eastern) and Yugo-Vostochnoe (South-eastern) deposits as well as that of the Severny (Northern) underground Ni-Cu mine are indicated on Fig. 23. Most of the ores are low-grade sulphide dissemination in the lowermost peridotites. The Zapolyarninskoe (Trans-Arctic) deposit is somewhat enigmatic as it is located in a tectonic zone in the country rock 'black shales' of the Productive Formation beneath the central part of the intrusion.

The northern part of the intrusion is up to 540 m thick and can be followed for 2.2 km, and dips at about 50° to the SW down to a depth of 3,500 m (Superdeep Drillhole intersection) and still continues further down. As a whole the intrusion is concordant with the country rocks, 'black shales' of the Productive Formation with cross-cutting relations in some locations. The intrusion is divided into seven zones (Smol'kin 1977) which are, from the



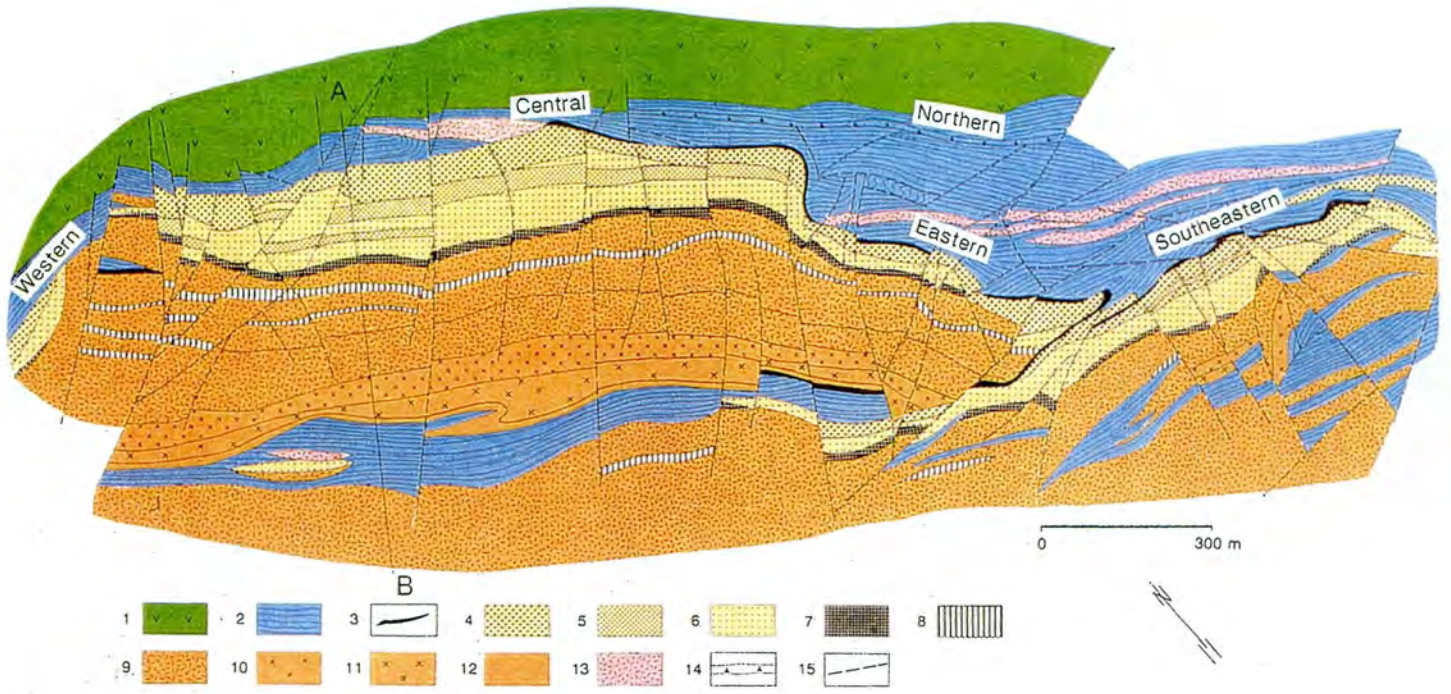


Fig. 23. Geological map of the Pilgijärvi differentiated intrusion (Smol'kin 1977, Hanski 1992).

Legend: 1, *Kolasjoki Volcanic Formation*: tholeiitic basalt; *Productive Formation*: 2, 'black shales'; *Pilgijärvi differentiated intrusion*: 3, marginal zones; 4, peridotite with disseminated Ni-Cu ore; 5, wehrlite; 6, olivinite; 7, intermediate zone (olivine pyroxenite, kazanskite, kosvite); 8, pyroxenite; 9, gabbro; 10, coarse-grained gabbro; 11, pegmatitic and essexitic gabbro; 12, diorite; 13, gabbro-diabase sill comagmatic with tholeiites of the Pilgijärvi Volcanic Formation; 14, sulphide Ni-Cu ore in a tectonic zone; 15, fault.

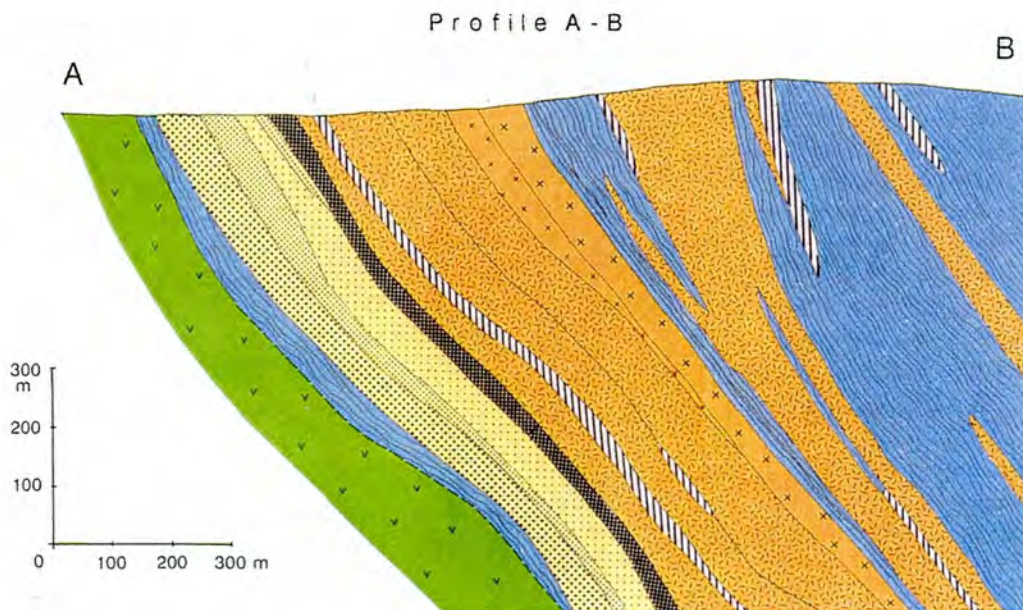


Fig. 24  
Vertical profile across the Pilgijärvi intrusion along the line A-B (Fig. 23). Ornamentation as in Fig. 23. Section is from Hanski 1992.

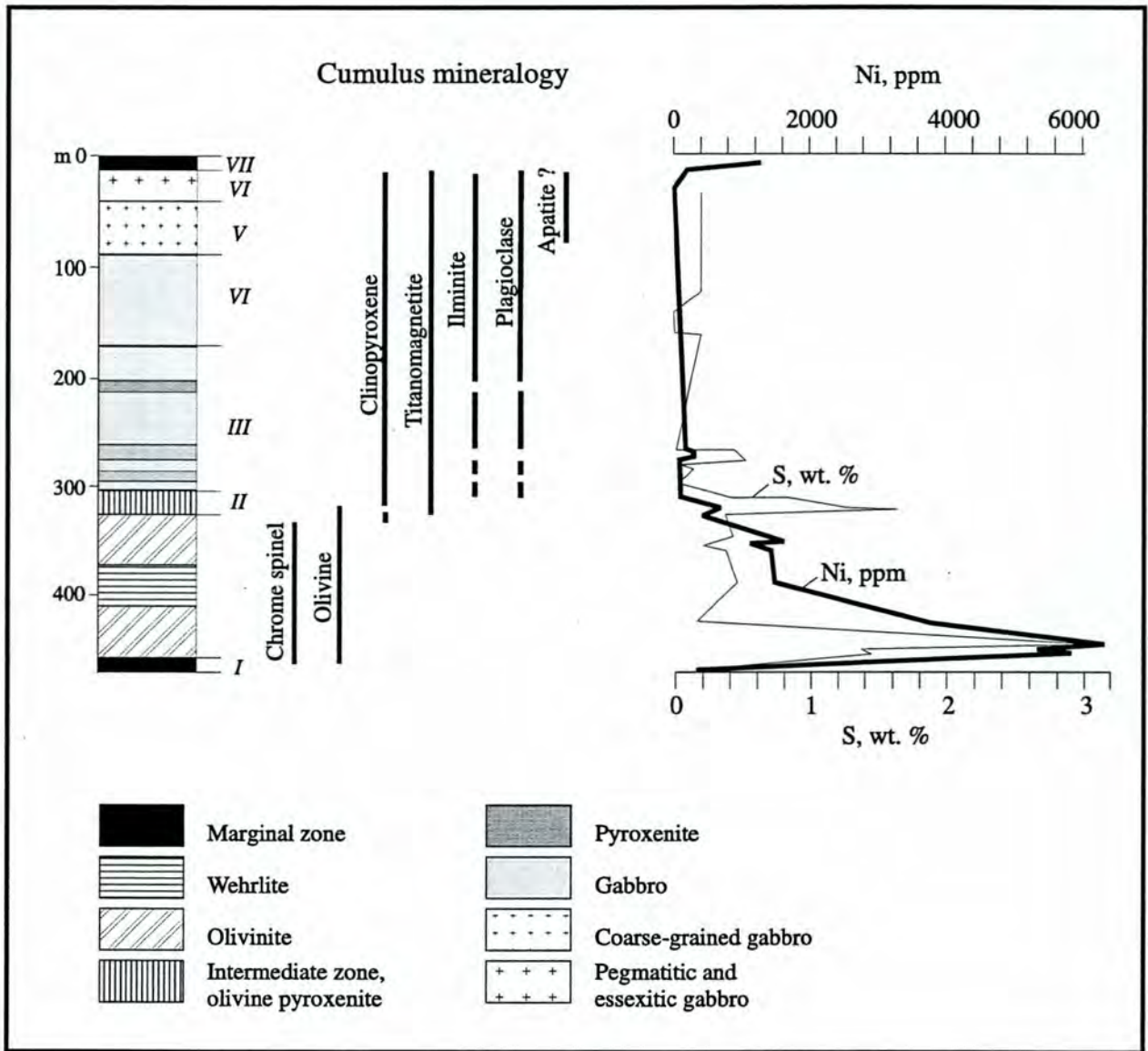


Fig. 25 The zones, cumulus mineralogy and variation of Ni and S across the Pilgijärvi differentiated intrusion (Hanski 1992). The description of the zones see in the text.



base upwards: (I) the lower marginal zone, (II) the wehrlite-olivinite zone, (III) the intermediate zone, (IV) the gabbro-pyroxenite zone, (V) the gabbro zone, (VI) the essexitic gabbro zone, (VII) the upper marginal zone (Fig. 25). Boundaries between these zones are gradational. Primary flow structures such as banding, cross-bedding, preferred orientation of primary minerals are developed in mafic rocks. Country rock xenoliths have been found in the gabbroic part of the intrusion, mostly at the contacts between different zones.

All type of ores known in the Pechenga ore field are present in the Pilgujärvi intrusion. Participants will get a chance to examine Ni-rich massive ores, brecciated massive ores, high-grade disseminated ores (named locally a 'grey ore'), as well as lower-grade disseminated ores.

**Locality 17. The Severny underground Ni-Cu mine at 39°45'00"E 69°24'00"N (Fig. 1, 2).**

**Massive Ni-Cu ores located in a tectonic in the country rock 'black shales' of the Productive Formation beneath the central part of the Pilgujärvi intrusion.**

The final and most exiting target of the Pechenga excursion is the Severny (Northern) underground Ni-Cu mine. This mine is located on the northern margin of the Central Zhdanovsky quarry and exploits rich sulphide Ni-Cu ores of the Zapolyarninskoe (Trans-Arctic) deposit. The deposit is located in a tectonic zone which separates the Productive formation 'black shales' from the Kolasjoki Volcanic Formation. It is located at the foot of the Productive Formation beneath the central

part of the Pilgujärvi intrusion and the Central ore body of the Zdanovsky deposit. The Zapolyarninskoe (Trans-Arctic) deposit is a sheet-like body, 1,000 m in length along strike, dipping 50° south down to 2,000 m with a thickness from 2 to 50 m (Fig. 26).

The ore body is composed of highly tectonised and altered ultramafic rocks (serpentine-chlorite-talc rocks and talcites) containing ores. The latter are represented by two main types, namely (i) serpentinite-hosted disseminated and vein-disseminated ores, and (ii) ore breccias. The ore breccia consist of 'black shale' and serpentinite fragments of different size which are cemented by sulphide ground-mass. The size of fragments varies from 0.1 cm up to 2-3 m. A multiphase deformation led to a complex structural development of the ore body, resulting in the formation of at least three generations of ore breccias and three populations of sulphide minerals. The latter are pyrrhotite, pentlandite, chalcopyrite and magnetite. An enhanced content of As and platinum group elements distinguishes the Zapolyarninskoe (Trans-Arctic) deposit from others in the Pechenga Ore Field. The Ni content ranges from 1 to 12 wt. % with the average value of 2.12 wt. %. The ore proportion is very high; in places ultramafic rocks are not present at all and the ore-mass is located at the foot of the Productive Formation.

It is believed that the Zapolyarninskoe (Trans-Arctic) ore body was formed as result of the intrusion of a silicate-sulphide melt into the tectonic zone during the extensional tectonics. Later deformations followed by metamorphic-hydrothermal events led to the formation of a complex textural and mineralogical development of the ore body.



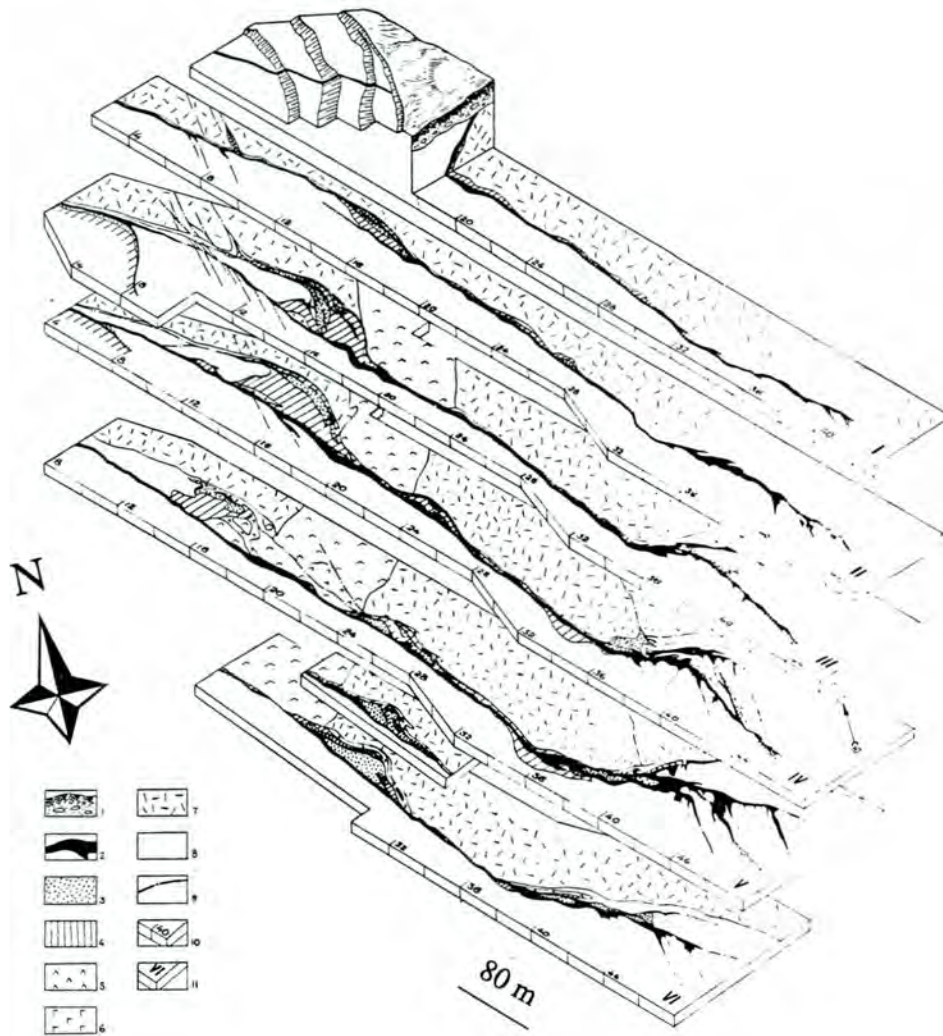


Fig. 26 Block diagram of the Zapolyarninskoe (Trans-Arctic) Ni-Cu deposit showing the geology and distribution of ore bodies as a function of depth.

1, overburden; 2, massive sulphide ore and ore breccia; 3, high-grade disseminated ore in serpentine-chlorite-talc rock and talcite (Ni>1 wt. %); 4, low-grade disseminated ore in serpentine-chlorite-talc rock and talcite (Ni<1 wt. %); 5, serpentine-chlorite-talc rock and talcite; 6, gabbro; 7, Kolasjoki Volcanic Formation; 8, Productive Formation 'black shale'; 9, fault; 10, profile and its number; 11, horizon and its number.

The line-space between profiles is 20 m, the distance between each horizon is 60 m.

## References

Hanski, E.J. 1992: Petrology of the Pechenga ferropicrites and cogenetic, Ni-bearing gabbro-whirlite intrusions, Kola Peninsula, Russia. Geological Survey of Finland, Bulletin 367, 1-196.

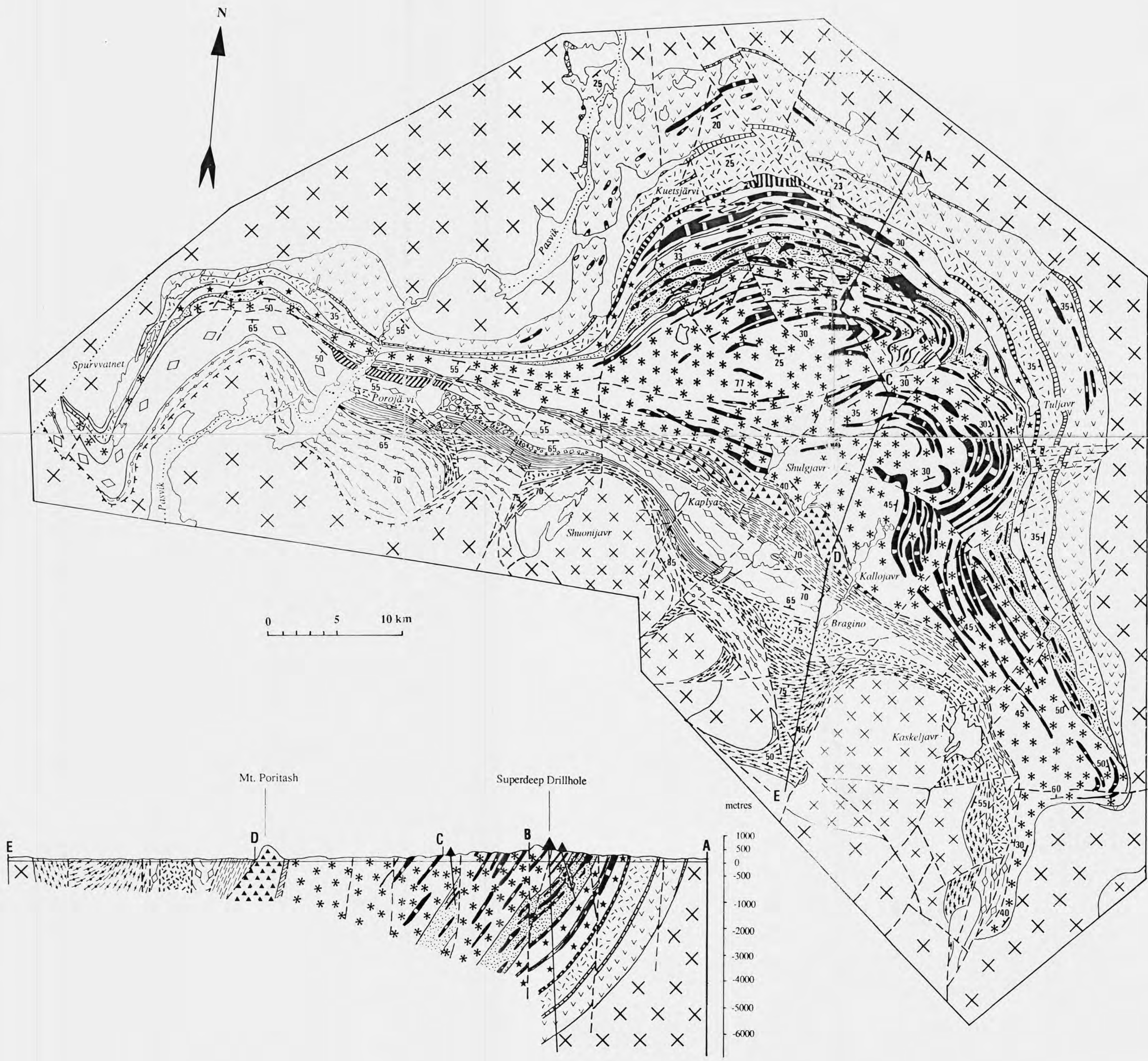
Smol'kin, V.F., 1977: Petrology of the Pilgjarvi ore-bearing intrusion (Pechenga). VINITI, No. 2114-77, 1-216.



# G E O L O G I C A L M A P O F T H E P A S V I K - P E C H E N G A B E L T

by  
V. A. MOKROUSOV, L. S. MOLOTKOV (Central Kola Geological Expedition, Monchegorsk), G. JUVE, V. A. MELEZHNIK, L. P. NILSSON,  
B. A. STURT, (Geological Survey of Norway, Trondheim), D. M. RAMSAY (University of Glasgow, Glasgow), P. K. SKUF'IN (Geological Institute  
Russian Academy of Sciences, Apatity).

Compiled in 1994/95 by V. A. MELEZHNIK (Geological Survey of Norway, Trondheim)



**LEGEND**

**PETSAMO SUPERGROUP (2.45-1.85 Ga)**

**SOUTH PECHENGA/LANGVANNET GROUPS (1.95-1.85 Ga)**

**METASUPRACRUSTAL ROCKS**

- LAKE PESTCHANO Formation
- THOLEIITIC PILLOWED AND AMYGDALOIDAL BASALT
- TAL'YA Formation
- SANDSTONE WITH THIN BANDS OF SILTSTONE
- KASESJOKI Formation
- ANDESITIC VOLCANOCLASTIC SANDSTONE
- ANDESITIC VOLCANOCLASTIC POLYMICT CONGLOMERATE
- KAPLYA Formation
- SYNOGENIC ANDESITIC AND DACITIC LAVA AND TUFF, EXPLOSION BRECCIA (COLD AND HOT LAHAR), MENNEL Formation
- SYNOGENIC PICRITIC BASALT, PICRITIC LAVA, LAVA-BRECCIA, TUFF, PICRITIC SEDIMENT
- FAGERMO Formation
- SYNOGENIC ULTRAMAFIC PILLOWED AND MASSIVE LAVA, LAVA-BRECCIA, TUFF, ULTRAMAFIC SEDIMENT
- BRAGINO Formation
- SYNOGENIC ANDESITIC AND DACITIC LAVA, TUFF, TUFFITE, ANDESITIC VOLCANOCLASTIC SEDIMENT, SUBORDINATE BASALT AND PICRITE, BONINITIC ANDESITE
- KALLOJAVR Formation
- C<sub>org</sub> AND SULPHUR-RICH SANDSTONE, SILTSTONE, MUDSTONE WITH CHERTY QUARTZITE AND SUBORDINATE BASALT AND ANDESITE
- LANGVANNET GROUP (undivided)
- BASALT, ANDESITE, ANDESITIC VOLCANOCLASTIC SEDIMENT, C<sub>org</sub> AND SULPHUR-RICH SANDSTONE, CHERTY QUARTZITE, AMPHIBOLE SCHIST

**METAINTRUSIVE ROCKS**

- MOUNTAIN SUBVOLCANIC OROGENIC ANDESITE, DACITE, RHYOLITE

**NORTH PECHENGA GROUP (2.45-1.95 Ga)**

**METASUPRACRUSTAL ROCKS**

- PILGJAVR VOLCANIC FORMATION
- THOLEIITIC PILLOWED AND MASSIVE BASALT, BASALTIC LAVA-BRECCIA, RHYOLITIC AND DACITIC EXPLOSION BRECCIA (COLD AND HOT LAHAR)
- ULTRAMAFIC (FERROPICRITIC) FLOW, SILL AND INTRUSION (undivided)
- PILGJAVR SEDIMENTARY FORMATION
- ULTRAMAFIC (FERROPICRITIC) LAVA, TUFF AND TUFFITE, C<sub>org</sub> AND SULPHUR RICH GREYWACKE AND ARKOSIC SANDSTONE, SILTSTONE, MUDSTONE
- ULTRAMAFIC (FERROPICRITIC) EXPLOSION BRECCIA (only in the cross-section)
- KOLASJOKI VOLCANIC FORMATION
- THOLEIITIC BASALT WITH PILLOW AND STRUCTURE, BASALTIC TUFF AND TUFFITE
- C<sub>org</sub> AND SULPHUR-RICH SANDSTONE AND SILTSTONE
- KOLASJOKI SEDIMENTARY FORMATION
- TUFFIC CARBONACEOUS SILTSTONE, Mn-RICH DOLOSTONE, STROMATOLITIC DOLOSTONE, DOLOLITHITE, JASPER, RED-COLOURED CURRENT-BEDDED HAEMATITE-RICH SANDSTONE, POLYMICT CONGLOMERATE
- KUETSJARVI VOLCANIC FORMATION
- AMYGDALOIDAL AND COLUMNAR JOINTED SUB-ALKALINE BASALT, AMYGDALOIDAL ALKALINE BASALT, ANDESITE, DACITE, RHYOLITE AND MUGEARITE
- BROWNISH RED VOLCANOCLASTIC CONGLOMERATE, VOLCANOCLASTIC MUDSTONE WITH VOLCANIC BOMBS, SILTSTONE
- KUETSJARVI SEDIMENTARY FORMATION
- RED AND MULTICOLOURED DOLOSTONE, ONCOLITHIC DOLOLITE, RIPPLE MARKED DOLOLITHITE, DOLOMITIC BRUCCIA AND CONGLOMERATE, RED COLOURED ARKOSIC AND QUARTZITIC SANDSTONE
- AHMALAHTI VOLCANIC FORMATION
- PORPHYRITIC AND AMYGDALOIDAL SUB-ALKALINE BASALT, BASALTIC ANDESITE, DACITE, KOMATIITIC ANDESITE, MAFIC AND ULTRAMAFIC TUFF, GREYWACKE SANDSTONE
- NEVERSKRUKK FORMATION
- BASALTIC TUFF, ARKOSIC SANDSTONE, GRITSTONE, BASAL POLYMICT CONGLOMERATE AND BRECCIA

**METAINTRUSIVE ROCKS**

- GABBRO AND GABBRO-DOLERITE SILL (undivided)
- SYNOGENIC GRANITE, GRANODIORITE, DIORITE

**ARCHAEOAN ROCKS (2.9-2.5 Ga)**

- TONALITE, GRANITE, GNEISS, AMPHIBOLITE, MAFIC AND ULTRAMAFIC INTRUSIONS

**GEOLOGICAL SYMBOLS**

- LITHOLOGICAL BOUNDARY (unspecified)
- FAULT (unspecified)
- INFERRED THRUST BOUNDARY
- STRIKE AND DIP OF BEDDING
- DRILLHOLE